EBC
Energy in Buildings and Communities Programme

International Energy Agency, EBC Annex 68

Indoor Air Quality Design and Control in Low-Energy Residential Buildings

Subtask 5: Field measurements and case studies

Energy in Buildings and Communities Technology Collaboration Programme

October 2020

EBC
Energy in Buildings and Communities Programme

International Energy Agency, EBC Annex 68

Indoor Air Quality Design and Control in Low-Energy Residential Buildings
Subtask 5: Field measurements and case studies

Energy in Buildings and Communities Programme

October 2020

Subtask 5 co-leaders:

Jelle Laverge (jelle.laverge@ugent.be), Ghent University, Belgium
Fitsum Tariku (fitsum_tariku@bcit.ca), British Columbia Institute of Technology, Canada

Editors:

Sarah L. Paralovo, Ghent University, Belgium

Contributing Authors:

Alula Assefa, BCIT Building Science Centre of Excellence, Canada
Esfand Burman, UCL Institute for Environmental Design and Engineering, UK
Klaas De Jonge, Ghent University, Belgium
Gaëlle Guyot, Cerema; University of Savoie Mont Blanc, France
Roman Jaques, BRANZ, New Zealand
Manfred Plagmann, BRANZ, New Zealand
Shahrzad Pedram, BCIT Building Science Centre of Excellence, Canada
Gabriel Rojas-Kopeinig, University of Innsbruck, Austria
Maarten Spruyt, VITO, Belgium
Marianne Stranger, VITO, Belgium

Published as report number 431 by the Department of Civil Engineering, Technical University of Denmark, Brovej, Building 118, DTU, DK-2800, Denmark.

ISBN: 87-7877-530-2

EAN: 9788778775306

Participating countries in EBC:

Australia, Austria, Belgium, Canada, P.R. China, Czech Republic, Denmark, Finland, France, Germany, Ireland, Italy, Japan, Republic of Korea, the Netherlands, New Zealand, Norway, Portugal, Singapore, Spain, Sweden, Switzerland, United Kingdom and the United States of America.

Additional copies of this report may be obtained from:

EBC Bookshop
C/o AECOM Ltd
The Colmore Building
Colmore Circus Queensway
Birmingham B4 6AT
United Kingdom
Web: www.iea-ebc.org

Email: essu@iea-ebc.org

Preface

The International Energy Agency

The International Energy Agency (IEA) was established in 1974 within the framework of the Organisation for Economic Co-operation and Development (OECD) to implement an international energy programme. A basic aim of the IEA is to foster international co-operation among the 30 IEA participating countries and to increase energy security through energy research, development and demonstration in the fields of technologies for energy efficiency and renewable energy sources.

The IEA Energy in Buildings and Communities Programme

The IEA co-ordinates international energy research and development (R&D) activities through a comprehensive portfolio of Technology Collaboration Programmes. The mission of the IEA Energy in Buildings and Communities (IEA EBC) Technology Collaboration Programme is to develop and facilitate the integration of technologies and processes for energy efficiency and conservation into healthy, low emission, and sustainable buildings and communities, through innovation and research. (Until March 2013, the IEA EBC Programme was known as the IEA Energy Conservation in Buildings and Community Systems Programme, ECBCS.)

The R&D strategies of the IEA EBC Programme are derived from research drivers, national programmes within IEA countries, and the IEA Future Buildings Forum Think Tank Workshops. These R&D strategies aim to exploit technological opportunities to save energy in the buildings sector, and to remove technical obstacles to market penetration of new energy efficient technologies. The R&D strategies apply to residential, commercial, office buildings and community systems, and will impact the building industry in five areas of focus for R&D activities:

- Integrated planning and building design
- Building energy systems
- Building envelope
- Community scale methods
- Real building energy use

The Executive Committee

Overall control of the IEA EBC Programme is maintained by an Executive Committee, which not only monitors existing projects, but also identifies new strategic areas in which collaborative efforts may be beneficial. As the Programme is based on a contract with the IEA, the projects are legally established as Annexes to the IEA EBC Implementing Agreement. At the present time, the following projects have been initiated by the IEA EBC Executive Committee, with completed projects identified by (*) and joint projects with the IEA Solar Heating and Cooling Technology Collaboration Programme by (☼):

Annex 1: Load Energy Determination of Buildings (*)
Annex 2: Ekistics and Advanced Community Energy Systems (*)
Annex 3: Energy Conservation in Residential Buildings (*)
Annex 4: Glasgow Commercial Building Monitoring (*)
Annex 5: Air Infiltration and Ventilation Centre
Annex 6: Energy Systems and Design of Communities (*)
Annex 7: Local Government Energy Planning (*)
Annex 8: Inhabitants Behaviour with Regard to Ventilation (*)
Annex 9: Minimum Ventilation Rates (*)
Annex 10: Building HVAC System Simulation (*)

Annex 11: Energy Auditing (*)
Annex 12: Windows and Fenestration (*)
Annex 13: Energy Management in Hospitals (*)
Annex 14: Condensation and Energy (*)
Annex 15: Energy Efficiency in Schools (*)
Annex 16: BEMS 1- User Interfaces and System Integration (*)
Annex 17: BEMS 2- Evaluation and Emulation Techniques (*)
Annex 18: Demand Controlled Ventilation Systems (*)
Annex 19: Low Slope Roof Systems (*)
Annex 20: Air Flow Patterns within Buildings (*)
Annex 21: Thermal Modelling (*)
Annex 22: Energy Efficient Communities (*)
Annex 23: Multi Zone Air Flow Modelling (COMIS) (*)
Annex 24: Heat, Air and Moisture Transfer in Envelopes (*)
Annex 25: Real time HVAC Simulation (*)
Annex 26: Energy Efficient Ventilation of Large Enclosures (*)
Annex 27: Evaluation and Demonstration of Domestic Ventilation Systems (*)
Annex 28: Low Energy Cooling Systems (*)
Annex 29: ☼ Daylight in Buildings (*)
Annex 30: Bringing Simulation to Application (*)
Annex 31: Energy-Related Environmental Impact of Buildings (*)
Annex 32: Integral Building Envelope Performance Assessment (*)
Annex 33: Advanced Local Energy Planning (*)
Annex 34: Computer-Aided Evaluation of HVAC System Performance (*)
Annex 35: Design of Energy Efficient Hybrid Ventilation (HYBVENT) (*)
Annex 36: Retrofitting of Educational Buildings (*)
Annex 37: Low Exergy Systems for Heating and Cooling of Buildings (LowEx) (*)
Annex 38: ☼ Solar Sustainable Housing (*)
Annex 39: High Performance Insulation Systems (*)
Annex 40: Building Commissioning to Improve Energy Performance (*)
Annex 41: Whole Building Heat, Air and Moisture Response (MOIST-ENG) (*)
Annex 42: The Simulation of Building-Integrated Fuel Cell and Other Cogeneration Systems (FC+COGEN-SIM) (*)
Annex 43: ☼ Testing and Validation of Building Energy Simulation Tools (*)
Annex 44: Integrating Environmentally Responsive Elements in Buildings (*)
Annex 45: Energy Efficient Electric Lighting for Buildings (*)
Annex 46: Holistic Assessment Tool-kit on Energy Efficient Retrofit Measures for Government Buildings (EnERGo) (*)
Annex 47: Cost-Effective Commissioning for Existing and Low Energy Buildings (*)
Annex 48: Heat Pumping and Reversible Air Conditioning (*)
Annex 49: Low Exergy Systems for High Performance Buildings and Communities (*)
Annex 50: Prefabricated Systems for Low Energy Renovation of Residential Buildings (*)
Annex 51: Energy Efficient Communities (*)
Annex 52: ☼ Towards Net Zero Energy Solar Buildings (*)
Annex 53: Total Energy Use in Buildings: Analysis and Evaluation Methods (*)
Annex 54: Integration of Micro-Generation and Related Energy Technologies in Buildings (*)
Annex 55: Reliability of Energy Efficient Building Retrofitting - Probability Assessment of Performance and Cost (RAP-RETRO) (*)
Annex 56: Cost Effective Energy and CO2 Emissions Optimization in Building Renovation (*)
Annex 57: Evaluation of Embodied Energy and CO2 Equivalent Emissions for Building Construction (*)
Annex 58: Reliable Building Energy Performance Characterisation Based on Full Scale Dynamic Measurements (*)
Annex 59: High Temperature Cooling and Low Temperature Heating in Buildings (*)
Annex 60: New Generation Computational Tools for Building and Community Energy Systems (*)
Annex 61: Business and Technical Concepts for Deep Energy Retrofit of Public Buildings (*)

Annex 62: Ventilative Cooling (*)
Annex 63: Implementation of Energy Strategies in Communities (*)
Annex 64: LowEx Communities - Optimised Performance of Energy Supply Systems with Exergy Principles (*)

Annex 65: Long-Term Performance of Super-Insulating Materials in Building Components and Systems (*)
Annex 66: Definition and Simulation of Occupant Behavior in Buildings (*)
Annex 67: Energy Flexible Buildings
Annex 68: Indoor Air Quality Design and Control in Low Energy Residential Buildings
Annex 69: Strategy and Practice of Adaptive Thermal Comfort in Low Energy Buildings
Annex 70: Energy Epidemiology: Analysis of Real Building Energy Use at Scale
Annex 71: Building Energy Performance Assessment Based on In-situ Measurements
Annex 72: Assessing Life Cycle Related Environmental Impacts Caused by Buildings
Annex 73: Towards Net Zero Energy Resilient Public Communities
Annex 74: Competition and Living Lab Platform
Annex 75: Cost-effective Building Renovation at District Level Combining Energy Efficiency and Renewables
Annex 76: ☼ Deep Renovation of Historic Buildings Towards Lowest Possible Energy Demand and CO_2 Emissions
Annex 77: ☼ Integrated Solutions for Daylight and Electric Lighting
Annex 78: Supplementing Ventilation with Gas-phase Air Cleaning, Implementation and Energy Implications
Annex 79: Occupant -Centric Building Design and Operation
Annex 80: Resilient Cooling
Annex 81: Data-Driven Smart Buildings

Working Group - Energy Efficiency in Educational Buildings (*)
Working Group - Indicators of Energy Efficiency in Cold Climate Buildings (*)
Working Group - Annex 36 Extension: The Energy Concept Adviser (*)
Working Group - HVAC Energy Calculation Methodologies for Non-residential Buildings
Working Group - Cities and Communities
Working Group - Building Energy Codes
Working Group - International Building Materials Database

Summary

IEA-EBC Annex 68: Indoor Air Quality Design and Control in Low Energy Residential Buildings investigates how to ensure that future low energy buildings are able to improve their energy performance while still providing comfortable and healthy indoor environments. More specifically, Subtask 5 of Annex 68 has dealt with generation of data for the verification of the models and strategies developed in the other Annex 68 Subtasks through controlled field tests and case study presentations.

Thus one of the main goals of Subtask 5 was to run measurement campaigns in well-known field test buildings, focusing on testing and demonstrating in practice which low energy operational strategies can be used that will provide amenable indoor environments. For this, a series of field tests with increasing complexity were performed. The two other goals were to present a selection of past case studies and provide an overview of available measurement techniques for those setting up new campaigns.

This document contains a comprehensive summary of existing measurement methods for indoor air quality (IAQ) and ventilation assessments, intended to serve as a guide for researchers and practitioners (Chapter 1) as well as the complete report of the experiments conducted as part of Subtask 5. The series of experiments started from a 1 room/1pollutant situation (Chapter 2) and was escaladed to an occupied house (Chapters 3-6). Finally, a collection of case study measurement campaigns from annex participants is presented in a standardized format (Chapter 7).

From our activities in ST5, we can conclude that there is a wide range of different methods available to measure a variety of IAQ indicators, each method with its own working principles and practical limitations. Consequently, choosing the most adequate method for a specific measurement campaign can prove to be a not-so-simple task. The same characteristic of a method can be considered an advantage or a disadvantage depending on the objectives of the specific assessment to be performed.

Although the selection of measurement method should ultimately be done on a case-to-case basis, some general recommendations are described below:

- **Comprehensiveness x focus**: it is important that every assessment measures at least one IAQ indicator (e.g. TVOC, formaldehyde, $PM_{2.5}$) and one ventilation indicator (e.g. average air change rate, CO_2 concentration), as both concepts are intrinsically connected;
- **Official surveys**: If the goal of the assessment is to verify compliance with guidelines or, more importantly, with legislation, or if the results are intended to have any type of official character, the measurement methods should be the standard ones, complying with the ISO 16000 and other relevant official standards, if applicable (e.g. NAAQS, Gilliam et al., 2016). If the survey is of academic or purely exploratory nature, alternative methods can be applied;
- **Time scale**: If the assessment intends to observe variations over short-term periods (e.g. variation of pollutant levels due to point events, or variation of air change rate over working hours), the measurement methods chosen should be based on active techniques with automatic data storage (low-cost sensors may be used if deeper characterization of the species of pollutants is not needed). If the intention is to observe the average situation over longer periods or if it is enough to characterize the indoor air by a limited number of samples, simpler methods can be employed (e.g. passive sampling, gravimetry, grab samples);

- **Spatial scale**: If the intention is to assess many different sites (e.g. large-scale regional surveys) or if the assessed site presents a considerable spatial heterogeneity (e.g. multi-zone buildings), it is advisable to select lower-cost measurement methods for specific IAQ indicators and invest in simultaneous sampling at the different sites/points of the heterogeneous site.
- **Occupancy**: If occupants will be present at the site during the course of the assessment (e.g. workplace or home survey), the selected measurement methods should not cause excessive disturbance to the environment (e.g. noise, smell, clutter). Passive methods and/or small, silent sensors tend to be preferred in such cases.

Due to the complex interconnections between building properties, energy use, occupancy and IAQ, the reporting of a case study should, in order to understand the significance of the reported IAQ data, include a general description of the building and its relevant components (envelope, interior finishing, mechanical systems and ventilation), the boundary conditions during the measurements, the measurement plan and measurement equipment. Ideally, it should also provide the reader with a short 'lessons learned' section.

Table of content

Chapter 1: Measurement methods guide for IAQ and ventilation assessments

1.1 Introduction

The rise of the energy-efficient buildings concept, such as the passive building concept originally proposed by W. Feist (Foster et al., 2016), is pushing the new buildings to become more and more airtight over time. To enhance energy savings even more, parallel efforts are being made to limit space heating energy consumption by lowering the ventilation rate to the minimum necessary based on the 'demand'. However, doing so may negatively impact the indoor air quality (IAQ), as ventilation is a crucial factor in determining the accumulation of pollutants in indoor environments (EPA, 1994).

That was the motivation behind the creation of the IEA EBC Annex 68 project: Indoor Air Quality Design and Control in Low Energy Residential Buildings. The main goal of Annex 68 has been to investigate strategies to ensure that future low energy buildings can improve their energy performances while still providing comfortable and healthy indoor environments. In this context, it is of uttermost importance that the means employed to assess the IAQ in such buildings are the most adequate and as reliable as possible. Thus, the aim of this review is to present a wide array of possible methods currently used to measure different parameters of IAQ.

A good IAQ assessment must:

- Be comprehensive: the assessment planning must include not only the monitoring of the pollutants of interest (i.e. gaseous compounds, organic and/or inorganic, solid particles, bioaerosols or a combination of those), but preferably also scan for non-targeted pollutants and provide information on basic ventilation parameters (building ventilation type, designed air change rate, actual/measured air change rate);
- Utilize reliable and accurate measurement methods: considering the relevance of IAQ monitoring both from a health perspective and from the energy performance perspective, it is critical to ensure that the important IAQ indicators are measured sufficiently and adequately.

The ISO 16000 series provides a detailed guide on how to execute adequate indoor air pollution measurements. The different parts of ISO 16000 describe several aspects of a sampling strategy to be observed, including the conditions of interest for the particular substances or groups of substances, such as the dependence of indoor air pollution concentrations on e.g. humidity or temperature. ISO 16000 also deals with actual procedures for measurements of individual substances.

The following sections present an overview of the most common methods currently used to measure IAQ pollutants and ventilation parameters.

1.2 Measurement methods: IAQ pollutants

A wide range of substances is commonly found in any indoor environment, varying in physicochemical properties, toxicity level and originating sources. For each group of substances, there are usually at least a few different sampling and analytical methods. Sampling methods can be either active or passive, depending if they require the use of electricity or not. Active methods are those which employ pumping systems to collect air, while passive methods rely on diffusion and sorption processes to capture the pollutants of interest. The different measurement techniques also vary with regards to the

method used to obtain the results and their timescale. Online monitors can automatically record real-time results, in a timescale that can reach seconds, whereas passive samplers (and some active ones too) need a longer sampling period and, afterwards, the resulting samples must go through an extraction/analytical lab process in order to produce results with timescales varying from hours to several days or weeks. A measurement method might monitor several different substances at a time, or one single compound, depending on the sampling and analytical procedure. The selection of measurement method must always be carefully considered, taking into account the questions which must be answered, the timescale of interest, the level of accuracy required, the logistical capabilities of the project and the available budget.

The financial costs involved in performing each method can vary widely. Some commercial sensors are very affordable, e.g. the cheapest gases sensors can be purchased from €10 to €30, and some PM sensors cost less than €10. However, such cheap sensors have lower accuracy in measuring absolute values. Other portable sensors with better accuracy can be acquired up to €300. On the other hand, high-accuracy instruments used for professional applications, requiring a higher level of reliability and low detection limits, are generally quite costly, with prices reaching tens of thousands of euros. Passive methods are generally cheaper than active ones, but the costs involved in post-analysis of samples should also be taken into account.

The following sections of this review describe a wide range of measurement methods for different pollutants present in the indoor air. The first subsection deals with solid phase pollutants, most commonly known as particulate matter. The second subsection deals with gas phase pollutants. The third one also deals with gaseous pollutant, but more specifically, with radioactive gaseous pollutants. The fourth and final subsection deals with pollutants from biological origin.

1.2.1 Particulate matter (PM)

Several measurement methods are available to monitor different characteristics of particulate matter suspended in air, which can be used both in indoor and outdoor environments. The simplest methods involve the collection of particles in suitable collection media, but several options of sensors for continuous monitoring are commercially available.

PM measurement methods can be divided between those which measure solely concentration (concentration methods) and those capable of determining, along with the concentration, the particle size distribution (size distribution methods). The most common PM measurement methods are classified as concentration methods and size distribution methods in Figure 1.

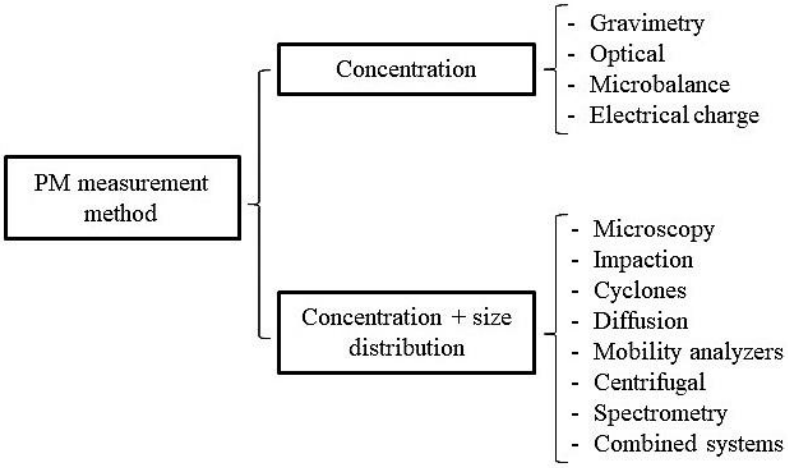

Figure 1 - Methods used for PM measurement (Adapted from Amaral et al., 2015).

1.2.1.1 Concentration measurement methods

The property of most common interest regarding PM pollution is the PM mass concentration, usually expressed in units of micrograms or milligrams per cubic meter of air. In some applications, the PM concentration may also be expressed in terms of number of particles or surface area (Vincent, 2007). The measuring principle for concentration measurements varies depending on the method, being either gravimetric, optical, microbalance or electrical charge (Amaral et al., 2015):

- **Gravimetric**: PM concentration is determined by simply weighing a filter before and after air sampling;
- **Optical**: A light beam is lit through the air sample, and the PM concentration is inferred by the difference between the intensity of the incident light and the intensity of the light detected after interaction with the particles present in the sample;
- **Microbalance**: PM is collected over the surface of an oscillatory microbalance element, altering the frequency of oscillation, from which the PM concentration is inferred;
- **Electrical charge**: PM concentration is determined by applying electrical charge to the particles.

More detailed information regarding the types of PM concentration measurement methods can be found in section A.1 of the appendix at the end of this document. Concentration measurement methods do not provide information on other PM properties, such as particle size or chemical composition, but it is possible to combine some of these methods with other techniques so as to provide more comprehensive PM characterization. Most of the devices used for PM concentration measurement are portable or have smaller versions to allow for easier logistics in the field. However, virtually all PM measurement methods require forced airflow sampling (i.e. pumping), hindering their use for personal sampling (although personal pumps are available and some methods are adapted in this sense).

1.2.1.2 Size distribution measurement methods

The second property of most common interest regarding PM is the size distribution of the particles, considering the different potential health impacts associated with different particle sizes (WHO, 2006). Size distribution methods measure the size of the particles, which can be represented by the diameter (mobility, aerodynamic or other equivalent diameters), along with the concentration of particles in each size range. The particle size is measured based on properties such as geometric size, inertia, mobility, electrical mobility and optical properties (Giechaskiel et al., 2014). In general, the measurement of particle size distribution is done by a combination of several techniques, involving charging of particles, particle size classification (impactors, cyclones or mobility classifiers) and detection (optical counters or electrometers) (Amaral et al., 2015). As shown in Figure 1, the methods used for PM size distribution measurement can be sub-divided into 8 categories:

- **Microscopy**: PM is collected on filters, which are then are properly treated to improve visibility and analyzed individually with a microscope;
- **Impaction**: PM is separated in two or more parcels of known particle size by using multiple impact stages/filters (impactors) or multiple orifices, then the PM concentration of each parcel is determined via gravimetry;
- **Cyclones**: Airflow is forced through a cyclone to select the particles' aerodynamic diameter. The larger particles deposit on the cyclone walls, while the smaller particles are collected by an after-filter;
- **Diffusion**: Specific for measurement of ultrafine PM, this method classifies particles by size based on their diffusion coefficients;

- **Mobility analyzers**: A well-defined charge distribution is applied to the PM via bipolar diffusion charging, and then the particles are classified with an electrostatic classifier.
- **Centrifugal**: PM is subjected to electrostatic and centrifugal forces simultaneously, and the particles are classified based on their mass-to-charge ratio;
- **Spectrometry**: Particle dimensions are measured by spectrometers based on particle mobility;
- **Combined systems**: Instruments that combine two or more of the aforementioned techniques.

Although there are exceptions, the devices used to determine PM size distribution are in general larger in size and relatively costly, rendering them less portable when compared to the devices performing solely PM concentration measurements. More details about the methods to measure PM size distribution are presented in section A.2 of the appendix at the end of this document.

1.2.2 Gaseous compounds

Gaseous pollutants in indoor environments may originate from a wide range of different sources. They might be inorganic or organic substances, which may exist permanently in gaseous form (e.g. CO, NO_2, NH_3, SO_2) or coexist in gaseous and liquid/aqueous forms, being released due to difference in vapor pressure. When planning an IAQ assessment, it is crucial to determine which measurement method must be used in order to cover all relevant gases and vapors. If inorganic gases and organic vapors occur simultaneously, then it is necessary to determine, prior to the assessment, which different sampling systems should be applied to cover all the substances of interest. One way of classifying the different measurement methods for gaseous substances is based on the type of air sampling process, as summarized in Figure 2 (Hebisch et al., 2009). Gases and vapors present in the indoor environment can be separated from the air by selective collection in/on an appropriate medium, i.e. they can be enriched in a collection medium (methods with enrichment) or, alternatively, the indoor air can be analyzed in its original state (methods without enrichment). In both cases, the analytical determination can be performed directly on location (e.g. using direct-reading monitors) or later in the laboratory. Generally, the same lab analytical methods (usually gas or liquid chromatography for organic gases and ion chromatography, spectrophotometry UV/Vis or IR spectroscopy for inorganic compounds) may be used for the analysis of samples collected with or without enrichment techniques.

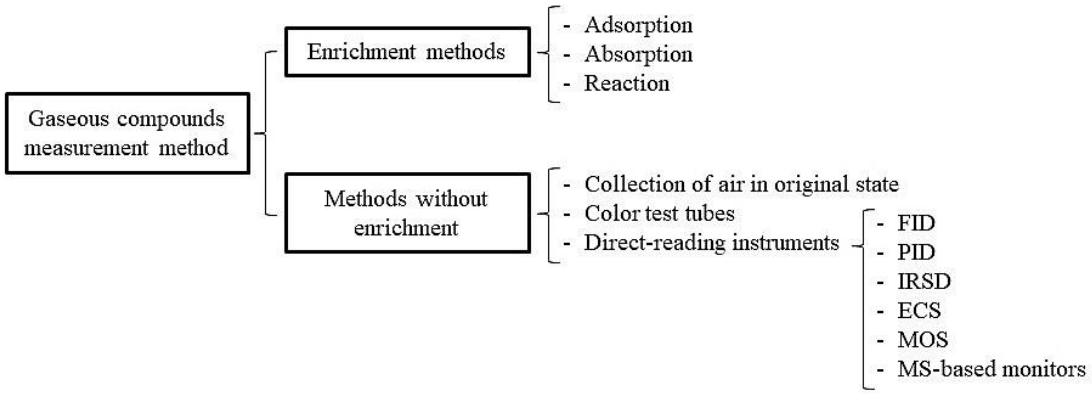

Figure 2 - Measurement methods for gases and vapors sampling in IAQ assessments (Adapted from Hebisch et al., 2009).

1.2.2.1 Enrichment methods

For sampling with enrichment, the substances to be determined can be adsorbed onto a solid collection phase, absorbed in a solution or can react with other substance(s) of the collection medium. After the collection period in situ, the samples need to be prepared for subsequent lab analysis (Hebisch et al., 2009). This type of sampling can be performed either actively (i.e. using a pump system for suction of

air) or passively (i.e. by means of diffusion), depending on the substance and type of assessment being performed. Both samplers and pumps may be personal or stationary. Active sampling is mostly used in applications which require higher time resolution (since pumping increases the airflow rate and consequently the volume of air sampled in the same period, compared to a passive sampler) and in which noise is not a concern (e.g. sampling in unoccupied spaces). For all enrichment methods, it is imperative to know the volume of air corresponding to each sample, as the gas concentration is determined by dividing the amount of analyte captured in the sampling medium by the total volume of air, which passed through such medium during the sampling period. An advantage of this type of sampling is that, in general, lower detection limits can be achieved. On the other hand, sampling with enrichment generates samples, which must be later transported and analyzed in lab for the determination of gas concentration. The chosen analytical method will depend on the substance(s) of interest and on the sampling type. As summarized in Figure 2, enrichments methods for gaseous pollutants measurement can be sub-divided in the following 3 categories:

- **Adsorption**: The substance(s) of interest is enriched by physically adsorbing onto a sampling surface;
- **Absorption**: The substance(s) of interest is enriched by being absorbed/dissolved by a sampling medium;
- **Reaction**: A chemical reaction between the substance of interest and the sampling medium allows the indirect measurement of the pollutant by measuring the reaction product(s).

More details about the methods used to measure gaseous compounds via enrichment can be found in section A.3 of the appendix at the end of this document.

1.2.2.2 Methods without enrichment

Measurement methods without enrichment analyze the air with no alterations to its original state. The different methods using this type of approach are thus distinguished by the analytical methods employed to obtain the results, i.e. to determine the concentration of the substance of interest in the air being sampled. The method can either deliver the result instantly on location (i.e. direct reading) or by analysis in laboratory after sample collection in a suitable vessel (Hebisch et al., 2009). As shown in Figure 2, gaseous compounds measurement methods without enrichment can be sub-divided into the categories:

- **Collection of air in its original state**: An air sample is collected, unaltered, using a gas storage vessel/flask, a cannister or a gas sample bag;
- **Color test tubes**: The presence and/or concentration of the substance of interest is determined by means of an instantaneous (on-site) reaction between the substance and the tube filling, which leads to a change in color;
- **Direct-reading instruments**: Automated devices which combine on-site/real-time air sampling and analysis; can be based on many different principles.

More detailed information regarding the non-enrichment measurement methods for gases and vapors (e.g. the different types of direct-reading instruments available) can be found in section A.4 of the appendix at the end of this document.

1.2.3 Radioactive gaseous pollutants

Radioactive gaseous pollution is measured in IAQ assessments in terms of radon concentration. Radon is a noble gas, occurring naturally in the atmosphere. The radon isotope ^{222}Rn is the main constituent

of indoor radon. This isotope is radioactive and can be found in large quantities in the soil. ^{222}Rn comes from radium disintegration, which in its turn comes from uranium disintegration. Radon can infiltrate inside a room through the building floor or it may exist in the construction materials (Namieśnik et al. 1992; Ciobanu et al., 2016). Radon is of great health concern: according to the EPA (2009), it is the second leading cause of lung cancer in the U.S., being estimated to be responsible for around 21,000 deaths.

Radon measurement techniques are classified based on three characteristics: (1) time resolution, (2) whether the technique measures ^{222}Rn or its decay products, and (3) radioactive detection of the type of emission (either alpha or beta particles or gamma radiation resulting from radioactive decay) (Baskaran, 2016).

1.2.3.1 Sampling of radon and/or its decay products

The time resolution of each measurement method is determined by the sampling technique, which may be accomplished by three main ways (EPA, 1990):

- **Grab sampling**: essentially is the taking of an instantaneous sample, i.e. the sampling takes place over a short period at a specific point in space. The analysis can be carried out in situ or in lab, after a specified period, using different techniques. Grab samples can be collected in flasks, in stainless steel containers or by absorption onto cold plates or activated charcoal.
- **Integrated sampling**: the sampling consists of an accumulation over time of physical quantities (e.g. number of nuclear traces, number of electrical charges) related to the decay of radon and/or its decay products. Analysis is carried out at the end of the accumulation period, providing a single average concentration value for that period. Generally, a period of at least one week is necessary to include a minimum number of daily variation cycles.
- **Continuous sampling**: consists of the continuous taking of multiple point samples (or of integrated samples in short periods) in closely spaced time intervals. Analysis is carried out simultaneously or only slightly later. This type of sampling allows the determination of patterns in the variation of concentration over the entire sampling time.

1.2.3.2 Measurement of radon concentration

Measurements of radon can be done either directly or indirectly (i.e. by measuring its progeny). Radon may be separated from its decay products during sampling, and the concentration of either or both can then be analytically determined. Separation is typically accomplished by allowing radon to diffuse through a passive barrier (e.g. foam rubber). The decay products, which rapidly adsorb onto solid surfaces, cannot pass through such barriers.

Most analytical methods for radon and its decay products actually measure emitted radiation instead of concentration of the targeted species, although the two are directly related in the absence of other radioactive material (EPA, 1990). In the decay of ^{222}Rn, three alpha-particles (from the decay of ^{222}Rn, ^{218}Po, ^{214}Po) and 2 beta-particles (from the decay of ^{214}Pb and ^{214}Bi) along with a number of gamma-ray lines are produced (Baskaran, 2016). The emission rate of any of these may be measured by the adequate instrumentation.

Although a large number of radon-measuring devices are available, the actual analysis of radon and/or its decay products is typically done using a scintillation phosphor mounted on a photomultiplier, an ionization chamber, a thermoluminescent dosimeter (TLD) or a visual or automatic image processing method (EPA, 1990). The 6 following methods are the most utilized for measuring radon:

- **Scintillation flasks**: Consist of plates (for samples of radon collected on filters) and/or cells (for gaseous and liquid samples) which are coated with silver-activated zinc sulfide phosphor and a transparent surface (viewing window), to which a photomultiplier tube is coupled. When an alpha particle strikes the phosphor, a flash of light is produced;
- **Online detectors**: Devices used for automated and continuous radon monitoring, usually based on pulse ionization chambers, scintillation detectors or silicon PIN diodes;
- **Electrets**: Electrically charged Teflon discs act as electric field sources and sensors. When an alpha particle decays in the detector chamber, the air is ionized and the total charge on the electret decreases;
- **Thermoluminescent dosimeter (TLD)**: Ionizing radiation is determined by measuring the intensity of light emitted from a crystal (thermoluminescent in response to ionizing radiation) when it is heated;
- **Track detectors**: Dosimeters based on solid-state nuclear track detectors; a piece of appropriate plastic material is exposed to the air sample, and when the alpha particles strike the surface of the plastic, microscopic gouge marks are made;
- **Solid media collection**: Radon is captured onto activated charcoal by adsorption; the resulting sample can then be analyzed via different methods.

More details about the different radon measurement methods can be found in section A.5 of the appendix at the end of this document.

1.2.4 Biological pollutants

Biological contaminants are, or are produced by, living beings. Bioaerosols consist of aerosols originated biologically such as metabolites, toxins or fragments of microorganisms, ubiquitously present in indoor environments, including bacteria, viruses, mold, animal-originated material (e.g. dander, hair, insects' body parts, saliva, urine and feces particles), house dust, mites and pollen. Many of these biological contaminants can be inhaled, potentially triggering allergic reactions, infectious and respiratory diseases and even cancer (Kim et al., 2018).

1.2.4.1 Sampling of bioaerosols

The assessment of biological contaminants in indoor air starts with the sampling procedure. Any method for separating particles from air (e.g. sedimentation, filtration, inertial impaction, impingement in liquids, thermal and electrostatic precipitation) can be applied to collect such contaminants (Kim et al., 2018). Bioaerosol samples are usually collected into liquid media or on solid filters as a way of keeping the viability of the biological components (i.e. ability to multiply when provided the appropriate conditions) (Lehtinen et al., 2013). After the suspended particles have been collected in a suitable medium, the total number of cells present can then be counted and identified. The most common methods used to collect bioaerosol samples in IAQ studies are:

- **Impaction plates**: Same principle applied to common PM sampling for gravimetry, but employing plates of solid nutrient media instead of common filters;
- **Rotorod**: Rotating slit or slit-to-agar sampler, in which a large plate of nutrient medium is placed on a turntable beneath a stationary slit inlet;
- **Electrostatic precipitator**: Incoming bioaerosol is electrically charged at the inlet and then subjected to a precipitating electric field. Precipitated particles are collected onto agar plates;
- **Impingers**: Particles are collected in an appropriate liquid media.

More information regarding the different methods for bioaerosol sampling can be found in section A.6 of the appendix at the end of this document.

1.2.4.2 Analysis of bioaerosol samples

Once the biological particles have been adequately collected from the air, using one of the methods mentioned in section 1.2.4.1, they can be counted, identified and analyzed by another set of different methods. The choice among the possible method depends on the type of bioaerosol to be analyzed, on the sampling method utilized and on what information is intended to be extracted. The 4 most common analytical methods used to characterize bioaerosol samples are the following:

- **Culture**: The viable bioaerosol is cultured in the appropriate nutrient medium after sampling, and later the organisms are identified by their distinctive individual colonies;
- **Microscopy and optical methods**: Bioaerosol particles are identified by their morphology using a microscope and/or by applying fluorescent probes to stain and determine specific bacterial groups or species in the sample;
- **Polymerase chain reaction (PCR)**: Used to detect and quantify microorganisms (viable and non-viable) by copying and amplifying specific regions of the genome for analyses.
- **Bioassays and immunological tests**: The concentration or potency of a substance is determined by its effect on living cells or tissues. Specifically in immunological tests, the presence of specific bioaerosols is assessed by measuring the levels of antibodies in the blood serum.

More information regarding the different methods for analysis of bioaerosol samples can be found in section A.7 of the appendix at the end of this document.

1.3 Measurement methods: Ventilation rates

Ventilation is the inward/outward transport of air to/from any enclosed space, by natural or mechanical means, intentional or unintentional (i.e. infiltration or exfiltration due to leakage), besides the air exchange between different rooms or zones inside the same space. Methods currently used for measuring ventilation rates either involve direct flow rate measurements at vent holes and ductwork combined with pressurization tests, or a tracer gas dilution/dispersion test. The first type is mostly used when the assessed building presents high airtightness and the airflows occur mainly mechanically in ductwork (Persily, 2016). In these cases, ventilation is almost entirely restricted to that generated by the mechanical system, making its measurement very straightforward. In buildings with low airtightness and/or using natural ventilation, a tracer gas test is a more appropriate method to measure the total (i.e. intentional plus unintentional) air change rate (Sherman, 1989; Persily, 2016). Finally, the ventilation rate due to leakage can be estimated using a pressurization test.

1.3.1 Tracer gas tests

Air that enters an indoor environment comes from a combination of infiltration and intentional ventilation. While the measurement of air flow rate through identifiable openings is possible by direct flow measurement, it is not practical to measure air flow through every gap and crack in the room envelope, or to measure air flow rate through more than one or two purpose provided openings at a time. It is possible to overcome this problem by the use of a tracer gas (Liddament, 1996). Tracer gas methods are used to determine the air movement across a boundary during normal operating conditions, i.e. with normal occupancy. The boundary could be the building shell, a zone within the building or a single room (McWilliams, 2003). Since tracer gas tests can be carried out in occupied buildings, during normal

occupants' activity, this type of testing is more convenient and accurate, considering the large effect occupancy has on a building's air change rate.

In a tracer gas test, the air is marked with an easily identifiable gas so that its bulk movement can be traced. By monitoring the injection rate and concentration of the tracer, the air change rate can be inferred. A good tracer gas presents the following basic desirable characteristics (Sherman, 1990):

- **Non-reactivity**: as conservation will be used to infer airflow, the tracer gas should not react chemically or physically with any part of the system being assessed;
- **Insensibility**: the presence of the tracer should not affect the processes being studied, i.e. the air flow;
- **Uniqueness**: the tracer must be able to be recognized from all other constituents of air, i.e. the tracer should ideally not be a normal constituent of indoor or outdoor air;
- **Measurability**: the true concentration and all injected tracer gas must be quantifiable through some sort of instrumentation.

Gases typically used as tracers include nitrous oxide (N_2O), sulphur hexafluoride (SF_6) and various perfluorocarbon tracers (PFTs). Although present in the atmosphere, carbon dioxide (CO_2), either as generated by occupants or released from cylinders, is also used (Liddament, 1996). The method for monitoring the tracer gas concentration will depend on the substance employed as tracer and on the intended accuracy and timescale of the results (see Section 1.2.2 for an overview of the available methods for monitoring gaseous compounds).

The basic principle involved in the tracer gas test is that of conservation of mass of both air and tracer gas as expressed in Equation 1, which is applicable to any gas diluted in the indoor air (Sherman, 1990).

$$V\frac{dC}{dt} = G(t) + Q(t)PC_{out} - Q(t)C(t) - L(t) \quad (1)$$

where V is the room volume (m^3), $C(t)$ is the indoor concentration of tracer gas (kg m^{-3}), C_{out} is the outdoor concentration of tracer gas (kg m^{-3}), $G(t)$ is the tracer gas emission rate (kg h^{-1}) and $Q(t)$ is the airflow through the room (m^3 h^{-1}). P is a dimensionless coefficient that accounts for the loss of tracer on entering the building due to the combined effects of particle filtration, gaseous air cleaning and losses on surfaces (P = 1 if there are no losses and P = 0 if none of the outdoor tracer enters the interior space). $L(t)$ is the rate at which the tracer is removed within the building by deposition, filtration, air cleaning, and chemical reaction.

It is important to notice that the expression of Equation 1 is only valid under a single-zone assumption. In ventilation measurements, a perfect zone is homogenous (the tracer or contaminant concentration is sufficiently uniform throughout the zone to be characterized by a single value), isolated (only communicates with the outside, an area whose concentration of tracer gas or contaminant is unaffected by the zone) and perfectly mixed (instantaneous mixing of incoming tracer gas or contaminant). Thus, tracer gas has to be well mixed in the test space, which is usually experimentally accomplished by using small mixing fans. Multiple sampling points can also be used to verify that the concentration is uniform across the zone (McWilliams, 2003). Additionally, the tracer concentration in the assessed space must be sufficiently low as to not alter the air density (Sagheby et al., 2012). Tracer techniques are then used to determine the flow from a test zone to/from the outside (but not within the zone or inter-zone). The vast majority of ventilation measurements involve a single-tracer gas deployed in a single zone. This technique is very useful for buildings that may be treated as a single zone (e.g. big box store) and for more complex buildings with isolatable sub-sections. Buildings in general are not single-zone systems

(e.g. dwellings without forced air HVAC), meaning that concentrations differ between zones, in which case a multi-zone mass balance equation must be used to account for the effects of ventilation and inter-zone airflows, as well as other transport phenomena (Sherman, 1990; Persily, 2016).
All tracer gas methods rely on the solution of the continuity equation to infer the ventilation from measurements of the concentrations and injected tracer flow rate. The continuity equation can be solved directly for the ventilation as follows (assuming the simplest case, P = 1, L = 0):

$$Q(t) = \frac{G(t) - V\frac{dC}{dt}}{C(t) - C_{out}} \quad (2)$$

The most common definition of air change rate (q) is the one of air flow per unit volume (h^{-1}), calculated as follows:

$$q = \frac{Q}{V} \quad (3)$$

It is not possible to solve Equation 1 on an instantaneous basis to find the ventilation, because of measurement problems, including mixing issues. Therefore, it is necessary to use time-series data to reduce the uncertainties to make the analysis possible. The exact analytical technique (regression, integral or averaging techniques) for inverting the measured data to find the ventilation depends on both the experimental technique used, the assumption made about the system, and the quantity of interest (Sherman, 1990).

Experimentally, the tracer gas method is conducted using one of the following techniques, depending on specific application:

- Concentration decay;
- Constant concentration;
- Constant emission;
- Long term average;
- Multi tracer analysis.

All these methods assume that the tracer gas is not present in the outdoor air and that all the tracer gas in the indoor air is originated from the study's source.

1.3.1.1 Concentration decay

The concentration decay method is the most straightforward and least disruptive one, requiring the smallest amount of equipment. It is used to obtain air exchange rates over short periods in small single zone buildings. In this method, a quantity of tracer gas is released into the assessed room and thoroughly mixed with the indoor air. The amount of tracer released is calculated on the basis of the maximum start concentration desired and should be released rapidly. If the air change rate is constant and no tracer gas is supplied (injection rate equal zero) to the room during the measurement period, the tracer gas concentration (*C(t)*) will decay exponentially, with the decay rate equal to the air change rate of the space in units of inverse time:

$$C(t) = C_0 e^{-qt} \quad (4)$$

Where C_0 is the concentration of tracer gas initially injected in the room, q is the air change rate and t is the total measurement period. Rearranging for the air change rate:

$$q = \frac{\ln C_0 - \ln C(t)}{t} \quad (5)$$

A straight line should be obtained when plotting the natural logarithm of tracer concentration against time, with the line's gradient being the air change rate in the room. If an approximately straight line is not obtained, then the room air cannot be considered sufficiently mixed, making the results invalid (Roulet and Vandaele, 1991; Liddament, 1996). Besides, the single-zone nature of the methods means that conducting a tracer gas decay test in only a single room of a building will not generally provide an accurate air change rate for that space or for the whole building. The problem with such testing is that the tracer gas mass balance of the room is impacted by airflows to and from other spaces, not just the outdoors. Therefore, calculating the tracer gas decay rate for a single room employs a tracer gas mass balance equation that ignores the impact of these other zones on the concentration in the space being considered. While a tracer gas decay test can be carried out in a single room in a multizone building, the result is not the air change rate. Therefore, the other tracer gas methods are usually more adequate than the decay method (Persily, 2016).

1.3.1.2 Constant concentration

The constant concentration method is used for continuous air change rate measurements in one or more zones, being particularly useful for conducting analyses in occupied buildings (Roulet and Vandaele, 1991; Liddament, 1996). It is a steady state technique in which an active control system is used to change the emission rate of tracer gas in order to maintain its concentration in the indoor air fixed at some target level (C_T). Thus, the mass balance equation is reduced to:

$$q = \frac{G(t)}{V C_T} \quad (6)$$

The air change rate is directly proportional to the tracer gas emission rate required to keep the indoor concentration constant. Injection and sampling must take place independently in each room. Injection takes place only in rooms in which fresh unseeded air enters and dilutes the tracer gas. For this reason, air flow between rooms is not detected. This method is advantageous because it enables accurate long-term measurements of average air change rates in situations where the air change varies and also because it registers such variations in detail. However, the necessary instrumentation is usually bulky and the test is difficult and time consuming to perform, with high costs involved, since there is the need for a gas concentration monitor and for some sort of tracer emission rate controller (Liddament, 1996; McWilliams, 2003).

1.3.1.3 Constant emission

A simplification of the constant concentration approach is constant tracer gas emission. The constant emission method is used for longer-term or continuous air change rate measurements in single zones. This method consists in injecting tracer gas at a constant rate into the assessed room and monitoring the concentration response. Assuming the injection rate (G) is constant, the single-zone mass balance (Equation 1) can be integrated and expressed as follows:

$$q = \frac{G}{V}\overline{\left(\frac{1}{C}\right)} - \frac{\ln\left({}^{C_2}/_{C_1}\right)}{t_2 - t_1} \quad (7)$$

Where C_1 and C_2 are the tracer gas concentrations at times t_1 and t_2, respectively, and C is the average concentration during the measurement period. If the airflow rate is constant, the tracer gas concentration will eventually reach steady state ($C_1 = C_2 = C_S$), and Equation 7 simplifies as follows:

$$q = \frac{G}{VC_S} \quad (8)$$

Considering that in the constant injection method, the tracer gas must be emitted continuously into the room throughout the whole measurement period, the cost and amount of tracer gas needed might be a concern. Thus, the use of a monitor to measure inexpensive tracer gas or that is capable of detecting and quantifying low concentrations should be considered if this method is applied (Roulet and Vandaele, 1991; Liddament, 1996).

An example of a simple constant emission method is presented by Sandberg and Sundberg (1987), in which the air change rate is estimated based on the emission of metabolic carbon dioxide in an occupied space, in which the occupants are considered a “tracer source” of constant emission rate. CO_2 concentration is monitored at fixed time intervals using inexpensive detector tubes from which the flow rate is evaluated.

1.3.1.4 Long term average

Tracer gas methods often employ active emitting and sampling techniques, i.e. techniques using pumps and electricity, which can be expensive and unpractical to transport to the site. Decay and constant emission tests can be easily adapted to passive techniques, i.e. techniques based on diffusion and absorption/adsorption processes for emission and sampling of tracer gas, respectively. Passive tracer gas techniques are commonly used to estimate the average air change rate into a building over an extended period of time, measuring long term tracer gas concentration averages. It is the most adequate approach to be used in occupied dwellings, offices or other large buildings. Test periods can vary from a few hours to several months. If more than one test gas is used, it is also possible to use this method to analyze air flow between zones (multi-tracer gas methods). This method is inexpensive and unobtrusive. It may easily be conducted by relatively unskilled operators. Analysis of samples is always undertaken off-site in a laboratory (Liddament, 1996; McWilliams, 2003).

Currently, passive techniques are based on the use of volatile perfluorocarbon tracers (PFTs) which may be detected in the air in very low concentrations. The tracer gas is emitted over a period of time within the test space and an exposed sampling tube is used to adsorb the gas over the pre-determined time period. The air change rate is calculated from the amount of gas emitted and collected by the emission and sampling tubes respectively. The sample tubes are taken to a lab where the tracer gas is desorbed and analyzed by means of gas chromatography (McWilliams, 2003).

The source typically consists of a small amount of volatile liquid PFT tracer placed in an emission tube (approximately 5 mm diameter and 30 mm length). The liquid evaporates into the test space at a rate strongly dependent on ambient air temperature. Usually the emission rate can be reasonably accurately inferred from records of the average daily indoor air temperature. Ideally, one emission and one detection tube should be used for each 50 m^3 of space. The sample tube is of similar dimension to the source tube, containing an adequate gas adsorbent such as activated charcoal in a porous mesh (Liddament, 1996). For detailed descriptions of passive methods for gaseous compounds monitoring, see Section 1.2.2.

The passive approach is only accurate if the air change rate remains reasonably constant over a period of time. This approach provides insufficient weighting to peaks in air change, such as those associated with airing, door opening or transient high infiltration driving forces, i.e. transient changes in conditions cannot be detected. Arguably, if the objective of the measurement is to estimate the average pollutant dose received by occupants in a space, resulting from a constant emitting pollutant source (e.g.

furnishings and fittings), this method provides a reliable result, in the same timescale as the pollution concentration measurements. However, it can ignore the benefit of ventilation for transient pollutant emissions (e.g. airing for washing and cooking) and underestimate ventilation related thermal losses (Liddament, 1996).

1.3.1.5 Multi-tracer analysis

The multi-tracer approach is used to determine the flow rate between zones (or rooms within a zone) and to identify cross contamination problems. It is important to keep in mind that the use of multi-tracers greatly amplifies the complexity of the tracer gas test, restricting this approach to the specialist field. Three different approaches are usually applied:

- **Multi-tracer decay**: The building is divided into separate zones, with a unique gas being emitted into each one. After mixing, the fans are switched off to prevent artificial air movement between rooms. The concentration decay in each zone, relevant to the specific tracer gas released into that zone is used to calculate a room air change rate. By combining the air change value for each room in a flow balance equation, the flow rate between each may be evaluated. In practice, a single tracer gas analyzer is used to undertake all measurements; this is normally based on a gas chromatograph that can separate each of the gases in a sample prior to analysis. Sometimes gas samples may be collected in bottles for subsequent laboratory analysis.
- **Multi-tracer constant concentration**: This approach enables the air flow pattern to be continuously observed. A unique tracer gas is emitted into each zone, and between zones, maintained in the zone at a constant concentration. The total air flow rate out of each zone (to adjacent zones or outside) is calculated from the tracer gas injection rate. By combining the air flow rates for each zone, the individual flow rates between zones may be determined.
- **Multi-tracer passive sampling**: The average air flow rate between zones may be determined using passive emission and sampling. Each zone is seeded with a different PFT gas and air flow rate between zones is calculated using the flow balancing approach of the previous methods (Sateri et al., 1989; Shinohara et al., 2010).

1.3.2 Pressurization tests

Pressurization testing is used to measure the airtightness, i.e. to determine the air leakage across a given boundary or envelope such as a building shell. Based on this measurement, the in- or exfiltration due to leakage can be estimated. The boundary can also be a portion of a building, such as a room or a zone. This type of test is highly important, considering that excessive air leakage can interfere with the design performance, energy and IAQ related, of ventilation systems. Fan pressurization is the technique most widely used to assess envelope leakage (McWilliams, 2003), and can be classified into two categories, steady and unsteady technique, according to the way in which they approach the measurement. The steady technique does it by establishing a steady state pressure difference across the envelope and recording the induced leakage rate of airflow through the envelope, whereas the unsteady technique, or dynamic air tightness measurement technique, analyses the pressure-flow correlation when the building envelope is exposed to varying pressure (Cooper et al., 2014).

1.3.2.1 Blower door test

In this method, the airtightness of a building as a whole is measured at pressures in excess of those that are naturally developed, but not so great that openings are artificially distorted by the pressurization process itself. A large fan is set up in an opening in the envelope (usually a door, hence the usual

denomination “blower door test”) and then used to create and maintain a pressure difference between the inside and outside of the building (normally between 20 Pa and 70 Pa). The flow rate through the fan is measured, usually with a calibrated orifice plate or nozzle. The test can be performed as one single point, normally at 50 Pa, or as multiple points over a range of induced pressures. If a multiple points test is performed, a curve can be fit, correlating the induced pressures and the flows through the fan, from which the total leakage can be derived (McWilliams, 2003). The maximum volume of space that may be pressurized is governed by the overall airtightness of the building and the available fan capacity (multiple fans can be used together). To determine airtightness in large, multizone buildings, it is possible to apply the blower door test in a floor-by-floor approach, isolating each floor of a building in order to do a fan pressurization test on each floor in succession. The adjacent floors are also pressurized so that there is no air leakage between floors. The sum of the leakages measured on each floor equals the total leakage for the building.

It is sometimes possible to use the building’s own mechanical ventilation system to carry out a pressurization test, in a method known as the air handler pressurization method (Kim et al, 2013). This method uses the air handlers (with outdoor air intakes) to create a pressure difference across the building envelope. The building leakage can be calculated when the outdoor airflow is measured with tracer gas or orifice flow plates (McWilliams, 2003).

1.3.2.2 Component airtightness testing

Airtightness testing of specific building components is necessary to check compliance with relevant standards and to check the quality of fitting. Standards verification is usually undertaken in the laboratory whereas the quality of fitting must be undertaken as an in situ test. Several methods of component testing are available, including (Liddament, 1996):

- **Reductive sealing**: The building pressurization test is repeated as components are systematically sealed with tape. This enables the in situ leakage characteristics of individual components to be assessed by deduction.
- **Pressure testing individual components**: A ‘pressure’ collection chamber is placed over the component and a standard pressurization test is performed. For improved accuracy, the test room may be pressurized to the same value as the collection chamber. This approach may be used for both laboratory and in situ testing.
- **Multi-fan techniques**: Pressurization testing using more than one fan may be used to infer leakage of specific components in situ, e.g. individual walls or between rooms, enabling the air leakage across specific walls including party walls, internal room walls and façade walls to be determined. An accurate method of estimating air leakage through party walls or facades is the pressure equalization or guarded pressurization technique, using two pressurization fans (Furbringer et al., 1988).
- **Combined pressure testing and tracer gas analysis**: Component leakage by combined pressure testing and tracer gas analysis can be applied when other methods prove to be difficult. An example includes evaluating ceiling leakage. The space above the ceiling may be too leaky for pressurization, while joints for reductive sealing are often inaccessible. Tracer gas is applied to one of the spaces (e.g. roof space) at approximate constant concentration. If weather conditions remain constant, this should be achievable by supplying gas at constant emission and waiting for an equilibrium concentration to be reached. The occupied space is depressurized to a suitable pressure. The ratio between occupied zone leakage and that of the ceiling/roof void interface is given by the ratio of roof void tracer gas concentration and the concentration in the dwelling.

1.3.2.3 Pulse technique

In common fan pressurization tests, an induced pressure of 50Pa is considered a standard for measuring the airtightness, because it is much higher than the level of pressure change caused by the wind and buoyancy effect (typically around 4Pa) so as to be able to neglect the errors caused by such effects in the test. However, this method presents some disadvantages related to errors associated with the extrapolation of the observed results to conditions of normal pressure and to disturbances to the indoor conditions caused by the high volumes of air that need to be dislocated during the test. The problem can be reduced if induced pressures are lower, but the lower the pressure becomes, the less accurate the measurement is, due to being close to the pressure generated by buoyancy and wind (McWiliams, 2003).

An alternative is the use of unsteady techniques, in which the required information is determined indirectly by measuring the pressure response to a known disturbance (Carey and Etheridge, 2001). This method is able to accurately generate a known air volume change to the building enclosure which makes the sources of error introduced by this technique less than the steady technique. The key part of unsteady techniques is to pressurize the assessed space to the desired pressure level by supplying or extracting air using pre-compressed or outdoor air. Then the pressure is varied by devices like a piston or left to decay naturally. During the pressure decay over a certain period of time, the correlation between the air leakage rate and pressure difference across the building envelope is recorded. Several methods can be used for the pressurization process in the unsteady technique, and the most common is pulse pressurization (Cooper et al., 2014).

The low pressure nozzle pulse technique, as described by Cooper et al. (2014), generates an instant pressure pulse in the assessed space by releasing compressed air into it via nozzle. The pressure pulse is left to decay naturally. This decay is monitored and used then to determine the building air tightness. This technique requires a minimal volume change (< 0.01%) to generate a pulse pressure in the order of 4 Pa.

1.3.3 Air flow patterns and turbulence

The measurement of flow velocity and air turbulence throughout a space use methods based on qualitative visualization approaches and/or quantitative anemometric techniques. There are a number of visualization techniques for the qualitative assessment of air flow patterns and turbulence. Particle Image Velocimetry (PIV) techniques are based on developing a two dimensional sheet of bright light which is directed across a section of the room. Smoke or small bubbles are then used to highlight the flow pattern. These may be photographed or recorded using a video camera (Liddament, 1996).

Quantitative evaluation of spatial air velocity and turbulence distribution is mostly given by anemometry. Anemometers must be very sensitive and are usually based on “hot wire” techniques. A resistance wire (the anemometer element) is heated while the current through the wire is monitored. Air speed fluctuations rapidly change the temperature and, therefore, the resistance of the wire. The resultant current change provides a measure of instantaneous air speed (turbulence). Hot wire anemometers are mostly used in test chamber studies where traverses are made across sections of the chamber to build up a complete pattern of air flow (Liddament, 1996). Although this method can be used in the field as well, hot wire sensors are very fragile. The use of acoustic sensors is an appropriate alternative (Van Schaik et al., 2010).

1.3.4 Air flow through ventilation openings

Flow measurements through individual ventilation openings are needed to ensure that the air flow rate and flow direction conforms to design requirements. Common applications include the monitoring of the air flow through passive ventilation stacks, the monitoring the performance of mechanical ventilation systems and the measurement of naturally or mechanically driven air flow through air inlets and outlets. It is important to notice that, by these methods, only the air flow through specific openings is measured, thus not providing the total air change rate, which includes air movement through infiltration openings. If the assessed structure is leaky, then only a fraction of the total air flow through the building (the mechanical, i.e. the intentional one) will be measured (Liddament, 1996).

Techniques are based on standard air flow measuring instrumentation, including:

- **Orifice plates and nozzles**: These are calibrated devices that are fitted in series with ductwork and have a known air flow rate versus pressure drop relationship. The flow rate is determined by measuring the pressure drop across the device. Long straight lengths of duct are needed both upstream and downstream of the system while the constriction imposed by the orifice or nozzle can impede flow.
- **Pitot static traverses**: Air velocity at a specific location is commonly measured using a pitot static tube. Duct air flow can be measured by inserting the tube into a prepared opening and measuring the air speed at several depths across the cross-section of the tube. The total flow rate is determined by integrating the results.
- **Anemometry**: Several types of anemometer are used to measure the flow rate through ducts and openings, including vane anemometers and hot wire anemometers. The vane anemometer is commonly used in servicing and commissioning since it is robust and is satisfactory for measuring relatively high air flow velocities.
- **Compensation method**: Vane anemometers can disrupt or impede the flow of air through an opening thus introducing error, especially if the flow rate is low. The compensation method uses a device (the flow finder) specifically designed to overcome this problem and to monitor the direction and rate of air flow through an opening. The flow finder is an active device containing its own calibrated fan, which is operable for flows up to 225 m^3/h. The funnel opening of the flow finder is placed over the opening through which the flow rate is to be measured forming an airtight seal. The internal fan speed is adjusted until there is zero pressure difference across the opening. The resultant flow rate through the device is thus equivalent to the undisturbed flow rate through the opening, i.e. the pressure drop caused by the own device is compensated. The impact of the measurement system on the rate of flow is therefore substantially minimized (Caillou, 2018).
- **Tracer gas injection**: Tracer gas injections can be used to measure air flow rates in ducts. The tracer gas is injected into the duct at a constant known rate. The flow rate of air through the duct is proportional to the tracer concentration measured in the duct.

The European standard EN 16211-2015 provides detailed descriptions of these air flow measurement methods and specifies the appropriateness of the different techniques for specific types of ventholes.

1.3.5 Leakage detection

Leakage detection is an important complementary measurement for the assessment of total ventilation. These measurements help to identify and locate sources of air leakage in buildings and building components. Leaks may be detected by fan pressurizing a building or an individual room and observing

the movement of smoke emitted from a smoke stick or puffer. This approach is very effective and easy to undertake. The smoke source is gently moved in the vicinity of potential sources of leaks during the course of the test. Leak locating and sealing may be simultaneously undertaken while conducting a routine pressurization test. However, air-tightness retrofit should only be undertaken in conjunction with the installation of a purpose provided (natural or mechanical) ventilation system to ensure the adequacy of ventilation. Alternatively, pressurization may be a purely qualitative action, undertaken to develop sufficient pressure to induce a strong flow of smoke through leakage openings. Ideally, the building or room should be pressurized so that the flow of smoke, from inside to outside, can be clearly identified. Thermography can also be used for leaks detection. Testing may be undertaken from either the inside or outside of the building. For indoor testing, the building or room is depressurized to allow the inflow of cold outdoor air. An interior thermographic scan will indicate the location of fabric leaks. Alternatively, scanning can be undertaken externally, in which case the building is pressurized and the sources of exfiltrating hot air are located. Either way, adequate experience is needed to interpret thermography results. For example, the presence of (ventilated) cavities in the construction can seriously affect the surface temperature. Other methods, which can be used for leak detection involve sound sources and microphones, although such methods are unlikely to be of value for routine investigations (Liddament, 1996).

1.3.6 Scale models

Scale models are useful in the study of ventilation in a building where the distribution of openings is well known. Flume models provide a method by which air movement, pollutant transport and temperature distribution can be predicted using scale models inserted in a water flume. In this type of measurement, a 1:20 to 1:100 scale model of the building is constructed using a transparent material. This simplified model keeps all the essential features controlling the ventilation process, including envelope openings and openings between individual rooms. This model is completely immersed in a glass sided water channel such that the pattern of flow can be observed using a video camera. Buoyancy induced flow (density stratification) is represented by sources of dense salt solution to which a tracer dye is added. The model and video camera are inverted so that the salt solution appears to rise. Cooling is similarly simulated using a less dense alcohol/water mixture. Quantitative measurements of flow velocities are made by measuring samples of salt solution taken from within the model. Automated image processing of the video film allow the measurement of dye intensities to give the instantaneous temperature distribution throughout the building, while flow velocities can be measured by particle tracking. Mixing and diffusion processes may also be quantified. Limitations of this type of experiment include the considerable laboratory space needed for its development and the impossibility to represent infiltration or other openings resulting from construction technique or poor site practice, unknown by definition (Liddament, 1996).

Other type of testing involving scale models is the wind tunnel testing. This type of test is used in order to get accurate information on wind pressure distribution over the outer walls of a building. For that, pressure taps connected via plastic tubing are placed on each face of a model of the assessed building, so that the pressure distribution can be determined. The model needs to be placed on a turntable so that pressure can be analyzed for the complete spectrum of wind direction. Wind speed is determined with respect to a specific datum height, normally corresponding to the height of the building. Upwind roughness is normally developed using an array of cubic blocks (Liddament, 1996). Smoke combined with photography is often used to provide visualization of the flow regime. A large wind tunnel is necessary to accurately represent the lower levels of the Earth’s turbulent boundary layer and to accommodate reasonably sized scale models of the building and its surroundings. Typical minimum scale for analysis of wind pressure distribution is 1:50, which means that large lab space is also necessary for such testing.

1.4 Recommendations

From the information laid out in the previous sections, it can be seen that there is a wide range of different methods available to measure a variety of IAQ indicators, each method with its own working principles and practical limitations. Consequently, choosing the most adequate method for a specific measurement campaign can prove to be a not-so-simple task. The same characteristic of a method can be considered an advantage or a disadvantage depending on the objectives of the specific assessment to be performed. These goals can be very diverse, e.g. IAQ assessment for health and safety checks, ventilation rate measurement for energy performance assessments, and research about the effect of a specific intervention. This means that the methods selection must be done on a case-to-case basis, taking into account the unique needs, intentions and logistic capabilities related to each planned IAQ assessment. Therefore, the key to select the most appropriate measurement methods to carry out a given IAQ assessment is to design in advance a detailed and thorough action plan, in which the specific objectives and intended outputs are very well-defined and clearly outlined.

Although the measurement method selection should ultimately be done on a case-to-case basis, general recommendations can be given based on overall goals common to groups of similar studies. Some of these general recommendations are described below:

- **Official surveys**: If the goal of the assessment is to verify compliance to guidelines or, more importantly, to legislation, or if the results are intended to have any type of official character, the measurement methods should be the standard ones, complying to the ISO 16000 norm and to other relevant official standards, e.g. NAAQS (EPA, 2018), if applicable. If the survey is of academic or purely exploratory nature, alternative methods can be applied;
- **Comprehensiveness x focus**: Ideally, an IAQ assessment would measure simultaneously all types of contaminants and ventilation parameters. However, due to time constraints, logistics and/or costs, it is understandable that the research team restrict the focus to specific compounds/indicators relevant to the research aim (e.g. exposure study, source identification, remediation, building structure assessment, ventilation system evaluation). Nevertheless, it is important that every assessment measures at least one IAQ indicator (e.g. TVOC, formaldehyde, $PM_{2.5}$) and one ventilation indicator (e.g. average air change rate, CO_2 concentration), as both concepts are intrinsically connected;
- **Time scale**: If the assessment intends to observe variations over short-term periods (e.g. pollutant levels variation due to point events, air change rate variation over working hours), the measurement methods chosen should be based on active techniques with automatic data storage (low-cost sensors may be used if deeper characterization of the pollutants species is not needed). If the intention is to observe the average situation over longer periods or if it is enough to characterize the indoor air by a limited number of samples, simpler methods can be employed (e.g. passive sampling, gravimetry, grab samples);
- **Time-series data**: Series of data measured with fine time intervals, which are analyzed by comparison with mathematical white, grey or black box models of the measured system to optimize parameters of the mathematical model can in some cases mean that a smaller number of sensors can be used to create a reliable representation of the measured reality (see IEA EBC Annex 58 and Annex 71 reports);
- **Spatial scale**: If the intention is to assess many different sites (e.g. large-scale regional surveys) or if the assessed site presents a considerable spatial heterogenicity (e.g. multi-zone buildings), it is advisable to select lower-cost measurement methods for specific IAQ indicators and invest in simultaneous sampling at the different sites/points of the heterogeneous site;

- **Occupancy**: If occupants will be present at the site during the course of the assessment (e.g. workplace or home survey), the selected measurement methods should not cause excessive disturbance to the environment (e.g. noise, smell, clutter). Passive methods and/or small, silent sensors tend to be preferred in such cases.

Due to the complex interconnections between building properties, energy use, occupancy and IAQ, the reporting of a case study should always include a general description of the building and its context, in order to understand the significance of the reported IAQ data. Next, all relevant components such as building envelope, interior finishing, mechanical systems and ventilation should be discussed. In addition to the measurement plan and measurement equipment, the boundary conditions during the measurements need to be clearly described. Ideally, the report also provides the reader with a short conclusions and 'lessons learned' section.

Chapter 2: Field test 1 - The Passys Cell

This chapter describes experiments in a Passys Cell, performed as a common exercise in the context of Subtask 5 of Annex 68. The two experiments consisted of the monitoring and modeling of a single-zone building, both based on the Passys Cell in Limelette, Belgium. The latter was also the basis of the common exercise in Subtask 3. The overall goal of both experiments was to simulate contaminant concentration, relative humidity and temperature in the building and to perform energetic analyis.

The following sections describe in detail the experiment and its outcomes, followed by the contributed reports of the 2 participating institutions.

2.1 The Passys Cell Experiment

2.1.1 Context

This section describes the experiment that is the subject of the common exercise in subtask 5 of annex 68. It is the first in a series that is conceived as a set of consecutive experiments with increasing complexity. The goal is to validate the collective ability of the annex participants to model and reliably predict the indoor air quality in a real building, from a very simple to a more complex and realistic situation.

The tiered experiments are

- A simple 1 room outdoor testbox with an isothermal diffusion source of 1 pollutant
- A studio with a number of selected materials as sources and varying T and RH as well as solar radiation
- An occupied single family dwelling

Some additional and intermediate experiments have also been set up and are reported below.

The subsequent sections describe the first experiment. The test cell is discussed first, followed by a description of the experiment and the modeling assignment. Annex participants that have a similar test cell available were also invited to perform repeated tests or perform variations on the experiment that address specific annex related issues, but unfortunately, due to practical limitations, this proved not to be feasible.

2.1.2 Test setup

The test is executed in a PASSYS cell, situated at the Limelette test site of the BBRI. The cell is freestanding, oriented more or less along the north/south axis (slightly rotated to the west).

A description of the envelope and dimensions of the cell can be found in Wouters and Vandaele (1990). The test cell used in this experiment is the last test cell in the original test setup described in the document that has been mounted on a mechanism that allows it to be rotated. During the test, it was in the original orientation (service room pointing north).

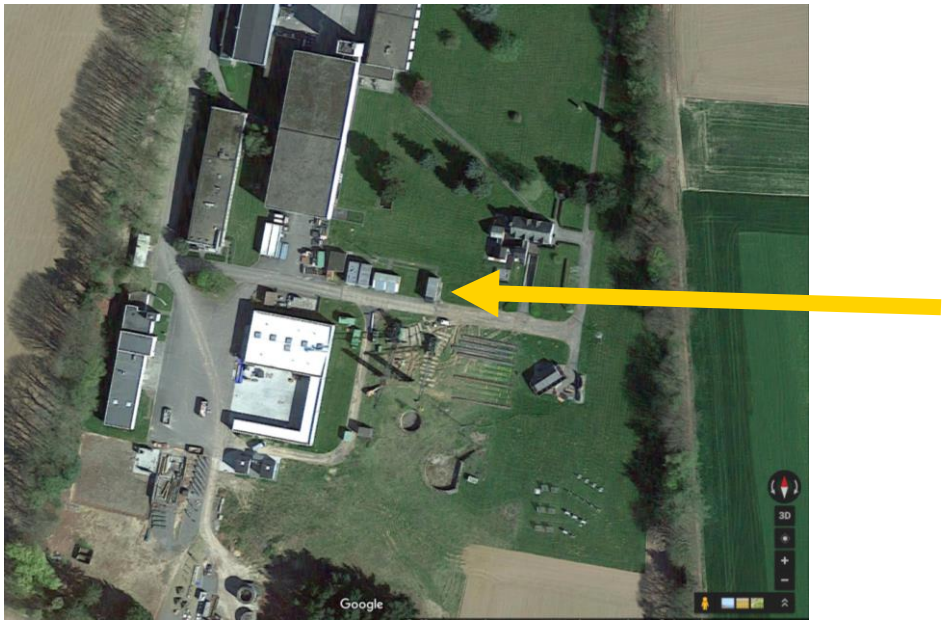

Figure 3 - The PASSYS cell

12 cm of additional EPS insulation and 1 mm of stainless steel cladding have been added to the interior walls, reducing the internal space to 2.46*2.46*4.86 m. The interior walls have all been painted with an unknown acrylic paint in the early 2000's. The cell is fitted with a 'calibration' test wall, that has exactly the same composition as the other walls and no windows.

2.1.3 Experiment description

A concreteplex panel has been fitted in the door between the test room and the service room. Flexible PU foam (2 mm) and clips make sure the panel fitting is airtight.

A 80 mm circular opening with a axial supply fan have been installed at 15 cm above the floor, a 150 mm flexible exhaust duct was installed at 15 cm from the top of the door panel. The exhaust duct exits the service room through a service opening at the front of the test cell, at ceiling height.

During the experiment, the small window in the front of the test cell (to the service room) is opened for fresh air supply. The test room is pressurized by the supply fan. The airtightness of the test room is 1.7 ACH50.

A mixing fan (http://www.bestron.com/en/dft27w.html?___from_store=en) is placed in the south-east corner of the test room, a concrete block with a height of 50 cm is sitting at 1,20 m from the south wall, on which the pollutant source, a glass bottle with freely diffusing Hexane, is placed.

The test room is heated to 27.5 °C by a single electric convector (http://www.produktinfo.conrad.com/datenblaetter/550000-574999/560075-an-01-ml-Konvektor_de_en_fr_nl.pdf) situated at 0.5 m from the south wall. The convector is controlled by a thermostat with external temperature probe and with a 0.1°C dead band. The external probe is positioned at the exact midpoint of the room (1.25 m height, at 1.25m from the side walls and 2.35m from the south wall.

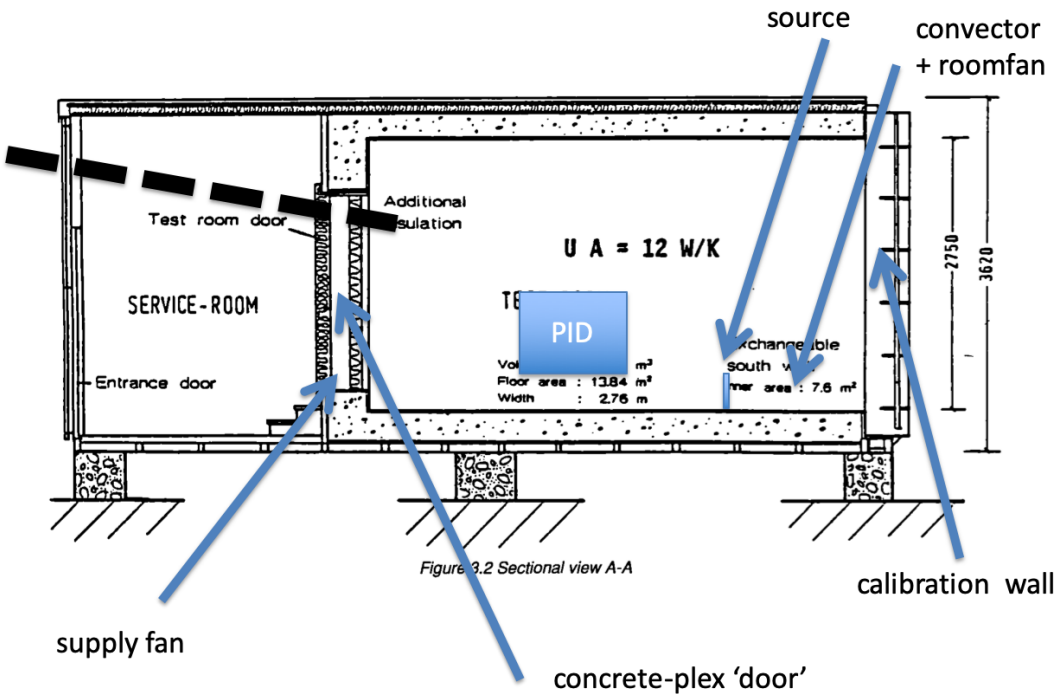

Figure 4 - Test and service rooms.

Temperatures are measured at 4 heights at 2 locations in the test room: 1 at the mid-point (where the thermostat probe is), and one at 40 cm from the south west corner. They are measured at 60 cm intervals starting at 35 cm from the ceiling using Onset HOBO U12-012 loggers (http://www.onsetcomp.com/products/data-loggers/u12-012).

The Hexane concentration in measured at the mid-point (where the thermostat probe is), with a Rosemount NGA2000 FID.

The test protocol is as follows:

Table 1 - Test protocol.

Phase	Time	Supply Ventilation rate	Source condition
1. Startup	Until steady state	1 ACH	Open
2. High	Day 1 00:00:00 (11/04)	1 ACH	Open
3. Low	Day 2 17:20:00	0.1 ACH	Open
4. High	Day 8 14:12:00	1 ACH	Open

2.1.4 Modeling exercise

The modeling exercise is very simple: model the concentration of Hexane in test cell during the experiment, using your own preferred modeling approach and tools. The results can be compared to the measurement data, available upon request.

2.2 CONTAM/TRNSYS Simulation

2.2.1 Context

A 1-zone building (based on the Passys Cell of Limelette) with a constant source of contaminant was modelled using CONTAM/TRNSYS to evaluate the contaminant concentration. The contaminant modelled in this simulation was the alkane hexane. The energy simulation tool TRNSYS was coupled with CONTAM to perform, in addition, an energetic analysis.

2.2.2 Building model and boundary conditions

Figures 5 and 6 show details of the models implemented in TRNSYS and in CONTAM, respectively. The building simulation tool TRNSYS works through types that represent components. Type 98 (here referred to as *"PassysCell_Limelette_coupled"*) allows the exchange of information between TRNSYS and CONTAM. CONTAM is able to calculate the air flows between the different zones of a building or between the ambient and the building (i.e. infiltration, ventilation, etc.), but is not able to perform any energetic analysis (e.g. calculation of temperature of the zone). TRNSYS receives as input the airflows from CONTAM and gives as output to CONTAM the temperatures of the zones. Type 9 (here referred to as *"Experimental_data"*) reads the experimental weather data from an external file.

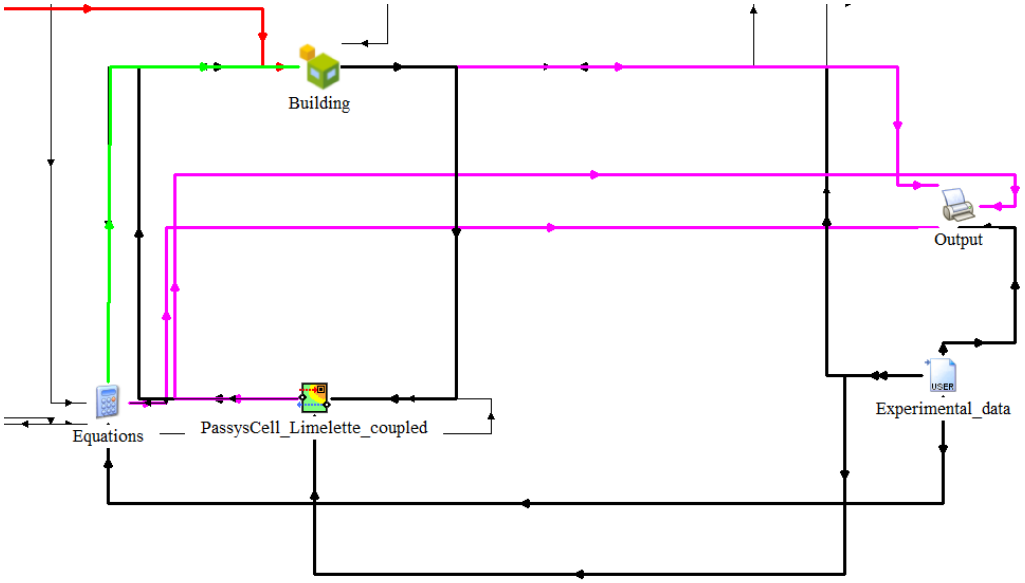

Figure 5 - Detail of the TRNSYS model

The main parameters of the performed simulations were:

- **Volume of building**: 29.4 m³
- **Climate**: Limelette (Belgium) experimental data
- **Simulation period**: 1 week (11 April - 17 April, experimental data available) with timestep of 1 minute
- **Air change rate**: variable, balanced ventilation system
- **Contaminant**: hexane
- **Contaminant emission rate**: constant, 490 ng min^{-1} (this value was chosen to enable the comparison with the results of Jos van Schijndel (Tue) and Marc Abadie (ULR))
- **Contaminant ambient concentration**: 0 ppm (constant)

- **Contaminant initial concentration in the building**: 0 ppm
- **Heating system**: electric radiator (convective part: 40%) controlled with the operative temperature (Tsetpoint of 27.5°C)
- Neither windows nor infiltration were considered

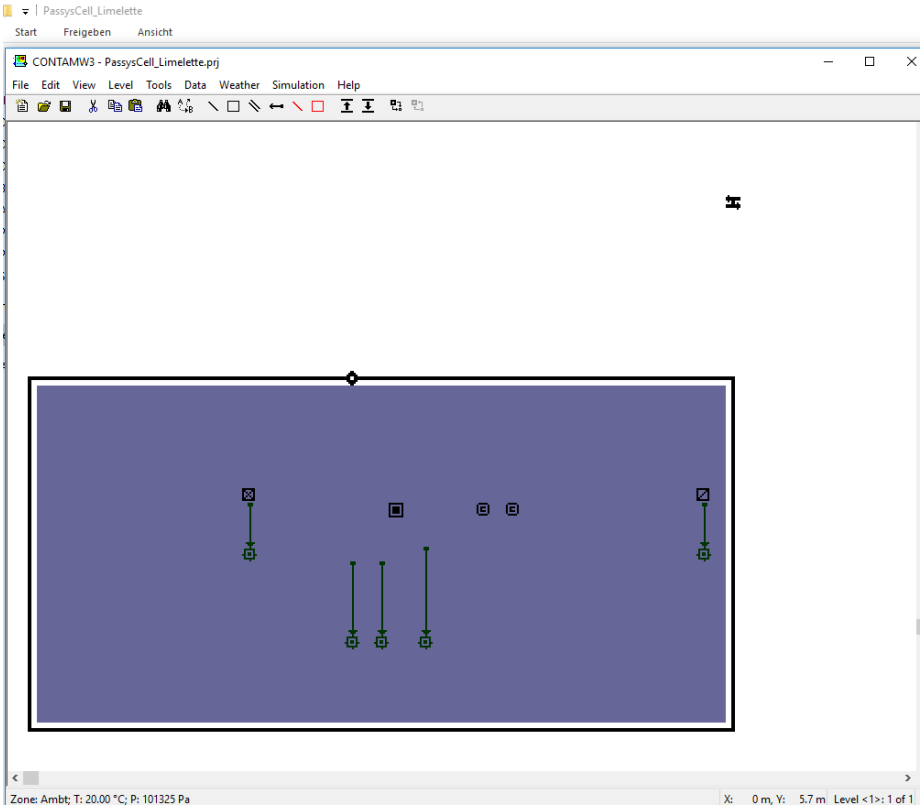

Figure 6 - Detail of the CONTAM model

2.2.3 Hexane concentration

A constant source of contaminant (hexane) and a variable air change rate of the building were considered in the simulation in order to study the influence of the ventilation rate on the hexane concentration. Figure 7 shows the concentration of hexane in the building. The evolution of the hexane concentration in the room is plausible and the stationary concentrations are comparable with the results obtained by the colleague Marc Abadie.

2.2.4 Energetic analysis

Figure 8 shows the ambient temperature and relative humidity used in the simulation. In TRNSYS, a type is used to read these information (experimental data from the site of Limelette). The experimental data were available just for the week from 11 April to 17 April and, consequently, only this period was simulated.

Figure 9 shows the temperatures of the building and how the air change rate influences also the distribution of the heating power to the convective and radiative node. The control of the heating equipment works perfectly because the operative temperature of the building is always equal to 27.5°C and the radiative part of the total power is always 60%. The heating power has always a convective part of 40%, but the convective temperature is lower than the radiative temperature just when the air

change rate is 1; when the air change rate is 0.1, the convective temperature is higher than the radiative temperature.

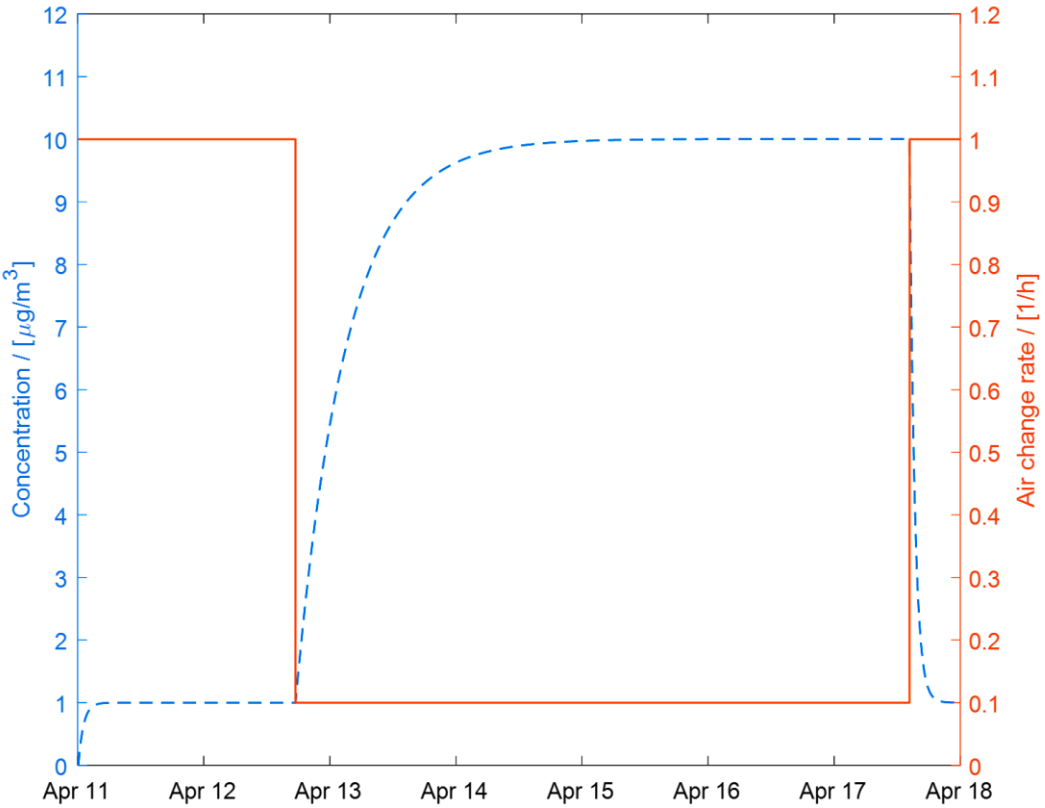

Figure 7 - Hexane concentration (left axis) and air change rate (right axis) versus time.

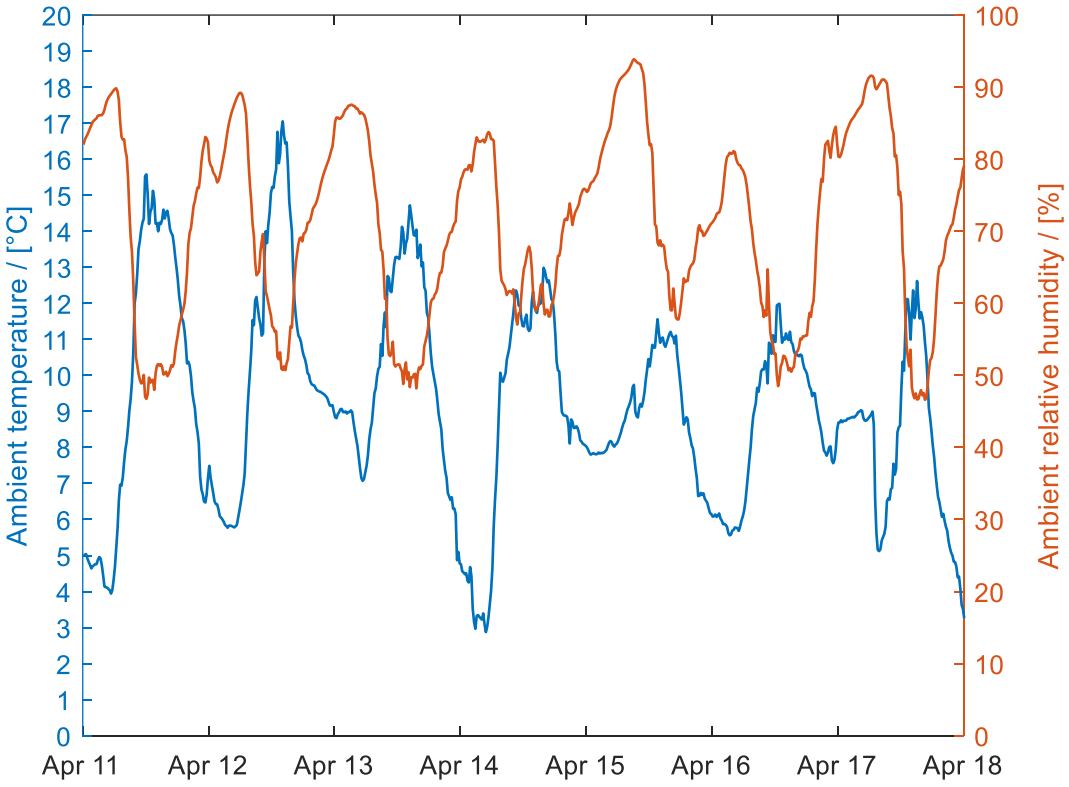

Figure 8 - External temperature (left axis) and relative humidity (right axis).

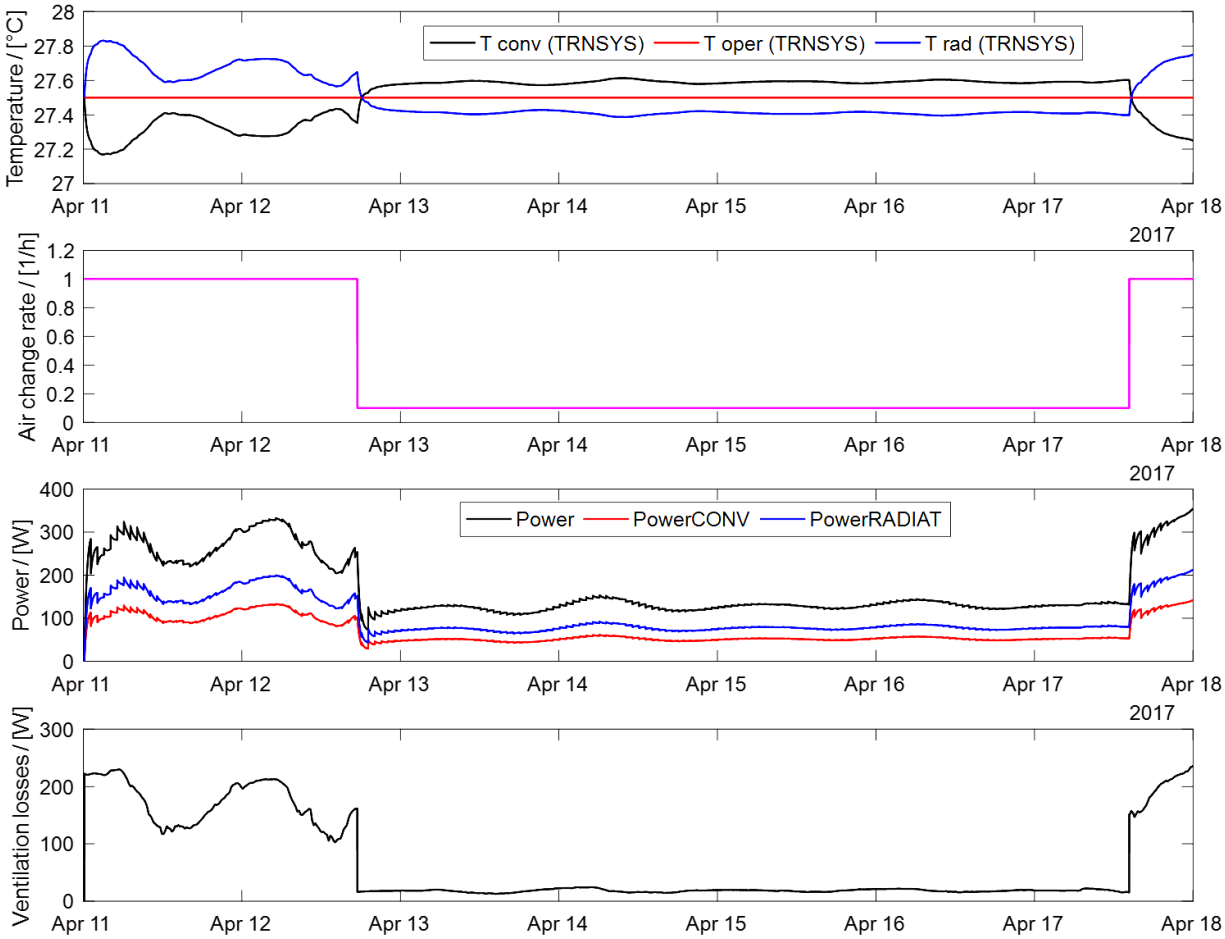

Figure 9 - Temperature of the building (top), air change rate, power of electric radiator and ventilation losses (bottom) versus time.

Table **2** shows the energetic balance of the building for the simulated period (1 week). The infiltration losses and the solar gains are put to zero.

Table 2 - Energetic balance of the building.

Transmission losses [kWh]	17.8
Ventilation Losses [kWh]	11.1
Infiltration losses [kWh]	/
Solar gains [kWh]	/
Heating demand [kWh]	**28.9**

2.3 TRNSYS/CONTAM vs. MATLAB/Simulink

2.3.1 Context

This is a variation on the actual experiment. A 1-zone building (based on the Passys Cell of Limelette) with a constant source of contaminant was modelled in CONTAM/TRNSYS and in MATLAB/Simulink to compare the results of contaminant concentration, energy demand, relative humidity and temperatures. The contaminant chosen to be modelled in this exercise was CO_2.

2.3.2 Building model and boundary conditions

Figure 10 shows a sketch of the building model.

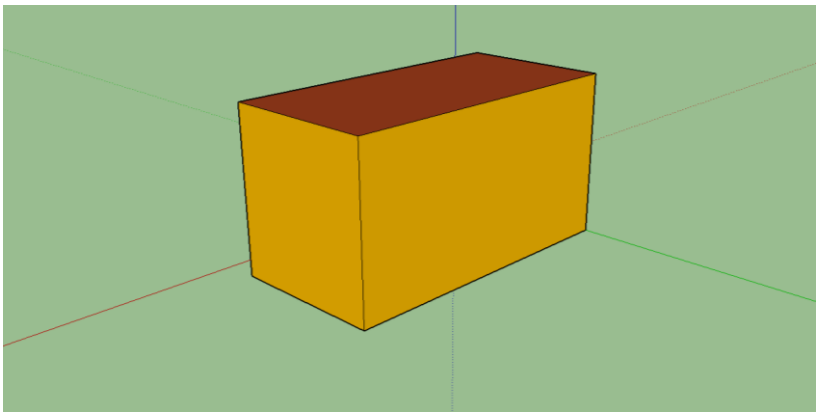

Figure 10 - Sketch of the building model.

The main parameters of the simulations were:

- **Volume of building**: 29.4 m^3
- **Climate**: Innsbruck
- **Simulation period**: 6 Months (January-June) with timestep of 10 minutes
- **Air change rate**: constant, 1 h^{-1}, balanced ventilation system
- **Contaminant**: CO_2
- **Contaminant emission rate:** constant, 1 person with low activity (7.08 mg s^{-1})
- **Internal gain**: 1 person (constant sensible gain of 60 W – 100% to convective node – and constant latent gain of 0.08 kg h^{-1})
- **Contaminant ambient concentration**: constant, 400 ppm
- **Contaminant initial concentration in the building**: 0 ppm
- **Heating system**: electric radiator controlled with the operative temperature (Tsetpoint of 22°C) and convective part of 100%
- Neither windows nor infiltration were considered

Table **3** shows the construction of the building model. In both building models, the external (h_e) and internal (h_i) heat transfer coefficients were equal to 17.7 W m^{-2} K^{-1} and 3.05 W m^{-2} K^{-1}, respectively (standard values in TRNSYS). Based on information about the Limelette Passys Cell, the floor is not directly connected to the ground temperature, but in both tools (Trnsys and Simulink) it is connected to the ambient temperature.

Table 3 - Walls construction of the building model.

Floor/Ceiling	Thickness [m]	Conductivity [W m^{-1} K^{-1}]	Resistance [m^2 K W^{-1}]	U - value* [W m^{-2} K^{-1}]
Pavement	0.02	0.13	0.15	**2.77**
Sand Pipes	0.04	0.6	0.07	
Concrete	0.2	1.6	0.13	
Inside Plaster	0.015	1.0	0.02	
Walls	Thickness [m]	Conductivivty [W m^{-1} K^{-1}]	Resistance [m^2 K W^{-1}]	U - value* [W m^{-2} K^{-1}]
Inside Plaster	0.01	1.0	0.01	**0.14**
Brick	0.3	0.7	0.43	
Insulation	0.2	0.03	6.67	
Outside Plaster	0.015	1.0	0.02	

* without convective heat transfer coefficient

2.3.3 CO_2 concentration comparison

A constant source of CO_2 (emission rate: 7.08 mg s^{-1}) is considered in the zone with an initial concentration of 0 ppm and constant ambient concentration of 400 ppm. Figure 11 shows that the comparison between the two tools is good and both provide results comparable with the analytical results. The stationary value of CO_2 concentration oscillates around the value of 870 ppm in both tools. The slight difference between the two tools could be caused by the calculation of pressure and density of air in the zone.

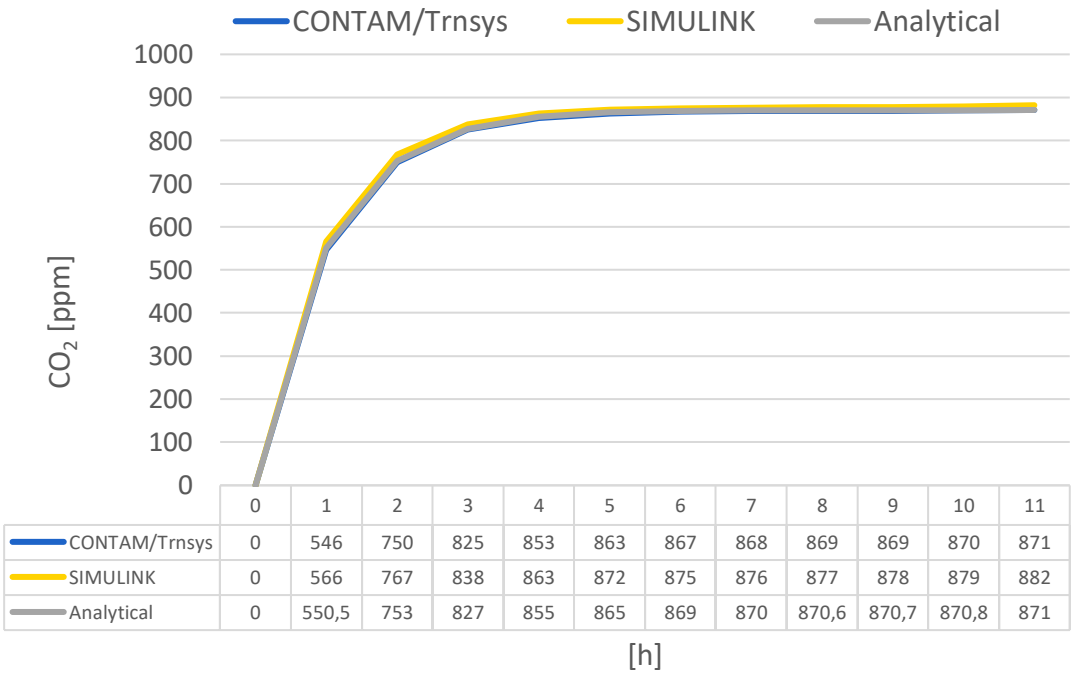

	0	1	2	3	4	5	6	7	8	9	10	11
CONTAM/Trnsys	0	546	750	825	853	863	867	868	869	869	870	871
SIMULINK	0	566	767	838	863	872	875	876	877	878	879	882
Analytical	0	550,5	753	827	855	865	869	870	870,6	870,7	870,8	871

Figure 11 - Transitory concentration of CO_2 in the zone.

2.3.4 Heating demand comparison

An electric radiator was modelled in Simulink and in TRNSYS to keep constant the operative temperature of the room (setpoint of 22°C). The thermal power of the electric radiator has a convective

part of 100%. In TRNSYS the electric radiator was modelled as an internal gain controlled with an iterative feedback controller (maximum heating power of 2500 W).

The heating demand of both tools (Table **4**) is in the same range (ca 3500 kWh). The deviation of the heating demand between the two tools is acceptable (+3% in TRNSYS). Infiltration losses and solar gains are always zero as expected. TRNSYS overestimates the transmission losses (+5%), while ventilation losses are slightly higher in Simulink (+3%).

Table 4 - Energetic balance of the zone for both tools.

	CONTAM/Trnsys	**Simulink**
Transmission losses [kWh]	3169	3020
Ventilation Losses [kWh]	680	704
Infiltration losses [kWh]	0	0
Internal gains [kWh]	260.6	260.6
Solar gains [kWh]	0	0
Heating demand [kWh]	**3587**	**3483**

The heating system in both tools is controlled according to the operative temperature with a setpoint of 22°C. The control of the heating system works properly (Figure 12) in both tools with a constant operative temperature of 22°C; the evolution of the radiative and convective temperature in TRNSYS and Simulink is comparable, even if the convective temperature is slightly higher in TRNSYS.

Simulink gives lower convective temperature (compared to TRNSYS) and higher ventilation losses. An explanation of this discrepancy can be given if the evolution of pressure (Figure 13) and density (Figure 14) are analyzed. TRNSYS uses a constant value of air density (1.15 kg m^{-3}) and the pressure of the room is slightly higher than the ambient pressure (because of the ventilation system implemented in CONTAM). In Simulink the pressure of air in the zone is higher and leads to a higher value of density (calculated in the model and not constant) in comparison to TRNSYS; this could be an explanation of the higher ventilation losses of Simulink, even if the convective temperature is slightly higher in TRNSYS.

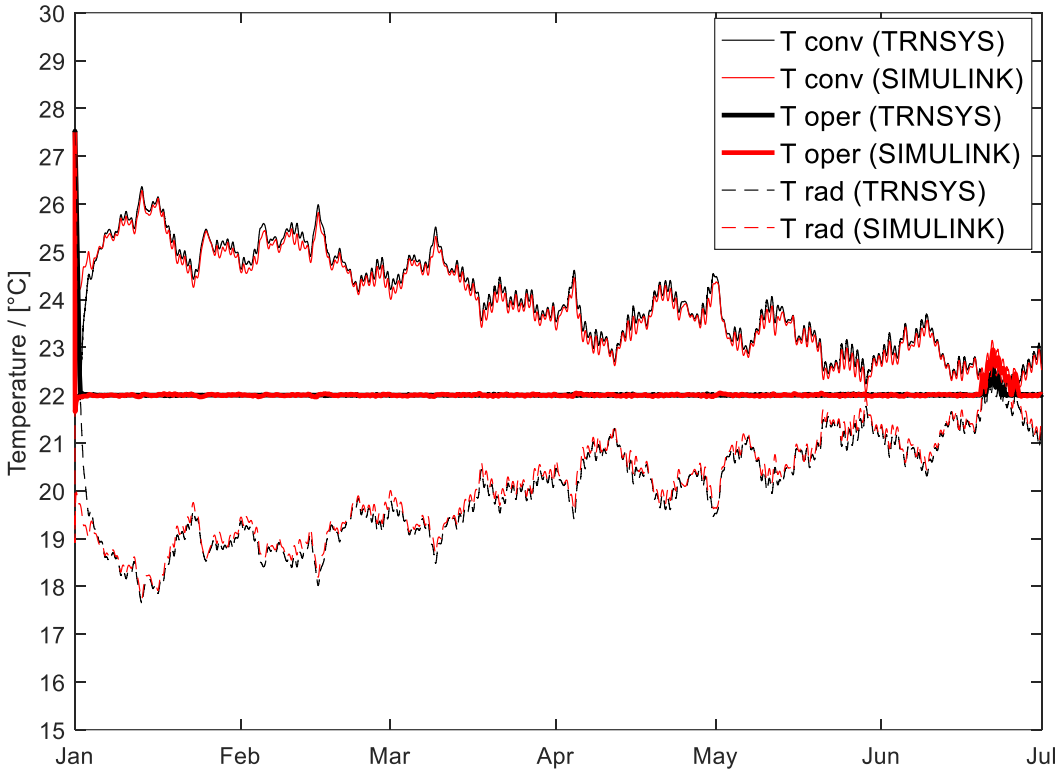

Figure 12 - Temperatures evolution for both tools.

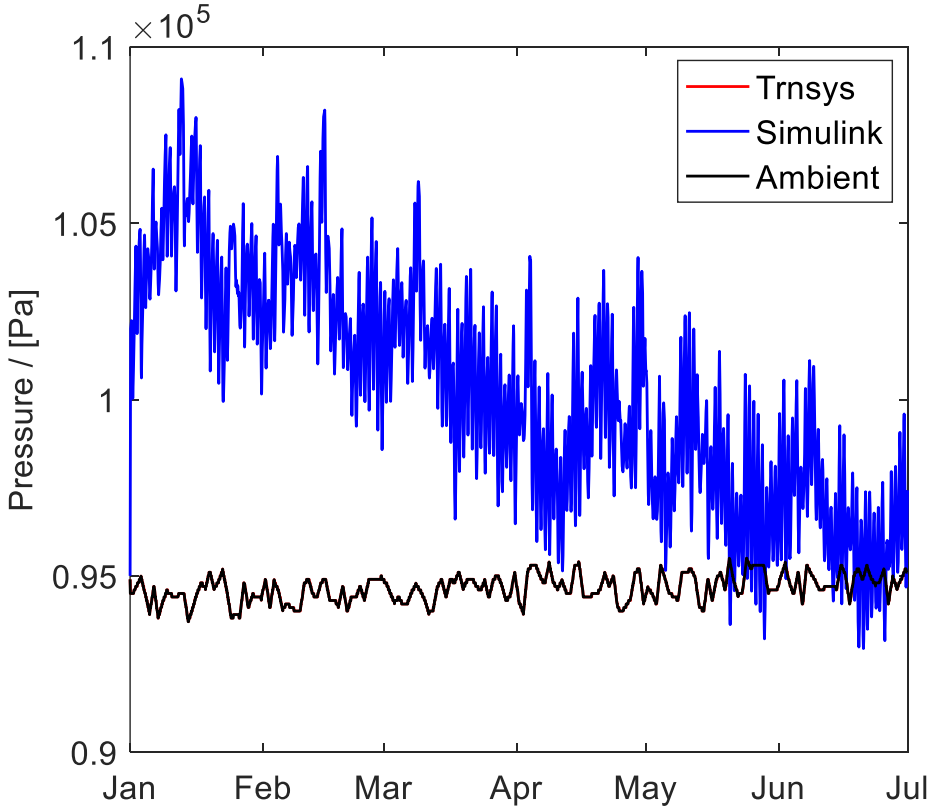

Figure 13 - Building pressure in TRNSYS and Simulink.

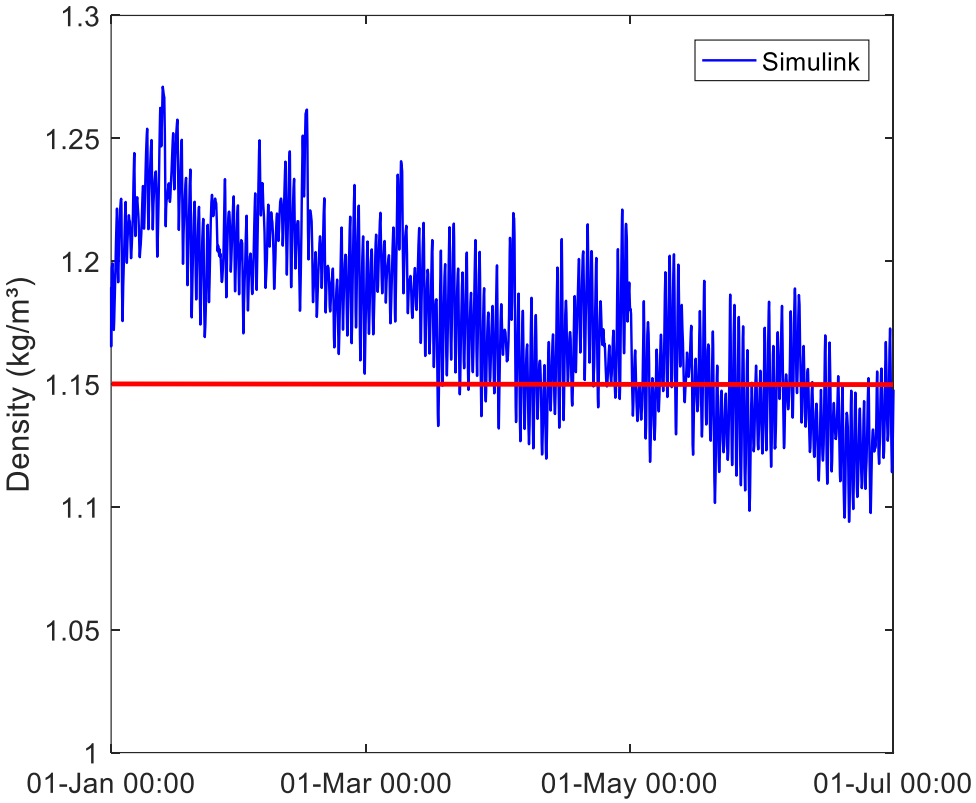

Figure 14 - Density of air in the building in Simulink and in TRNSYS (red line).

2.3.5 Relative humidity comparison

A constant latent gain of 0.08 kg h^{-1} (due to the presence of 1 person) and a balanced ventilation rate (1 h^{-1}) make the comparison of the relative humidity between the two tools interesting. In Simulink the hygrothermal walls model was considered, while in TRNSYS two humidity models could be chosen:

- **Simple Humidity model**: the transmission/storage of water through the walls of the building is not considered
- **Complex humidity model**:the hygrothermal properties of the walls are also considered

Four simulations were performed in TRNSYS to investigate the influence on the relative humidity of the humidity model and the comparison with the hygrothermal model used in SIMULINK (Figure 15).

The factor “C” represents the multiplication factor of the moisture capacitance of the thermal zone to take into account (approximately) the moisture capacitance of walls. The complex humidity model needs the definition of 6 parameters (Table **5**), which are difficult to evaluate in case of different walls construction. The comparison of relative humidity between the two tools is good.

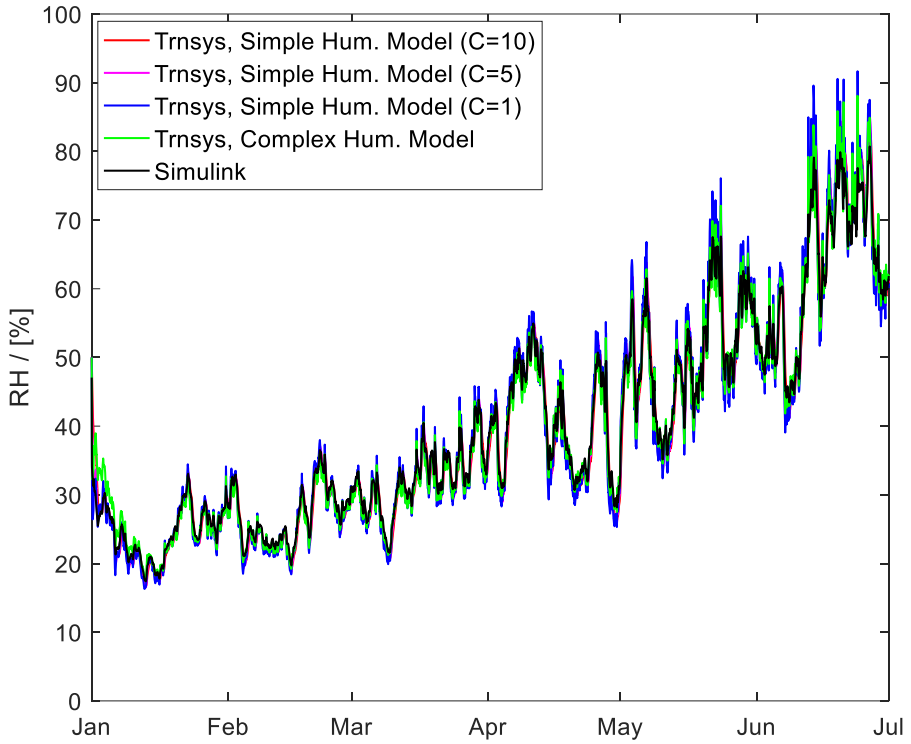

Figure 15 - Relative humidity of the building.

Table 5 - Coefficients implemented in TRNSYS for the definition of the complex humidity model.

Buffer storage model in TRNSYS - Coefficients		
	Surface buffer storage	**Deep buffer storage**
Gradient of sorptive isothermal line	0.02	1
Mass	240	8.5
Exchange coefficient	10	45

2.3.6 Open questions and possible next steps

The building model, used for this first comparison between TRNSYS/CONTAM and Simulink, is very simple and some parameters should be changed in order to make the comparison more realistic. The most important aspects to consider are:

- Distribution of the heating power and internal gain to the zone: At the moment, the convective part is 100% in both tools, but this value is not realistic and must be changed. A value of 100% was chosen because the definition of a radiative part caused unclear behaviour of the building model in TRNSYS. This unclear behavior should be further investigated to allow comparisons with a more realistic convective / radiative fraction.
- Implementation of an infiltration model.
- Implementation of a window to take into account solar gains.

Chapter 3: Field test 2 - The Dormitory experiment

This chapter describes a second field experiment executed in Belgium as part of Subtask 5 of Annex 68: the Dormitory experiment. The goal of this experiment was to test products emissions in field conditions, by monitoring the volatile organic compounds (VOCs) room concentration both before and after the placement of emitting products (sources), and to observe the influence of temperature and relative humidity over the products emissions under field conditions.

The following sections describe in detail the setup and outcomes of the experiment.

3.1 Context

This section describes the so-called Dormitory Experiment, an exercise developed in subtask 5 of Annex 68 between February and March 2018. It comprises a field test carried out in one dormitory suite located in VITO premises (Mol, Belgium). The goal of this experiment is to test products emissions in field conditions, by monitoring the volatile organic compounds (VOCs) room concentration both before and after the placement of emitting products (sources). This experiment also aimed at observing the influence of temperature and relative humidity over the products emissions under field conditions.

The subsequent sections describe the Dormitory Experiment in detail. The room characteristics are discussed first, followed by the description of the experiment setup and the results. The room conditions and characteristics are made available in order to allow the modeling of this experiment by Annex participants.

3.2 Test setup

The Dormitory Experiment was carried out in a single bedroom (with private bathroom) from first floor of the dormitory facility located in VITO premises, in the city of Mol, Belgium. The bedroom is furnished with a single bed, an IKEA desk, a chair, curtains and a wardrobe. In the bathroom, there is a sink, a shower and a vent fan. The products selected as sources in this experiment were OSB plates (involved in aluminum foil in one side to create a single emitting surface per plate; total emitting surface = 3 m^2) and a floor coating (applied onto aluminum foils; amount applied = 350 g; total emitting surface = 3.85 m^2). Figure 16 shows a scheme of the experiment setup, along with the chosen sampling points and the room characteristics.

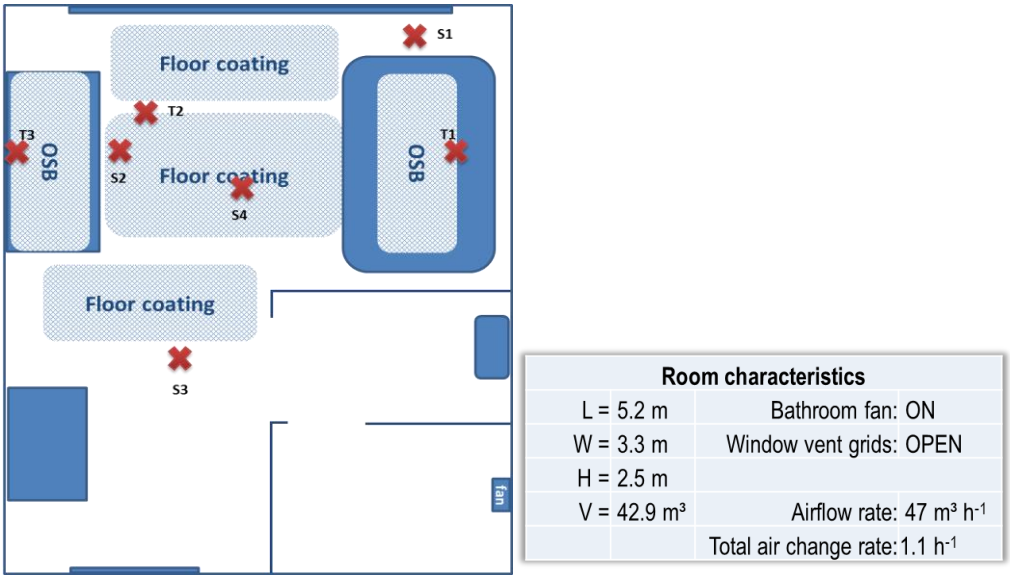

Figure 16 - Scheme of the setup for the Dormitory Experiment

The following devices were used to monitor temperature (T), relative humidity (RH), CO_2 and VOCs in different points of the room, both before (for background characterization) and after the placement of the sources:

- **Sift MS**: continuous VOCs monitoring;
- **FID monitor:** continuous total hydrocarbons (THC) monitoring;
- **ClimaBox:** continuous T, RH and CO_2 monitoring;
- **Radiellos:** time integrated VOCs/TVOCs passive monitoring;
- **UMEx:** time integrated aldehydes passive monitoring;
- **Testo loggers:** continuous T and RH monitoring;
- **SmartButton:** continuous T monitoring, attached to Radiello samplers
- **Flow finder:** instantaneous airflow measurement at vent holes.

The Sift MS, FID, ClimaBox, Radiello samplers and UMEx samplers were employed from start to finish, i.e. from the initial setup for background characterization until the test setup, when the sources were placed in the room. The Testo loggers were used, during the test setup, to monitor T and RH conditions directly onto the products surfaces (during the initial setup, they were placed in the central point, S4). The FlowFinder was used before the experiment to measure the constant airflow at the bathroom vent hole. Table 6 specifies which monitoring devices were present at each sampling point.

Table 6 - Monitoring devices per sampling point.

	Sampling points:						
	Innitial and Test setups				Test setup		
Device	S1	S2	S3	S4	T1	T2	T3
Radiello:	X	X	X				
UMEx:	X	X	X				
SmartButton:	X	X	X				
Testo:				X	X	X	X
ClimaBox:	X	X	X				
FID:				X			
Sift MS:				X			

Both the Sift MS and the FID monitors were placed inside a van, owned by VITO, parked below the window of the dormitory room, due to their size/weight and need for a computer to log the data. A long tube connected the monitors to sampling point S4. Figure 17 shows the van and the monitors inside it.

Figure 17 - VITO van containing the Sift MS and FID monitor.

Figure 18 shows a picture of the room during the test phase, in which the monitoring devices and sources can be seen.

Figure 18 - Dormitory room during the test phase

3.3 Experiment description

The Dormitory Experiment measurements started in February 15th 2018 and ended in March 7th 2018. The detailed description of the sampling period is given in Table 7.

Table 7 - Detailed description of the experiment's sampling period.

Phase	Date	Sources	Conditions	Remarks
1	15/02/2018	-	Normal	Background characterization
2	16/02/2018	2 materials	Normal	Materials placement
	17/02/2018	2 materials	Normal	
	18/02/2018	2 materials	Normal	
3	19/02/2018	2 materials	High RH	Shower on for 20min
	20/02/2018	2 materials	Normal	
	21/02/2018	2 materials	Normal	
	22/02/2018	2 materials	Normal	Leakage discovered and fixed
4	23/02/2018	2 materials	High T	Heater on at full capacity
	24/02/2018	2 materials	Normal	
	25/02/2018	2 materials	Normal	
	26/02/2018	2 materials	Normal	
5	27/02/2018	2 materials	High RH	Shower on for 20min
	28/02/2018	2 materials	Normal	
6	01/03/2018	2 materials	High T	Extra heater on for 3h30 FID stopped
	02/03/2018	2 materials	Normal	Sources removed FID restarted
7	03/03/2018	-	Normal	Decay evaluation
	04/03/2018	-	Normal	
	05/03/2018	-	Normal	
	06/03/2018	-	Normal	
	07/03/2018	-	Normal	

As shown in Table 7, some issues were faced during the course of the experiment. In February 22nd a leakage in the sampling tube connecting point S4 to the Sift MS and FID monitors in the van was discovered. Since the leakage start moment is unknown, these monitors measurements are not reliable until the leakage was fixed. Therefore, VOCs and THC concentration data for phases 1, 2 and 3 are reduced to those measured by the passive samplers. Besides that, the FID flame went out between March 1st and 2nd, meaning that there is a gap in the THC data for this period.

3.4 Results and discussion

3.4.1 Room conditions (T, RH, CO_2)

Figure 19 displays the T data measured during the whole period by the different devices. As observed in the chart, the average room temperature rose significantly when the heating system was set to full capacity (after the first straight dashed line), but it was not significantly affected by the placement of an electrical heater (second straight dashed line), which remained on for 3h30min. The loggers mostly recorded similar T values, with the exception of the ClimaBox logger placed at point S1 (CB1 in Figure 19). This logger recorded higher and less variable temperatures, which might be explained by its position (on the ground, close to the room heater and protected from direct sunlight). The other loggers recorded significant daily variation, following the variations in outdoor temperature. The Testo logger located at point T1 (Testo1 in Figure 19) recorded the largest T variation and the highest T values (almost reaching 40°C in 25/02), as T1 was the point which received the most sunlight out of the seven. Since the Testo loggers were used to monitor T closer to the products surfaces, this suggests that the products temperatures were affected more by the sunlight incidence than by the room temperature itself.

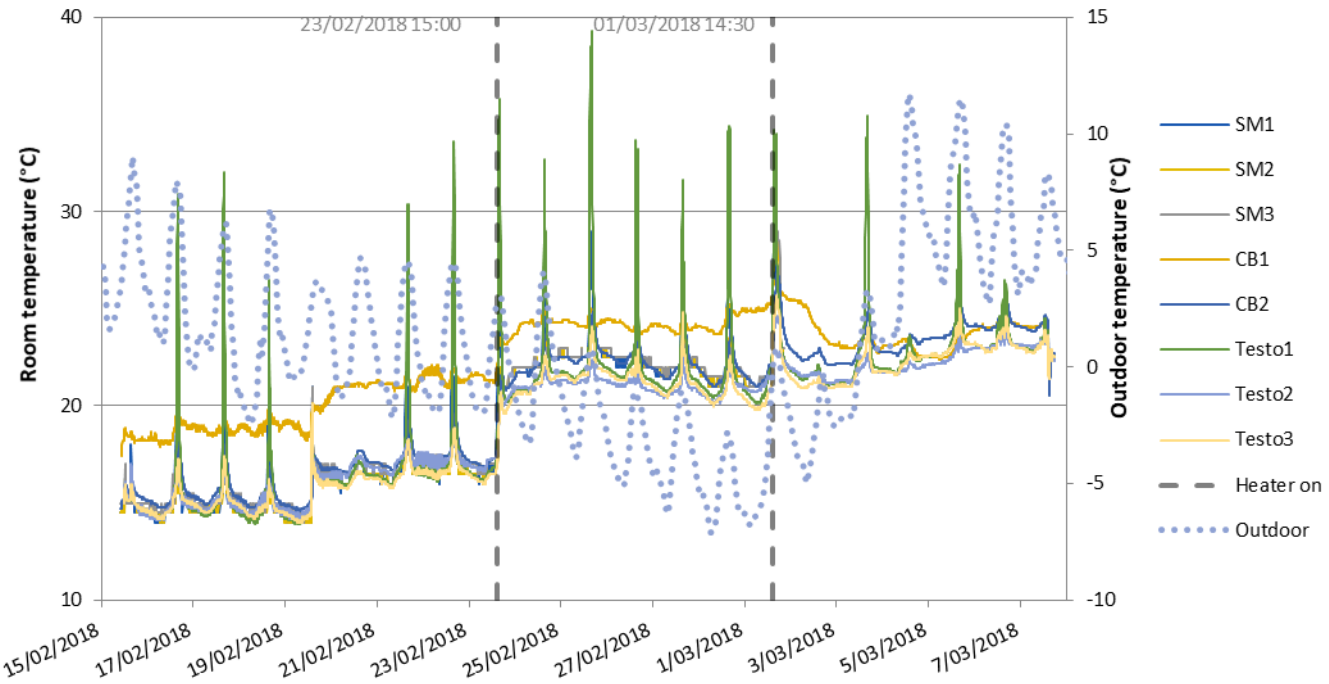

Figure 19 - Temperature measurements recorded by each device (SM1, 2 and 3: SmartButton loggers located a points S1, 2 and 3, respectively; CB1 and 2: ClimaBox loggers located at points S1 and 2, respectively; Testo1, 2 and 3: Testo loggers located at points T1, 2 and 3 respectively).

Figure 20 displays the RH data measured during the whole period by the different devices. The data recorded by the different loggers was very similar, except for CB1 (which presented lower average RH than the rest in the first half of the experiment) and Testo 1 (which recorded more variable RH data, reaching the lowest RH values). This might be connected to the locations of these loggers in the room, for the same reasons discussed above for temperature measurements. The highest RH values were measured during the two events when the shower was turned on, reaching almost 100% in both occasions after only 20min.

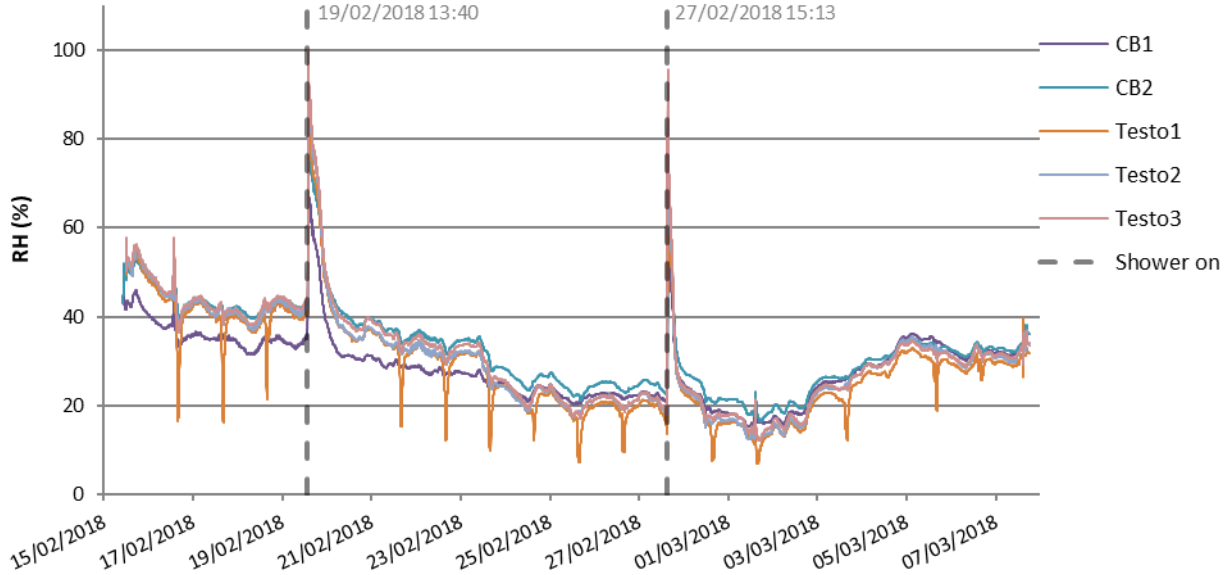

Figure 20 – Relative humidity measurements recorded by each device (CB1 and 2: ClimaBox loggers located at points S1 and 2, respectively; Testo1, 2 and 3: Testo loggers located at points T1, 2 and 3, respectively).

Figure 21 displays the CO_2 data measured during the whole period by the two ClimaBox devices. The chart shows that the CO_2 concentration in the assessed room was in average less variable than T and RH. Even though the recorded fluctuations were quite similar between the two devices, CB1 once again

recorded values somewhat different than CB2. The reason for this discrepancy is unclear, as the proximity to the heater should not affect the CO_2 concentration. Considering that CB1 presented disparities also in RH and T measurements (although in those cases the location of the device offers a plausible explanation for such disparities, as discussed above), it is possible that CB1 calibration done prior to the beginning of the experiment was hindered for some unknown reason. Nevertheless, both devices simultaneously detected CO_2 peaks coinciding with specific events which required a research team member presence in the room, due to CO_2 release from respiration. The two events linked to the placement of the products and of the electrical heater demanded more time and effort compared to the others, thus resulting in higher CO_2 peaks. This reinforces the importance of avoiding as much as possible the entrance during the course of this type of experiment.

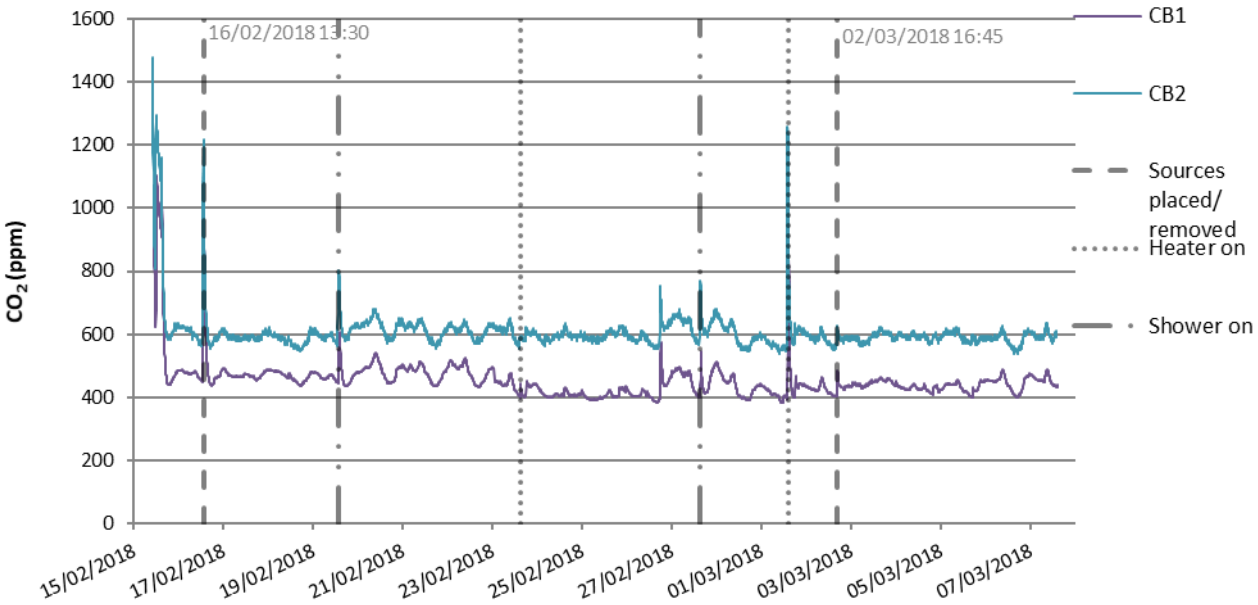

Figure 21 - CO_2 measurements recorded by CB1 and 2 (ClimaBox loggers from points S1 and 2, respectively).

3.4.2 Products emissions monitoring

Figure 22 contains the THC data measured by the FID during the Dormitory Experiment. First, the chart shows the significant effect of the leakage discovered in the sampling tube over the FID measurements. Before the leakage was fixed, the THC measurements were higher and presented strong fluctuation; after, the measurements showed much less variability. Nevertheless, the effect of the sources placement is still noticeable: the THC concentration rises rapidly and significantly above the "background", decaying to a level close to the initial after a period of approximately 2 days. Temperature (also plotted in Figure 22 chart) did not seem to influence THC release from the products, opposing the initial expectations. Even the highest temperature measured directly over the OSB plate did not increase the room THC concentration. Although previous test chamber tests proved that T increase does increase VOC emission from both products used as source, the present experiment suggests that such an emission increase is not enough to increase the room THC concentration as a whole. The gap in THC data due to the FID flame issue previously mentioned does not allow to clearly evaluate the effect of the products removal over the THC concentration. It does however seem like it caused the THC concentration to decrease slightly, suggesting that the selected products keep emitting an important amount of THC even after two weeks.

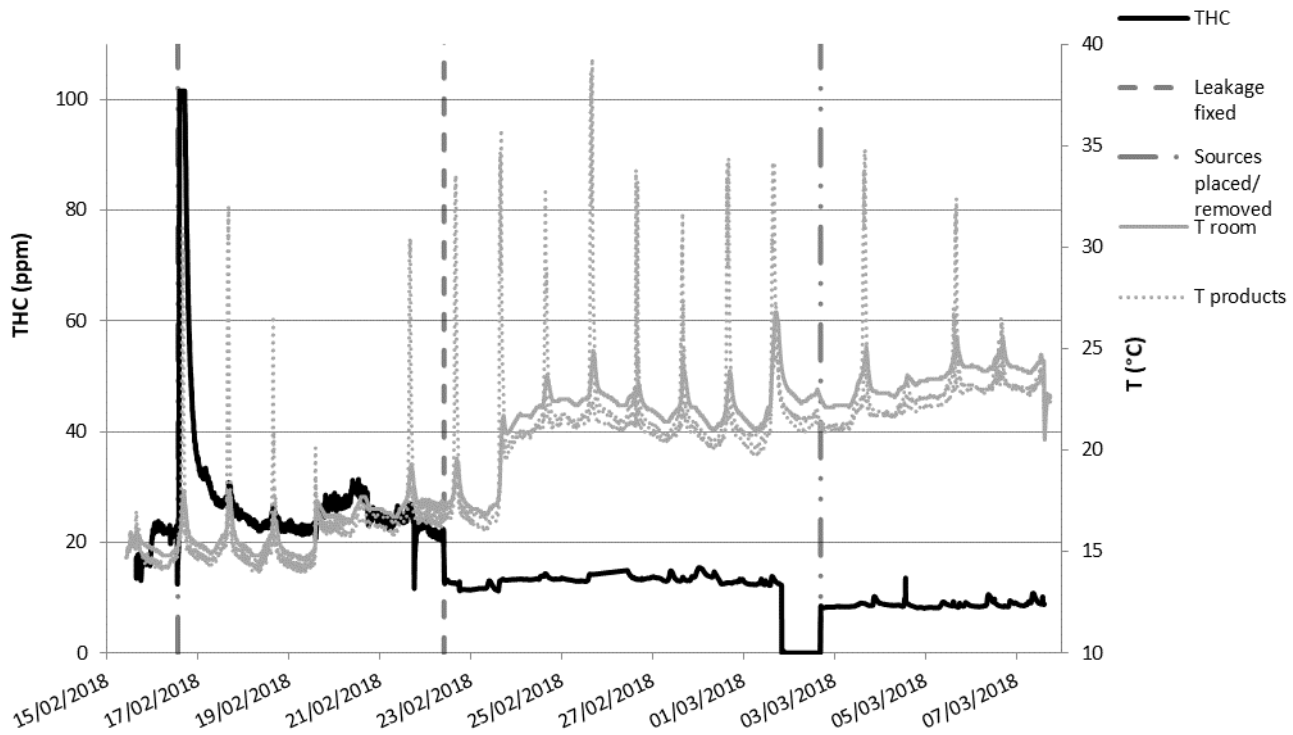

Figure 22 - Total hydrocarbons measurements recorded by FID ("T room" refers to the temperature data from the ClimaBox logger from point S2 and “T products” refers to the temperature data from the three Testo loggers).

Figure 23 presents the VOCs data monitored by the Sift MS (in ppm), including a set of aldehydes (acetaldehyde, benzaldehyde, formaldehyde, hexanal, pentanal and propanal), acetone, alpha—pinene and toluene.

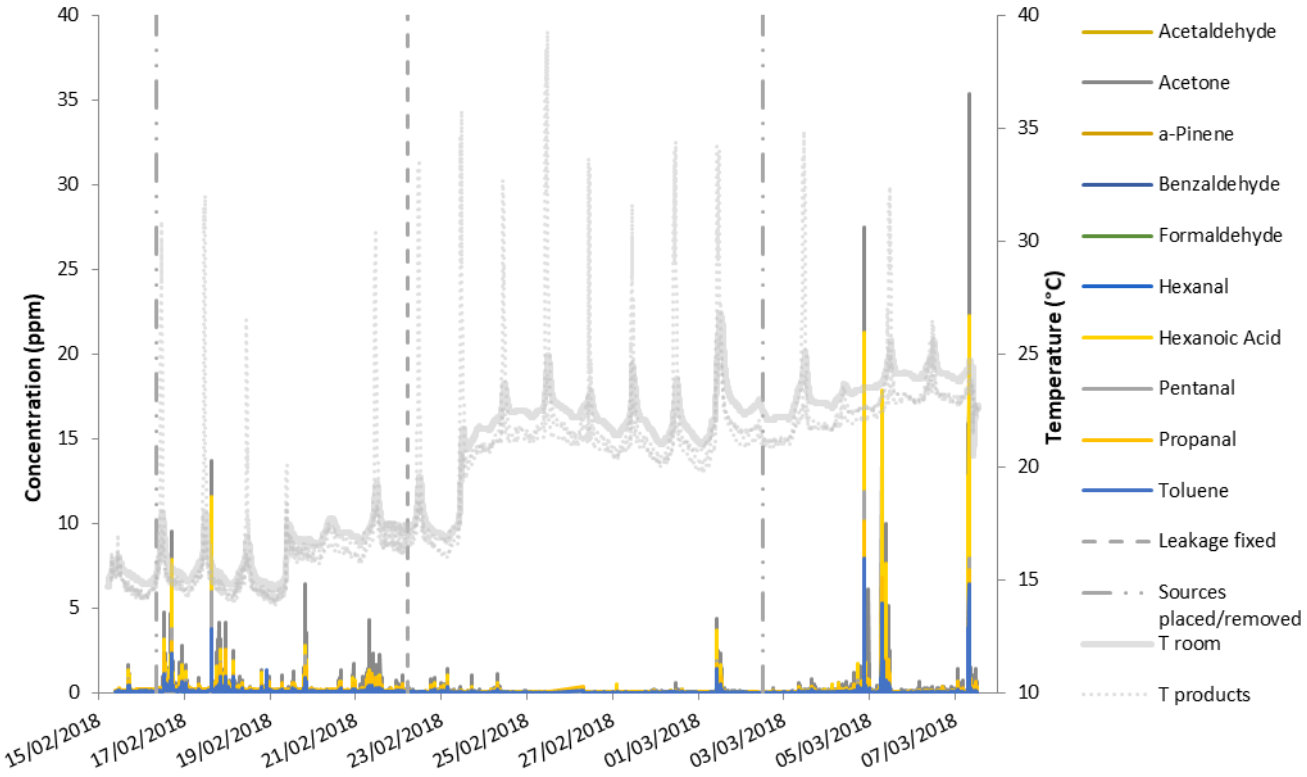

Figure 23 - VOCs data monitored by the Sift MS ("T room" refers to the temperature data from the ClimaBox logger from point S2 and “T products” refers to the temperature data from the three Testo loggers).

The concentration of VOCs presented an unusual behavior, with high peaks of very short duration, instead of an approximate curve decaying with time, as commonly observed in product emissions testing. Whereas the leakage did seem to have interfered in the measurements, the highest VOCs concentrations (namely of acetone and hexanoic acid) actually happened after the sources were removed from the room, again in disagreement with usual product emissions tests.

Although the reason for the unusual behavior of the data recorded by the FID and especially by the Sift MS is unclear, a possible explanation may be the extensive length of the sampling tube that had to be used between point S4 and the van containing the equipment. This tube was almost entirely outdoors, exposed to low temperatures (see Figure 17) for most of the sampling period, which could have led to condensation of a part of the VOCs inside the tube prior to reaching the equipment. The highest VOCs concentrations were registered by the Sift MS in the last days of the experiment, precisely when the outdoor temperatures rose, suggesting that some of the previously condensed VOCs in the tube were volatilized and added to the sampling flow coming from the room.

The results obtained after analysis of the passive samples (Radiello and UMEx) are presented in Figure 24. These results correspond to long term average values (1-day average background; 10-days average for the other samples). Although this type of measurement does not allow observing the actual concentration curve development, it still provides a very reliable overview of the accumulation of different VOCs due to the products emissions.

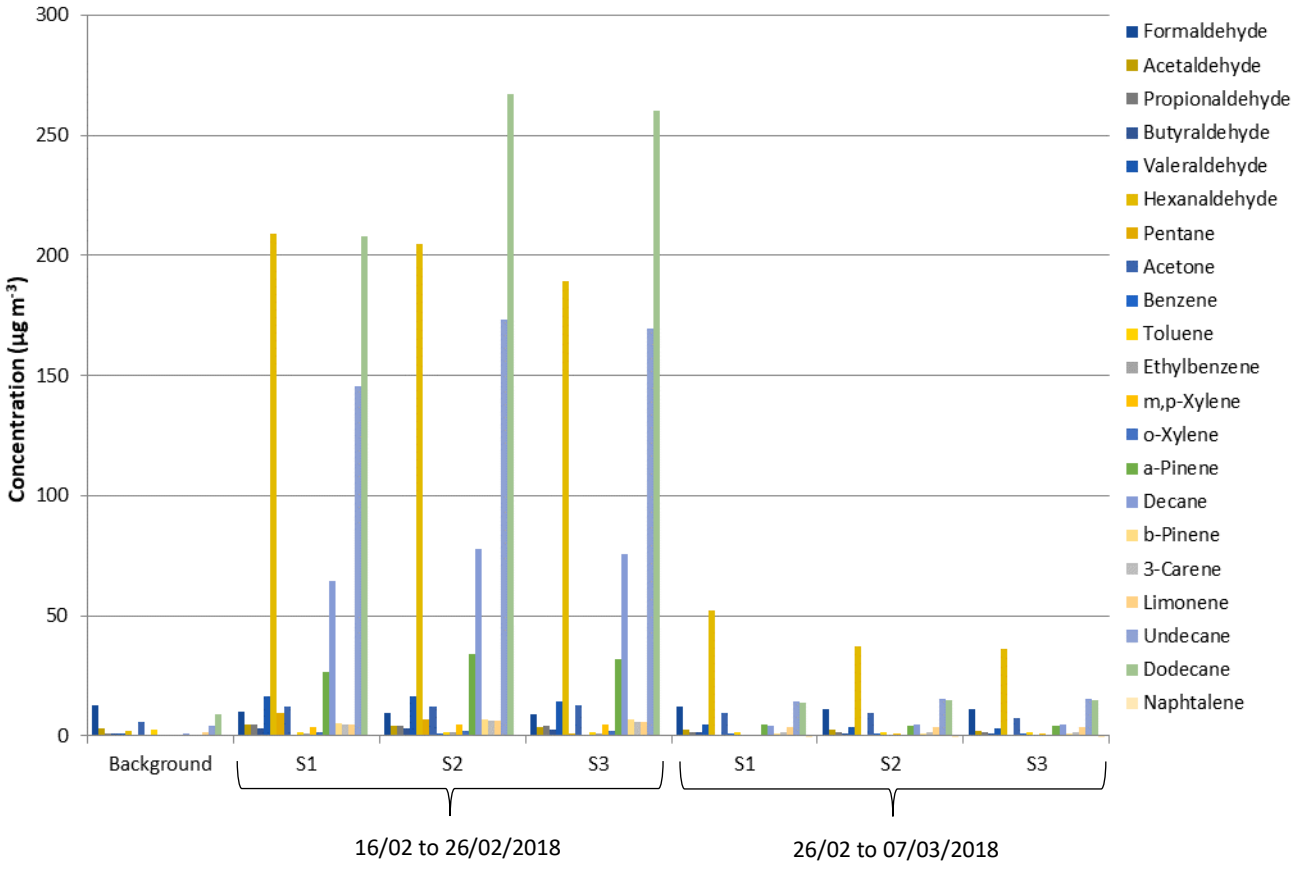

Figure 24 - VOCs average concentrations measured by passive sampling.

Observing Figure 24 chart, the highest VOCs concentrations were measured during the first period after the products placement, decreasing significantly in the second period. This is the expected trend, since the VOCs emission rates from the products decrease with time, resulting in lower room concentrations for an invariant air change rate. Dodecane reached the highest concentrations in the first period,

followed by the aldehyde hexanal, undecane, decane and a-pinene, in that order. In the second period, the highest average concentration was reached by hexanal, whereas all the other VOCs presented considerably lower average concentrations.

3.5 Final considerations

During the course of the Dormitory Experiment, some issues were observed, i.e. equipment malfunctions (leakage in the FID and Sift MS sampling tube, FID flame going out) and unusual/unexpected results from the FID and especially from the Sift MS, possibly due to a combination of the length and placing of the sampling tube with the low outdoor temperatures.

Therefore, the planning of the following experiments took this observations into account. Both the House and Office experiments were planned in such a way that the equipment could be placed closer to the assessed space, removing the need of a long sampling tube and therefore diminishing its susceptibility to the outdoor conditions. Also, in the following experiments extra care was taken in monitoring the operation of the equipment.

Chapter 4: Field test 3 - The House Experiment

4.1 Context

This section describes the House Experiment, the third experiment developed in subtask 5 of Annex 68. This experiment took place in November 2018 in a two-story house located in VITO premises (Mol, Belgium). Similarly to the Dormitory Experiment, the goal in this experiment is to test products emissions in field conditions by monitoring the volatile organic compounds (VOCs) room concentration both before and after the placement of emitting products (sources). In this experiment, however, the monitored space was occupied by two master students for the entirety of the experiment.

The subsequent sections describe the details of the House Experiment. The characteristics of the assessed space are discussed first, followed by the description of the experiment setup and the results. The room conditions and characteristics are made available in order to allow the modeling of this experiment by Annex participants.

4.2 Test setup

The House Experiment was carried out in the ground floor of the two-story house located in VITO premises, in the city of Mol, Belgium. The ground floor of the house has an open space comprising a dining room and a living room, a kitchen, an entrance hallway and a small hallway leading to the stairs to the second floor. The kitchen and entrance hall are separated from the open space by walls and doors. The house uses natural ventilation with manual window vent grids, which remained open during the experiment.

The experiment took place in the open space comprising the dining and living rooms. This open space is furnished with two couches, a center table between the couches, a dining table with four chairs, curtains, a bookcase close to the window and a shorter bookcase beside the dining table. The products selected as sources in this experiment were two OSB plates (identical to the ones used in the Dormitory Experiment, but this time not involved in aluminum foil; total emitting surface = 5,9 m^2) and an air freshener (Carrefour brand, gel type). Figure 25 shows a scheme of the experiment setup, along with the chosen sampling points and the space characteristics.

In this second phase, fewer devices were used for the monitoring of T, RH, CO_2 and VOCs compared to the Dormitory Experiment. The UMEx samplers were not available. The Testo loggers and SmartButtons were not used because it was observed during the Dormitory Experiment that their results were very similar to the results from the ClimaBox, and were therefore considered unnecessary. On their place, Omega loggers were used to monitor T, RH and CO_2 along with the ClimaBox. The FlowFinder was not used since the house does not have a mechanical ventilation system. Besides that, the Sift-MS was placed indoors instead of inside the van, in order to minimize the issues related to the length of the sampling tube. The FID monitor was not used due to the risk of explosion because of the hydrogen cylinder. The devices used in the House Experiment in different points of the room, both before (for background characterization) and after the placement of the sources, were:

- **Sift MS**: continuous VOCs monitoring;

- **ClimaBox:** continuous T, RH and CO_2 monitoring;
- **Omega loggers:** continuous T, RH and CO_2 monitoring;
- **Radiellos:** time integrated VOCs/TVOCs passive monitoring;

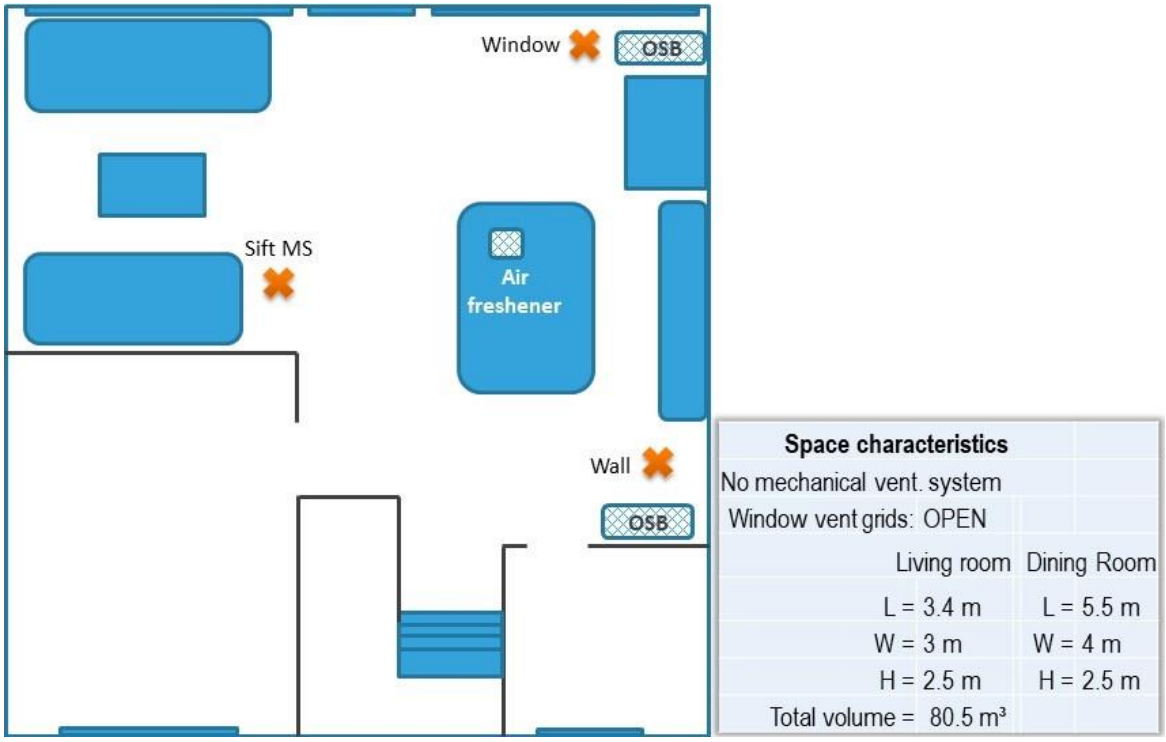

Figure 25 - Scheme of the setup for the House Experiment.

All the devices were employed from start to finish, i.e. from the initial setup for background characterization until the end of the test setup. Differently from the Dormitory Experiment, in the House Experiment only 3 sampling points were selected, since it was observed that the data recorded in most of the points in that previous phase were very similar. The greatest differences were observed only when comparing the point close to the window to the others. Thus, in the House Experiment, the points were selected to represent the conditions close to the window and away from the window (close to an inner wall). The Sift MS was positioned in a third, central point. Table 8 specifies which monitoring devices were present at each sampling point.

Table 8 - Monitoring devices per sampling point.

	Sampling points		
Device	**Window**	**Wall**	**Central**
Radiello:	X	X	
ClimaBox:	X		
Omega logger:		X	
Sift MS:			X

Figure 26 shows the assessed space during the test phase, with the monitoring devices and sources.

Figure 26 - House space (living room and dining room) during the experiment.

4.3 Experiment description

The House Experiment measurements started in November 7th 2018 and ended in November 16th 2018. The detailed description of the sampling period is given in Table 9.

Table 9 - Detailed description of the House Experiment's sampling period.

Phase	Date	Sources	Conditions	Remarks
1	07/11/2018	-	Normal	Background characterization
2	08/11/2018	2 materials	Normal	Materials placement
	09/11/2018	2 materials	Normal	
3	10/11/2018	-	-	Experiment paused
	11/11/2018	-	-	New background characterization
4	12/11/2018	2 materials	Normal	
	13/11/2018	2 materials	Normal	
	14/11/2018	2 materials	Normal	
5	15/11/2018	-	Normal	Decay evaluation
	16/11/2018	-	Normal	

As shown in Table 9, the experiment was paused during the weekend (10 and 11/11), as was requested by the occupants of the house, due to the intense noise of the Sift MS. However, the ClimaBox remained operational, and Sunday new Radiello samplers were placed in order to get a new background characterization, before bringing new sources to the house on Monday (12/11).

The occupancy pattern in the assessed space is shown in Figure 27. As indicated in the figure, the house occupants had guests over for a social gathering during the weekend, when the experiment was paused.

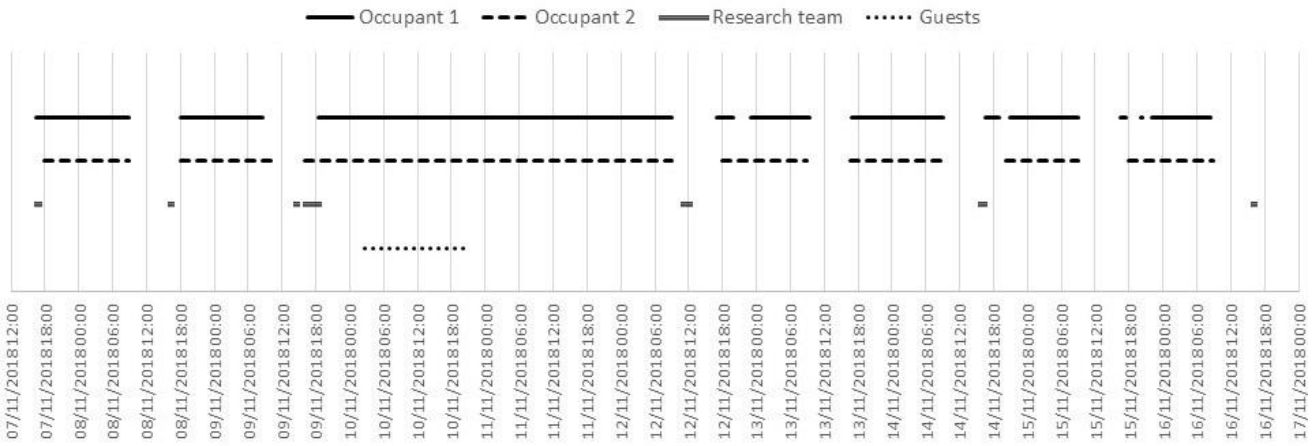

Figure 27 - Occupancy pattern in the assessed space during the House Experiment (lines indicate presence, whereas lack of lines indicate absence).

4.4 Results and discussion

4.4.1 Room conditions (T, RH, CO_2)

Figure 28 displays the T data measured during the House Experiment by the different devices, along with outdoor temperature data measured in VITO premises.

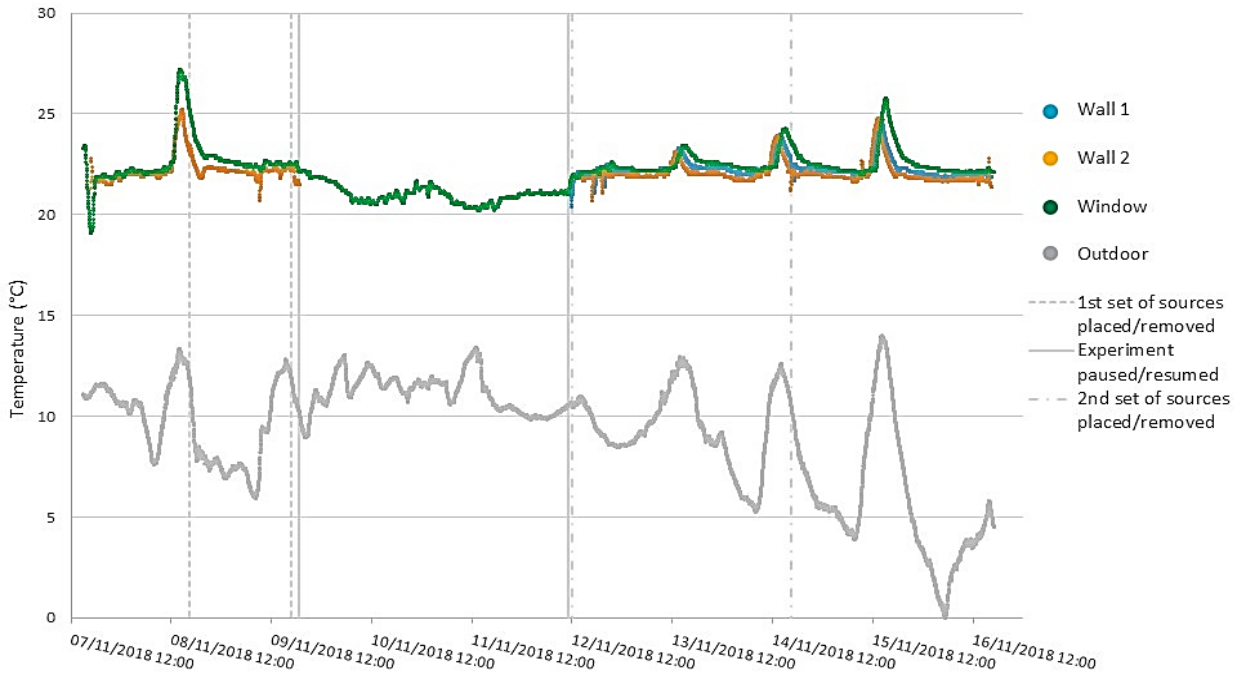

Figure 28 - Temperature measurements recorded by each device during the House Experiment (Wall 1 and 2: two Omega loggers positioned away from the windows; Window: ClimaBox logger located close to the window)

As observed in the chart, the indoor temperature during the House Experiment was considerably stable, with little deviation from the average (22°C). The greatest deviations are linked to larger variations in the outdoor temperatures, and can also be connected to increased sunlight incidence. The three devices presented very similar results, although it can be noticed that the device positioned close to the window recorded peaks higher than the other two, which can be related to the higher sunlight incidence in that spot.

Figure 29 displays the RH data measured during the House Experiment by the different devices. The three monitors recorded very similar RH data during the whole House Experiment. Thus, differently from what was observed for the temperature data, the position of the devices did not have a noticeable influence on the RH monitoring. The highest RH values (> 60%) were recorded during the experiment pause, which can be linked to the social gathering that the house occupants organized over the weekend.

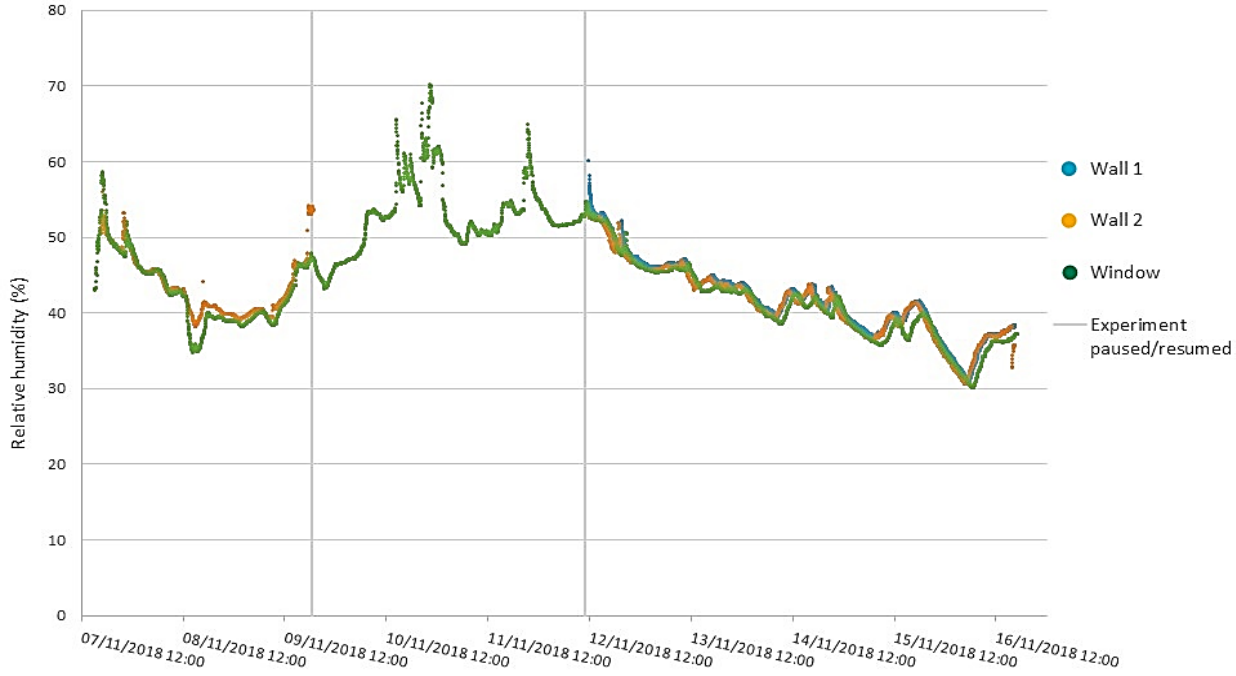

Figure 29 – Relative humidity measurements recorded by each device during the House Experiment (Wall 1 and 2: two Omega loggers positioned away from the windows; Window: ClimaBox logger located close to the window).

Figure 30 contains the CO_2 data recorded during the House Experiment by the different devices. The chart shows that the CO_2 data recorded by the two Omega loggers (both located at the same spot, away from the window) were very similar, whereas the ClimaBox logger located close to the window recorded higher values. No clear reason can be determined for this trend, except a possible decalibration of the CO_2 sensor of the ClimaBox logger. Nevertheless, the concentration fluctuations recorded by the ClimaBox are virtually the same as the ones measured by the Omega loggers. The CO_2 concentrations measured during the House Experiment were generally stable, even during the placement/removal of the source products, indicating a good ventilation of the assessed space. The highest concentrations of CO_2 happened during the experiment pause, when the house occupants hosted a social gathering.

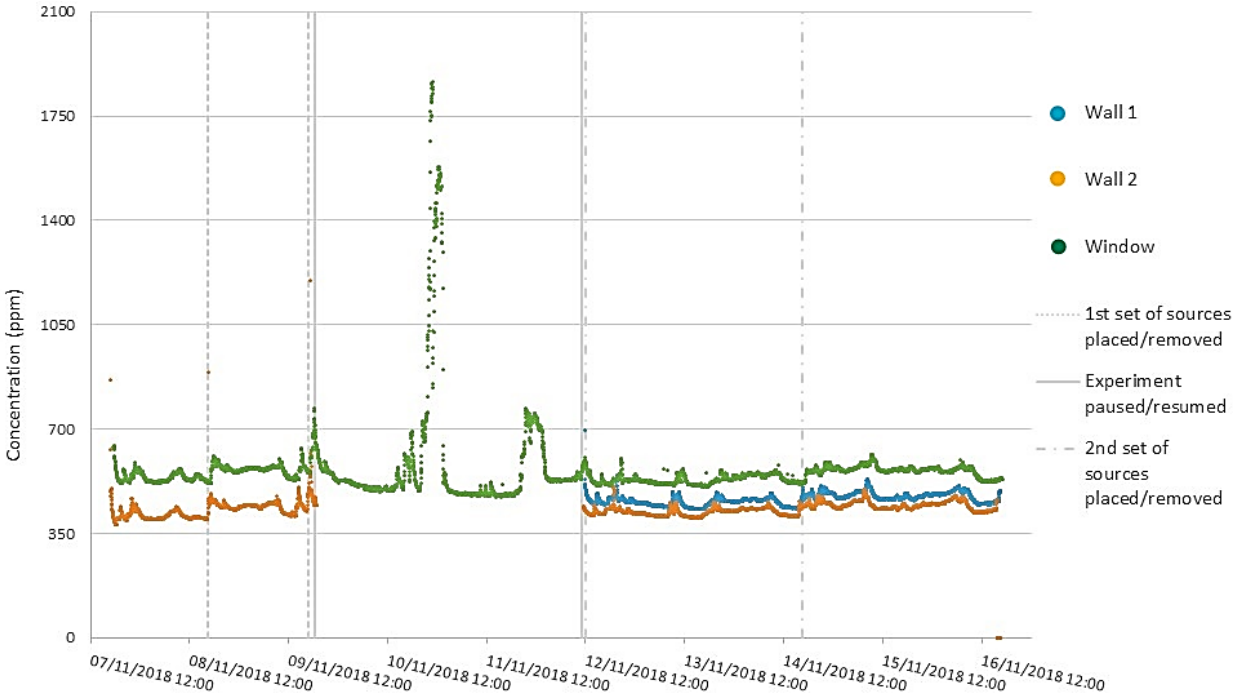

Figure 30 – CO_2 measurements recorded by each device during the House Experiment (Wall 1 and 2: two Omega loggers positioned away from the windows; Window: ClimaBox logger located close to the window).

4.4.2 Products emissions monitoring

Figure 31 displays the VOCs data measured by the Sift MS monitor during the House Experiment. The results recorded by the Sift MS followed a similar trend than the observed in the Dormitory Experiment, although the peak values reached were comparatively much lower (possibly due to the larger volume of the assessed space). On the other hand, the peaks of VOC concentration behaved more similarly to what was expected (exponential decay) than the peaks observed in the previous experiment, suggesting that moving the Sift MS indoors was effective. The placement of the first set of sources did not seem to influence the VOCs concentration, whereas the placement of the second set coincides exactly with the highest VOCs peak. This difference may be due to the fact that the OSB boards placed on 12/11 were slightly wet (it even caused a small but noticeable increase of RH, as can be seen in Figure 29). This occurrence coincides with a strong smell complaint from the occupants, reported around 17h of 12/11. These peak concentration values, however, decreased quite rapidly back to the base concentrations (~ 2h), indicating a high ventilation rate in the space.

The event with second highest VOCs concentrations coincided with the setting up of the experiment, when the equipment was being transported and set into place, the door to the outside was kept open (where the van was parked) and a lot of movement between indoor and outdoor was taking place. All this activity possibly allowed higher levels of VOCs to enter the space and caused re-emission of substances previously attached to surfaces. The third highest VOCs concentrations, happened between 14/11 and 15/11, could not be linked to any activities reported by the occupants. The VOCs found in highest concentrations were, in that order: hexanoic acid, a-pinene, acetone, formaldehyde, hexanal and toluene. The other compounds remained in lower concentrations (< 2ppm).

Figure 32 displays the average VOCs concentrations measured by the Radiello passive samplers during the House Experiment. Some results in Figure 32 were unexpected. First, very high average concentrations of dodecane (> 100 ppm) and especially decane (> 1000 ppm, bar not entirely shown) were measured. Second, the decane highest concentration happened during the background period

(which at least seems to be in agreement with the Sift MS results, which did show some relatively high VOCs concentrations). Third, the highest concentrations of dodecane happened after the first set of sources were removed. These unexpected results may be linked to the fact that the passive samplers were exposed for periods considered short for this type of sampling (1-3 days, recommended period is 7 days), due to time constraints regarding the equipment availability. After decane and dodecane, the other highest concentrations were measured for acetone (high concentrations with presence of the second set of sources), naphthalene and limonene (higher with presence of the first set of sources). All the other VOCs presented low average concentrations (< 3 µg m^{-3}).

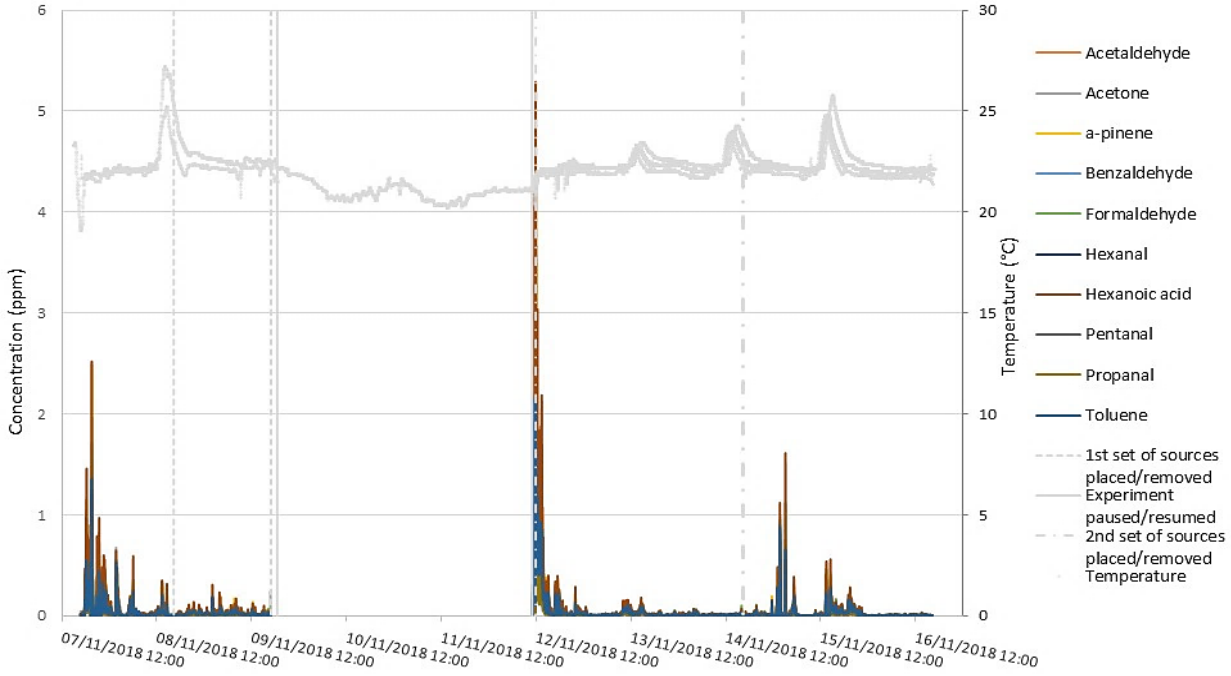

Figure 31 - VOCs data monitored by the Sift MS.

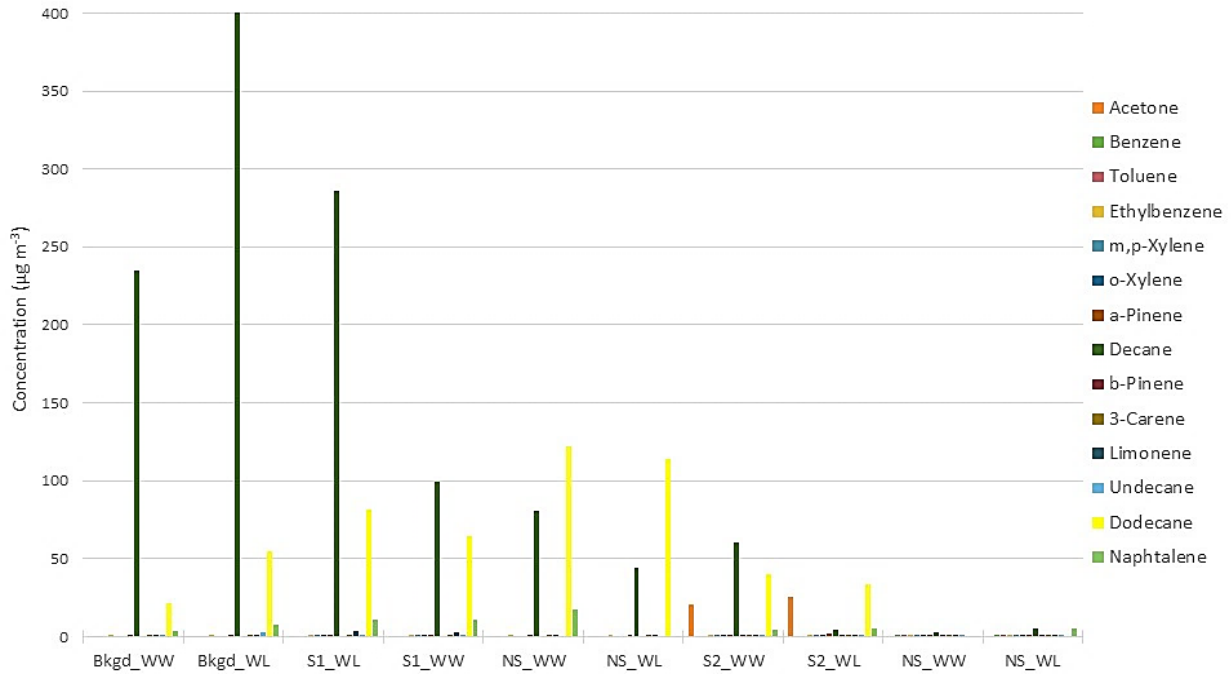

Figure 32 - VOCs average concentrations measured by passive sampling (Bkgd refers to the background samples; WW represents the point located next to the window; WL represents the point away from the window;

S1 and S2 refer to the samples taken with the presence of the sources; NS refers to the samples taken after the sources removal).

4.5 Final considerations

The House Experiment monitored VOCs emissions by two different source products for 9 days in an occupied house. The results recorded by the Sift MS indicate that placing it indoors, as suggested after analysis of the Dormitory Experiment results to dismiss the use of a long sampling tube, enhanced the measurement process. The VOCs concentrations were in general low, but a few concentration peaks were detected. The first concentration peak can be linked to the initial setup of the experiment (when all the research team movement and the devices transportation possibly increased the levels of VOCs) and the second one, which presented the highest concentrations, happened when the second set of sources was placed. This set differed from the first one because the OSB plates were slightly wet, which suggests that the water on the OSB surface can increase VOCs emissions.

The passive sampling results indicated very high concentration of decane and dodecane. However, these passive sampling results should be considered with care, since the sampling period applied in this experiment was shorter than the recommended. Therefore, it is recommended that, in the future, field experiment of this nature have a longer duration, in order to allow more adequate sampling periods for the passive samplers.

Chapter 5: Field test 4 - The Office Experiment

5.1 Context

This section describes the Office Experiment, the 4th of the experiments developed in subtask 5 of Annex 68. This experiment took place in December 2018 in an office space located in VITO premises (Mol, Belgium). This 4th experiment intended to replicate the Dormitory Experiment, testing products emissions in field conditions by monitoring the volatile organic compounds (VOCs) room concentration both before and after the placement of emitting products (sources), this time in an unoccupied office-like environment.

The subsequent sections describe the Office Experiment in detail. The characteristics of the assessed space are discussed first, followed by the description of the experiment setup and the results. The room conditions and characteristics are made available in order to allow the modeling of this experiment by Annex participants.

5.2 Test setup

The Office Experiment was carried out in the ground-floor office of a laboratory building of VITO, located in VITO premises in Mol, Belgium. Figure 33 shows a scheme of the experiment setup, along with the chosen sampling points and the space characteristics. The office uses natural ventilation with manual window vent grids, which remained open during the experiment. In order to maintain a constant air change rate in the space, a vent fan plus duct was installed at the only door to the office, which was then sealed with plastic wrapping as shown in Figure 34.

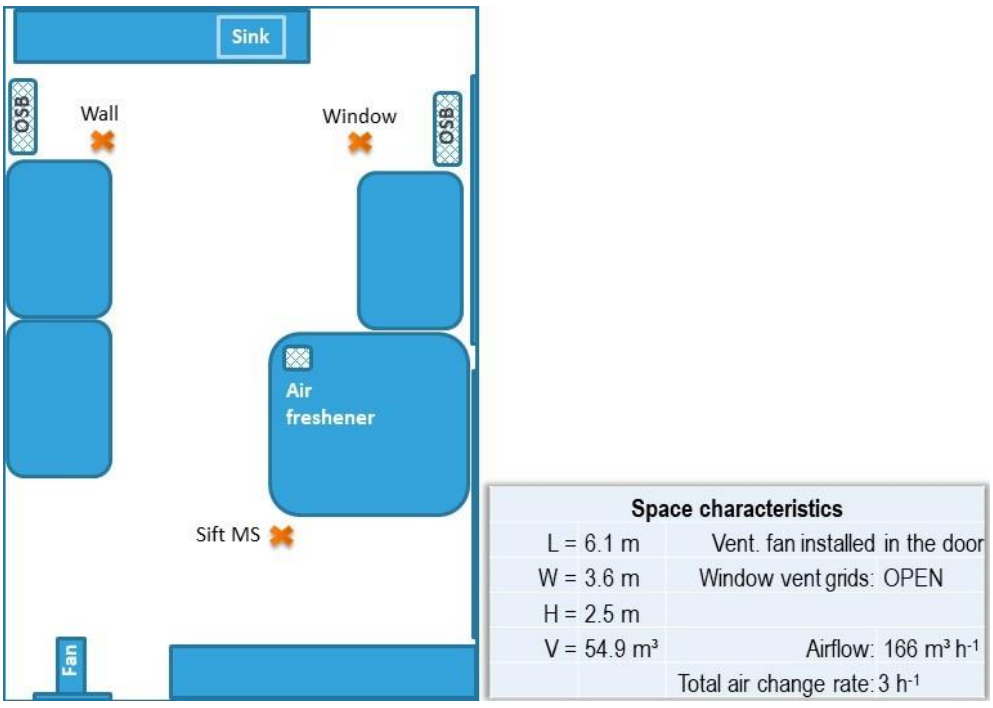

Figure 33 - Scheme of the setup for the Office Experiment.

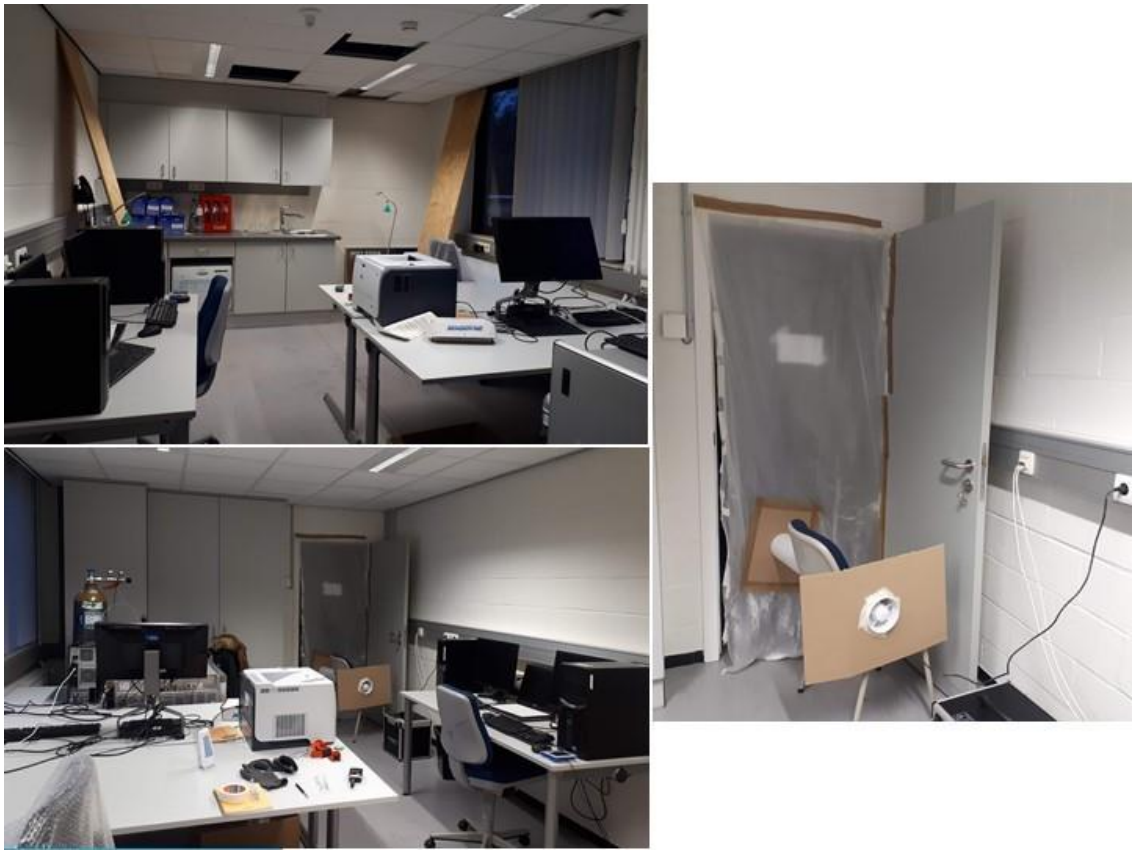

Figure 34 - Office space during the experiment.

As in the House Experiment, fewer monitoring devices were used in this third phase. For T, RH and CO_2 monitoring, only Omega loggers were used. The FlowFinder was used to determine the air flow provided by the fan installed at the door. Once again the Sift-MS was placed indoors and the FID monitor was not used (risk of explosion). The devices used in the Office Experiment in different points of the room, both before (for background characterization) and after the placement of the sources, were:

- **Sift MS**: continuous VOCs monitoring;
- **Omega loggers:** continuous T, RH and CO_2 monitoring;
- **Radiellos:** time integrated VOCs/TVOCs passive monitoring;
- **FlowFinder:** instantaneous airflow measurement at vent holes.

The office space is furnished with three computer desks, three rolling chairs, one simple chair, one document cabinet, a sink with a cupboard, three desktop sets and a printer (which remained turned off for the entirety of the experiment). The products selected as sources in this experiment were two OSB plates (identical to the ones used in the two previous phases, not involved in aluminum foil; total emitting surface = 5.9 m^2) and an air freshener (identical to the one used in the House Experiment; Carrefour brand, gel type).

All the devices were employed from start to finish, i.e. from the initial setup for background characterization until the end of the test setup. Similarly to the House Experiment, only 3 sampling points were selected: one point close to the window, one away from the window and one point exclusively for the Sift MS. Table 10 specifies the monitoring devices present at each sampling point.

Table 10 - Monitoring devices per sampling point.

	Sampling points		
Device	**Window**	**Wall**	**Central**
Radiello:	X	X	
Omega logger:	X	X	
Sift MS:			X

5.3 Experiment description

The Office Experiment measurements started in December 5th 2018 and ended in December 13th 2018. The detailed description of the sampling period is given in Table 11.

Table 11 - Detailed description of the Office Experiment's sampling period.

Phase	Date	Sources	Conditions	Remarks
1	05/12/2018	-	Normal	Background characterization
2	06/12/2018	2 materials	Normal	Materials placement
	07/12/2018	2 materials	Normal	
	08/12/2018	2 materials	Normal	
	09/12/2018	2 materials	Normal	
3	10/12/2018	2 materials	High RH	Faucet open from 15h11 to 15h51
4	10/12/2018	-	Normal	Decay evaluation
	11/12/2018	-	Normal	
	12/12/2018	-	Normal	
	13/12/2018	-	Normal	

5.4 Results and Discussion

5.4.4.1 Room conditions (T, RH, CO2)

Figure 35 displays the T data measured during the Office Experiment by the different devices, along with outdoor temperature data measured in VITO premises. The T data measured by both Omega loggers were quite similar, although the logger positioned close to the window consistently recorded slightly lower values. No daily peaks of higher T were observed, in contrast to the previous experiments, more likely due to a lack of direct sunlight incidence. It can also be observed that the T trend is not as stable as the one observed during the House Experiment, i.e. values of T present a clear descending tendency after 10/12, which can be linked to the decrease in outdoor T observed in the same period. This more intense link between indoor and outdoor temperature can be connected to the lack of occupancy in the office space, since the heating was not being adjusted for occupants comfort.

Figure 36 displays the RH data measured during the Office Experiment by the Omega loggers. The RH datasets are almost identical for the two devices, showing that the two chosen positions did not differ between themselves regarding RH levels, which is possibly connected to the high air change rate applied in the space. The average RH slightly decreased from 07/12 onwards. Opening the faucet for ~40 min caused only a small RH peak, going from 36% to 46%.

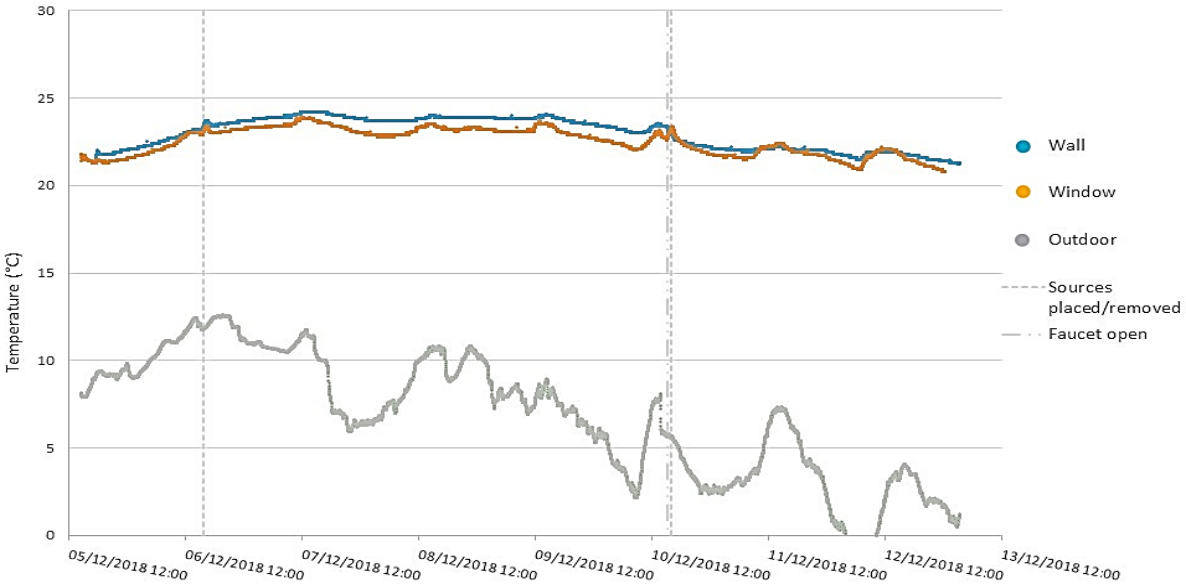

Figure 35 - Temperature measurements recorded by each device during the Office Experiment (Wall: Omega logger positioned away from the windows; Window: Omega logger positioned close to the window).

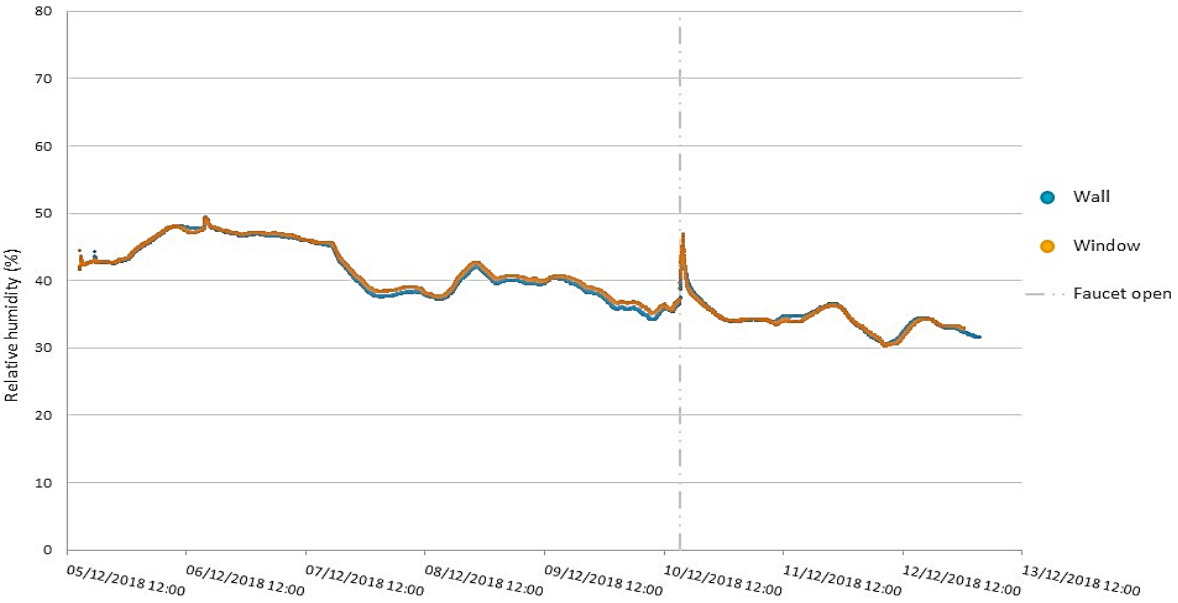

Figure 36 – Relative humidity measurements recorded by each device during the Office Experiment (Wall: Omega logger positioned away from the windows; Window: Omega logger positioned close to the window).

Figure 37 shows the CO_2 data recorded by the Omega loggers during the Office Experiment. As observed in the chart, the CO_2 concentrations during the Office Experiment were quite stable and low (~400 ppm) as expected, since the space was unoccupied for the duration of the experiment. Peaks reaching more than 600 ppm were recorded when the presence of a researcher was needed, i.e. during the placement and removal of the sources and during the faucet opening). In the last two days of the experiment, some variation on the previously very stable CO_2 concentration trend was observed.

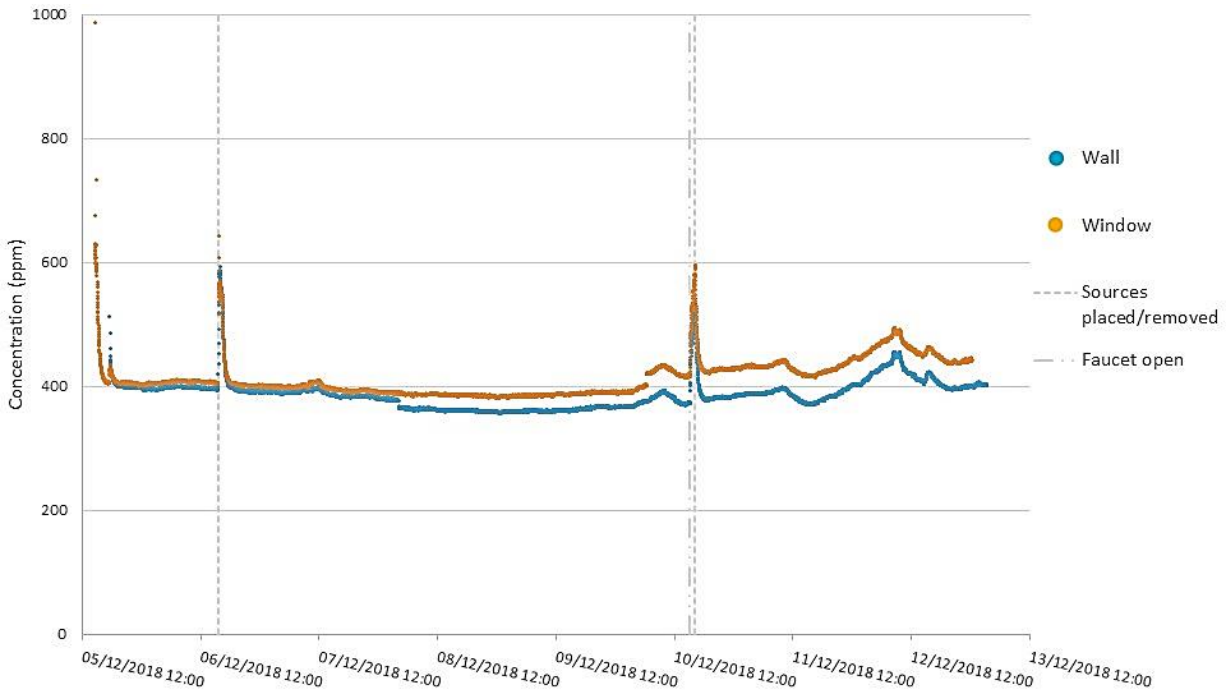

Figure 37 – CO_2 measurements recorded by each device during the Office Experiment (Wall: Omega logger positioned away from the windows; Window: Omega logger positioned close to the window).

5.4.4.2 Products emission monitoring

The VOCs data measured by the Sift MS during the Office Experiment are shown in Figure 38. The VOCs concentrations recorded by the Sift MS followed a similar trend than the observed in the two previous experiments. Both the magnitude of the peak values and the shape of said peaks were similar to those observed in the House Experiment. The highest VOCs concentrations were recorded before the placement of the sources. However, it is important to notice that the fan was installed to the door only after the placement of the Sift MS, and that this installation included the use of a long plastic sheet attached to the door opening by a considerable amount of adhesive tape (see Figure 34). Although most of the adhesive tape was placed on the outside, it is possible that it also acted as a VOCs source to the office for the whole duration of the experiment, possibly having its emission rate intensified whenever the adhesive taped had to be removed to allow entrance to the office (e.g. the second highest peaks occurred before opening the faucet, when extra adhesive tape had to be added to the door sealling). The VOCs found in highest concentrations were, in that order: acetone, hexanoic acid and propanal. The other compounds remained in lower concentrations (< 1ppm).

Figure 39 displays the average VOCs concentrations measured by the Radiello passive samplers during the Office Experiment. Observing Figure 39 chart, it can be noticed that the results from the Office Experiment were much lower than those observed in the previous experiments, probably due to the high air change rate. Unlike the House Experiment, the background samples presented very low concentrations of all VOCs. Dodecane presented the highest average concentrations, which happened after the removal of the sources. Acetone was the VOC with the second highest concentrations, measured with the presence of the sources. All the other VOCs presented very low average concentrations (< 2 µg m^{-3}).

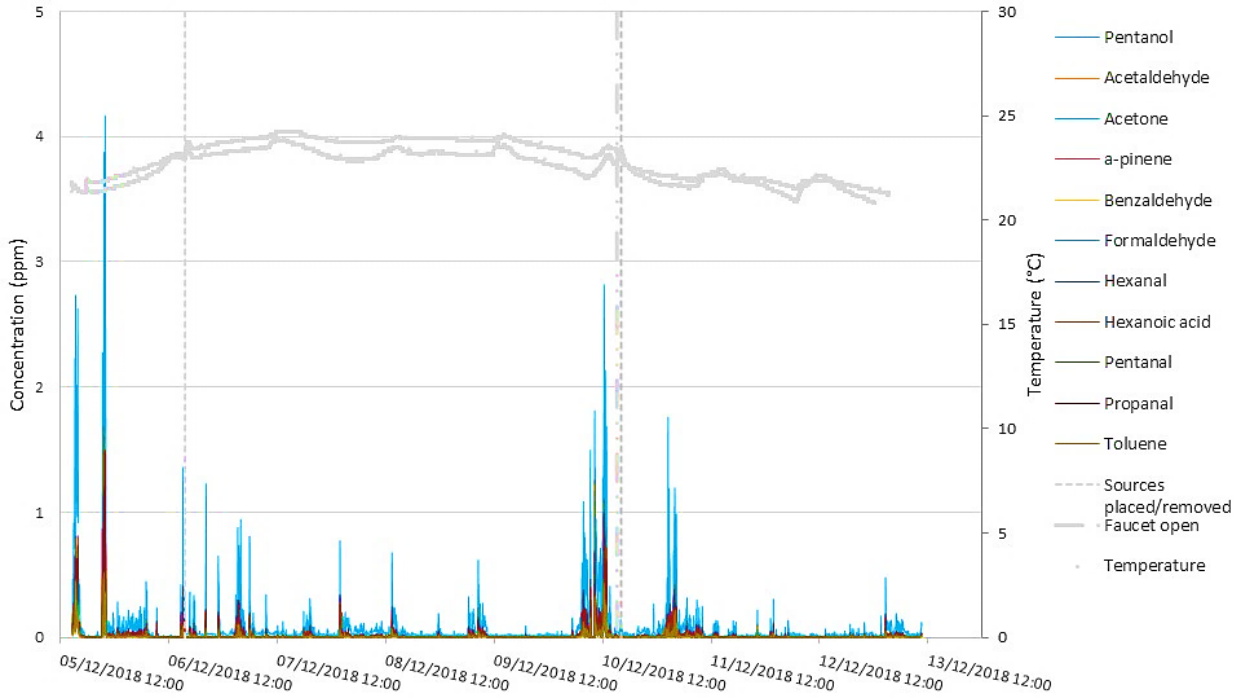

Figure 38 - VOCs data monitored by the Sift MS.

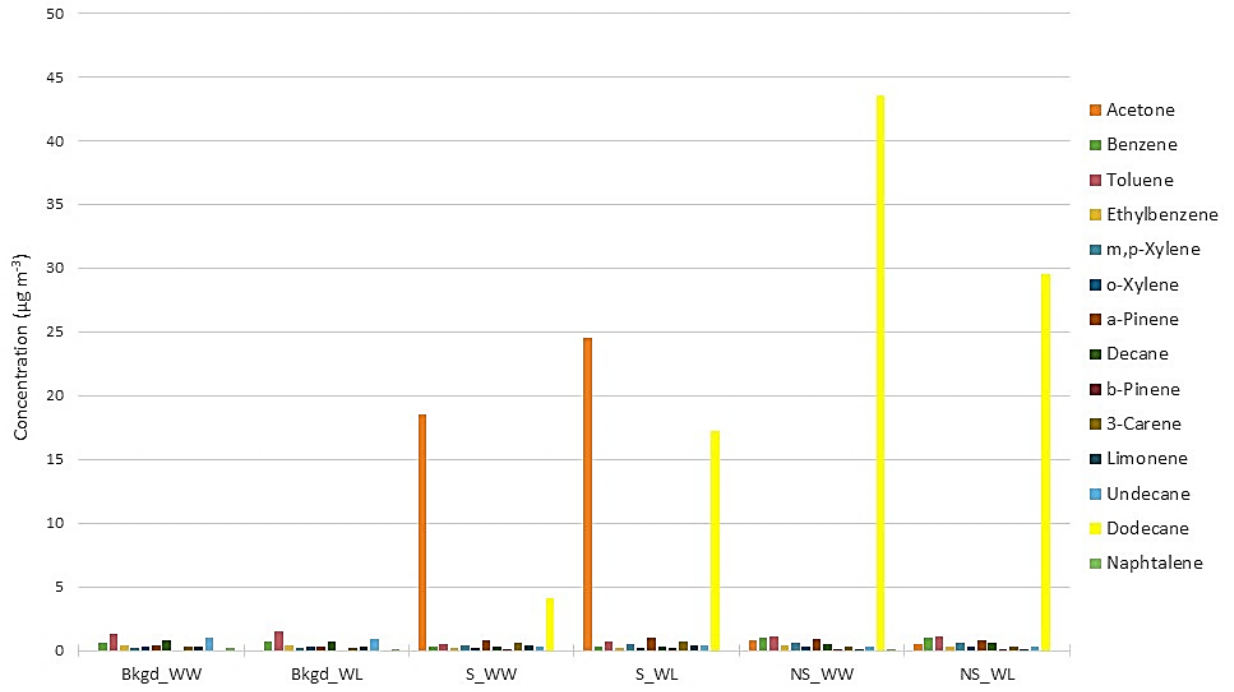

Figure 39 - VOCs average concentrations measured by passive sampling (Bkgd refers to the background samples; WW represents the point located next to the window; WL represents the point away from the window; S refers to the samples taken with the presence of sources and NS refers to the samples taken after the sources were removed).

5.5 Final Considerations

The Office Experiment monitored VOCs emissions by two different source products for 8 days in an unoccupied office space. The results recorded by the Sift MS were similar to those reported in the House Experiment in magnitude and trend. Moreover, the highest concentrations of VOCs were observed in the background period, before the placement of the sources. Peak concentrations during

the background period were also observed in the House Experiment, and the reason is probably analogous (movement and transportation of devices during the experiment setup increase the VOCs indoor levels) yet intensified here due to the installation of the plastic sealing to the door opening. On the other hand, the placement of the sources did not affect the Sift MS measurements. The passive sampling yielded generally low VOCs concentrations, except for dodecane and acetone. As already said in the final considerations of the House Experiment, these passive sampling results should be considered with care and it is recommended that future field experiment of this nature have a longer duration to allow more adequate sampling periods for the passive samplers.

Chapter 6: Field test 5 – The Dual Building

This chapter describes two field experiments executed in Canada in the context of Subtask 5 of Annex 68. The goal of the first experiment was to assess the impact of different heating systems' mode of heat transfer (radiative, forced air, or/and natural convective) on the indoor air temperatures and relative humidity distributions. In this experiment, the energy use and thermal comfort of buildings with different heating systems are compared. The goal of the second experiment was to study moisture buffering and ventilation strategies to control indoor humidity.

The following sections describe in detail the setup and outcomes of each experiment.

6.1 Energy use and thermal comfort of buildings with different heating systems

6.1.1 Context

The performance of a building can be characterized by its energy use, thermal comfort, indoor air quality, and durability. A good understanding of these indicators enables designers and engineers to design and optimize high-performance buildings that offer a healthy and comfortable indoor environment while at the same time being energy efficient. Buildings use different mechanical systems to create a comfortable living environment for occupants. The mode of heat transfer of the heating systems could be convective, radiative or combination of both. The thermal energy required to maintain the same indoor temperature using different heating systems with a different mode of heat transfer could be different. In addition to thermal energy, the thermal comfort of the living space could be different.

Most of the research work presented in the literature is conducted at steady or quasi-steady state conditions in a climate chamber with isothermal surfaces and constant temperature difference across the surfaces. Although the information generated is quite useful, it needs to be extended to building operations in a field as the actual environment is much more dynamic and complex, involving solar, wind wash, longwave radiation, rain, snow, and different thermal dynamics and loads on surfaces of different orientations at a given time.

In this work, the performance of four heating systems, namely, electrical baseboard heater (EBH), portable radiator heater (PRH), air-air heat pump (HP), and radiant floor heating (RFHS) (Figure 40), are studied in a field experimental setting. The space-heating systems RFHS, HP, EBH, and PRH represent surface heat source, forced air heating system, line heat source, and a unit heat source, respectively. The thermal energy used by the test buildings, as well as the thermal comfort, local thermal discomfort, temperature distribution, and RH distribution, is used to assess and compare the systems' performances.

EBH

PRH

HP

RFHS

Figure 40 - Heating systems considered in the study.

6.1.2 Experimental study

The approach followed to investigate these systems' performance involves running two different systems in two identical buildings (Figure 41) and measuring the buildings' energy use, indoor air environmental conditions (temperature and relative humidity at various points), and interior surface temperatures. The two full-scale identical test buildings, located at BCIT Burnaby campus, are exposed to similar outdoor climatic conditions and set to simulate small, detached residential buildings with identical building operating scenarios including setpoint, occupancy schedule, and ventilation rate and strategy.

a) STB b) NTB

Figure 41 - Whole Building Performance Research Laboratory (WBPRL).

The overall dimension of these buildings is 16 ft x 12 ft floor area and 10 ft height. The buildings are constructed using 2 by 6 woodframe standard walls with fiberglass insulation in the stud cavities. These buildings have insulated slab on grade, and 2 by 12 woodframe flat-roof construction. The buildings also have two double-glazed windows on the north and south walls of the buildings. Both buildings are equipped with generation of heat, moisture and CO_2 profiles of the desired type, reflecting simulated occupants' activity. The energy source for the four heating systems is electricity, and they have a heating capacity of 3.9 kW (RFHS), 2.3 kW (HP), 1.5 kW (EBH), and 1 kW (PRH). The flexibility that is available in operation and setup of the simulated occupancy loads and mechanical systems (heating and cooling), coupled with the exposure of the building to a similar outdoor climate, makes the test facility ideal for side-by-side comparative study.

6.1.2.1 Sensors and Sensor Layouts

The buildings have two separate rooms: a test room and a mechanical room (Figure 42). Each test room is equipped with sensors measuring air temperature, air velocity, globe temperature, relative humidity, and CO_2 concentration, while each mechanical room houses the air conditioning and ventilation systems and the DAQ equipment. Figure 42 shows the layout of the sensor in the test room. Sensors are positioned at four horizontal locations (L1, L2, L4, L5) and five vertical positions (P0, P2, P3, P4, PC) to map the indoor air temperature, relative humidity and CO_2 distributions in the test room. The temperature measurement is conducted at various levels ranging from floor to ceiling at different five locations. At the center of the test room globe, a thermometer is positioned for global thermal comfort calculation.

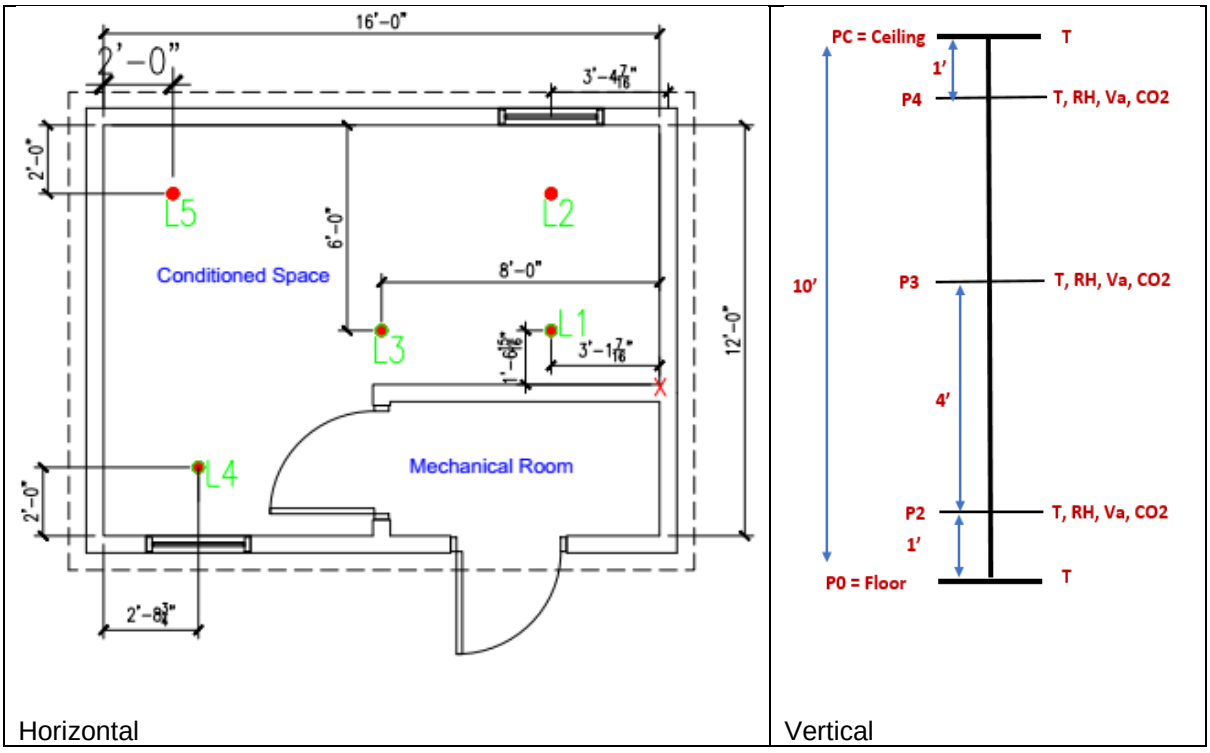

Figure 42 - Horizontal and vertical sensor locations.

The temperature, velocity and RH measurements at different points in the test room are used for local thermal comfort calculations. The interior surface temperatures of the walls in all the four orientations are measured at three vertical positions (one foot above the floor, mid-height, and one foot below the ceiling). Similarly, the temperatures at the wall corners, are measured at mid-height position, and the north and south windows at the center of the glass.

The energy consumption of the heating systems is recorded using an energy monitoring system (PowerScout 24), which is integrated into the test buildings' electric circuits and measures the amount of electric power drawn by the system. The PowerScout 24's reading is verified using an independent power meter, and by running the same heating systems in the two test buildings and comparing the buildings' readings.

6.1.2.2 Weather Condition During the Experimental Period

Figure 43 presents the outdoor weather condition, measured using an onsite rooftop weather station, during the experimental measurement period. The outdoor air temperature varies between –6°C to 12°C and the relative humidity varies between 24% and 100%. Solar radiation during the testing period varies with days with no solar radiation and days with limited solar radiation. Peak solar gain is less than 600 W m^{-2}.

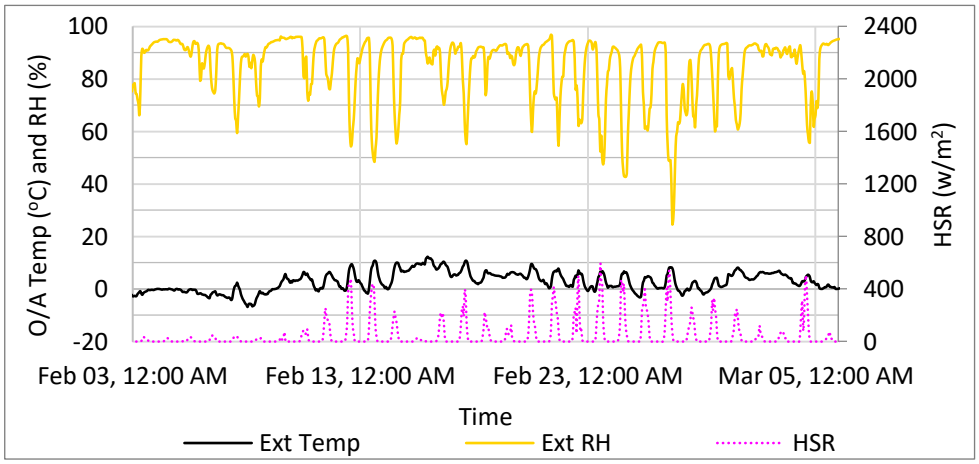

Figure 43 - Outdoor weather conditions over the measurement period.

6.1.3 Results and Discussion

6.1.3.1 Thermal Energy

The thermal energy comparison of the four heating systems is conducted using 24-hour total energy data from the four-day period side by side test period in which the maximum room temperature difference between the two test buildings is less than 0.5°C. Figure 44 shows the typical measurement parameters, which are the hourly thermal energy provided by the EBH and the HP over the four-day period along with the indoor temperature, outdoor temperature, and horizontal solar radiation. As shown in the figure, the thermal energy supplied by the heating systems have similar trends, and their magnitudes change with outdoor weather conditions to maintain similar indoor setpoint temperature.

The thermal energy comparison of the four heating systems is shown in Figure 45. Overall, all heating systems provided similar (small difference) thermal energy to maintain similar indoor air temperature. The test buildings used about 10 kWh to 14 kWh in days when the outdoor average temperatures were 7.1°C and 1.4°C, respectively. The slight difference in thermal energy between the portable heater and the other systems is associated with the location of the thermostats that control the systems. The PRH is controlled with an internal thermostat, whereas the other systems are controlled by a wall-mounted external thermostat.

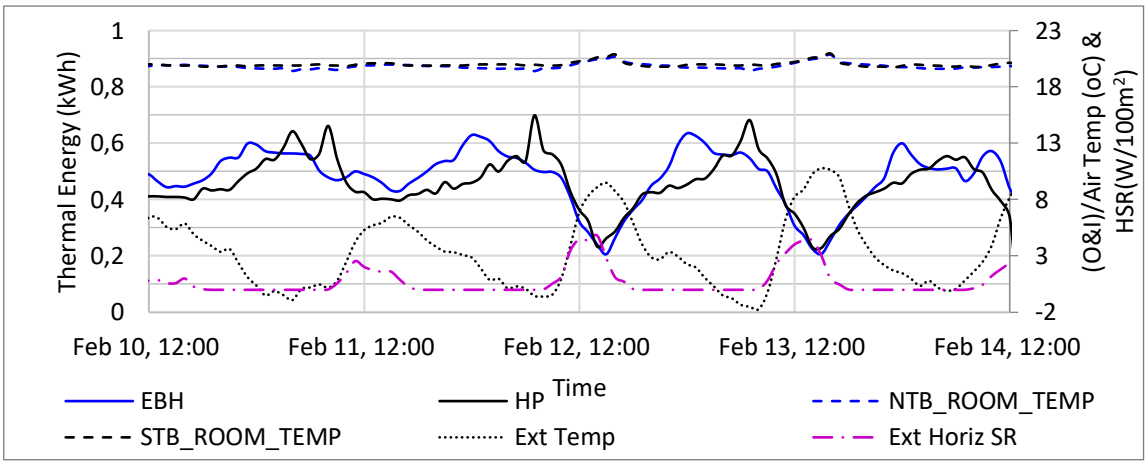

Figure 44 - Thermal energy profile of EBH and HP with indoor and outdoor conditions.

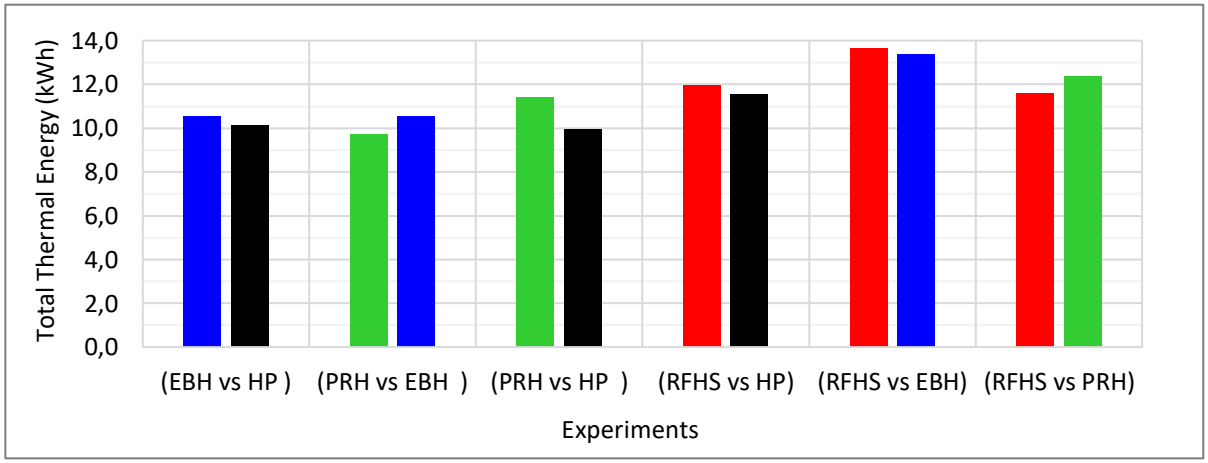

Figure 45 - One-day total thermal energy supply at the same outdoor and indoor environmental conditions.

6.1.3.2 Indoor Air Temperature Distribution

The indoor air temperature distributions of the test buildings while running the four heating systems are presented in Figure 46. The temperature readings in five horizontal locations (L1-L5) and three vertical positions (P2-P4) are plotted using a color gradient. To isolate the effect of the heating systems in the indoor air temperature and relative humidity conditions from other effects such as solar radiation, measurement data in early morning (6:00 am) are used. In all cases but RFHS, the indoor air temperature in the test buildings varies with distance from the floor. Higher temperatures are measured at P4, 1ft from the ceiling, and the colder at position P2, 1ft above the floor. The vertical temperature difference between P4 and P2 remain around 3°C for those three heating systems, but in the case of RFHS, the temperature difference is less than 0.4°C. In general, the temperature distribution when using RFHS is more uniform relative to a room with HP, EBH, or PRH, which is a difference of 0.5 and 3°C in air temperature distribution. The accuracy of the temperature sensor is ± 0.2.

Figure 46 - Indoor temperature distribution while using the four heating systems.

6.1.3.3 Indoor Humidity Distribution

The RH distribution for all heating systems mostly remains between 40% and 50%, with an average of 45% throughout the room, as shown in Figure 47**Error! Reference source not found.**. The RH distribution in the case of RFHS shows 45 ± 1% in all locations except L2 (> 46%), which is in front of the south window. While for the other heating systems, the RH distribution in the test rooms inversely follows the temperature distribution presented in Figure 49**Error! Reference source not found.**, relatively higher RH close to the floor (P2) and lower RH close to the ceiling (P4). The accuracy of the RH sensor is ± 2%.

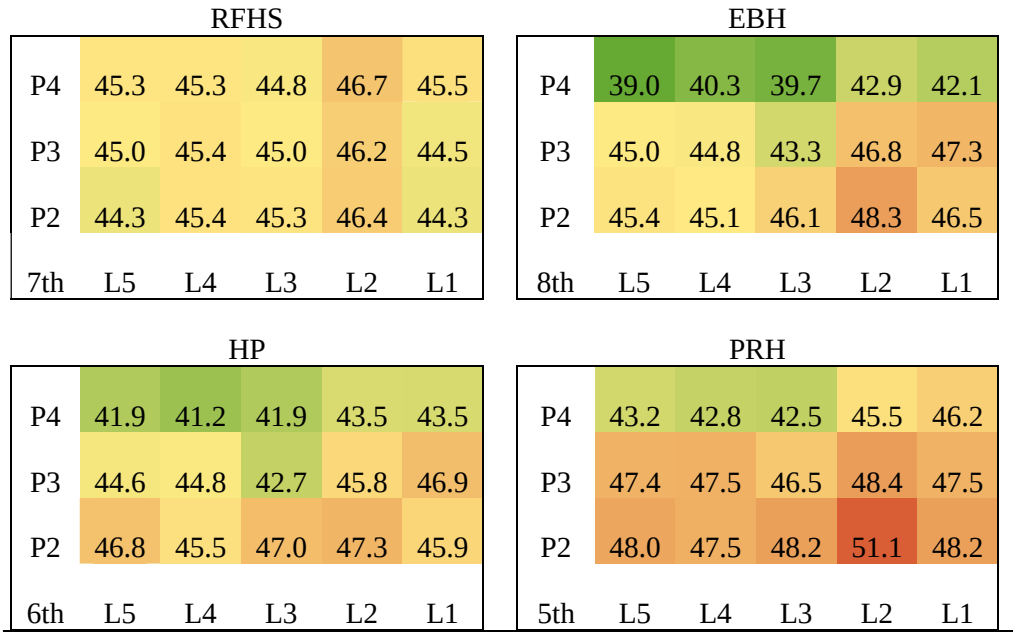

Figure 47 - Interior RH distribution while using the four heating systems.

6.1.3.4 Surface Temperature Distribution

This section presents the surface temperature distributions in the test buildings while running the four different heating systems (Figure 48). Profiling of surface temperature can help to identify potential durability problems in relation to condensation and mold growth as well as thermal discomfort related to occupants' radiative heat loss (or establishing mean radiant temperature). In the line and point heat source cases (EBH and PRH, respectively), the portions of the ceiling surface directly above the heat sources and the wall opposite to the heat sources are warmer when compared to other locations. Wall surfaces perpendicular to the heat sources or with low view factors, such as east wall, show lower surface temperatures. In general, the wall temperatures follow the room temperature profile, which means getting warmer with increases in vertical distance from the floor. The surface temperature distribution along the height of the walls (1 ft above the floor and 1ft below the ceiling—8 ft apart) can vary between 1.3°C to 2.4°C in the EBH, PRH and HP cases. The higher deviation belongs to EBH. In the cases of the RFHS, the surface temperature distributions are uniform within 0.7°C. The difference between the ceiling and floor temperatures in the EBH, PRH, and HP is 5.1°C, 3.6°C, and 4.1°C, respectively.

In the RFHS, the surface temperatures of the north and south windows are within 0.6°C difference. Whereas in the cases of EBH and HP, the south window is warmer than the north window by 1.3°C and 2.7°C, respectively. The difference is attributed to the fact that the south window is close to the heat sources, and the north window is not. The EBH and PRH are located below the south window, and the indoor header of the HP is installed on a wall facing the south window.

6.1.3.5 Thermal Comfort

This section presents the general and the local thermal comforts of the test buildings while they are operating the four heating systems. The buildings' thermal comfort is assessed through the determination of the percentage of people dissatisfied (PPD) with the buildings' indoor thermal condition. PPD values are calculated using the measured indoor air temperature, surface temperatures, relative humidity, and air velocity. For the thermal comfort calculation, a person sitting at the geometric center of a study/reading room with a typical winter clothing (1 CLO) and a metabolic activity rate 58.2 W m^{-2} (Met = 1, for light activity) are considered.

6.1.3.6 General Thermal comfort

Figure 49 shows the thermal comfort (in PPD) of the test buildings with EBH and HP systems. As it shows, their PPDs are higher than 20% and, according to ASHRAE 55, which limits the PPD to maximum of 20%, both buildings are thermally uncomfortable. In general, the thermal comfort of the buildings improves with an increase in outdoor temperature and solar radiation. It reaches its highest value around 3 pm, then gently falls. Although the indoor air temperatures of the two buildings are maintained close at 20°C throughout the day, the thermal comfort dissatisfactions are higher in early morning when there is no solar radiation and the outdoor air temperature is low. This is attributed to the lower mean radiant temperature (interior surface temperatures) in the morning as the result of the colder night temperature. During this time, the thermal comfort of the building with EBH has relatively lower thermal comfort when compared with the building with HP (33% vs 25% PPD). The thermal comfort difference between the systems can be attributed to difference in the mean radiant temperature. The HP fan circulates warm air in the test building, thereby increasing surface and mean radiant temperatures.

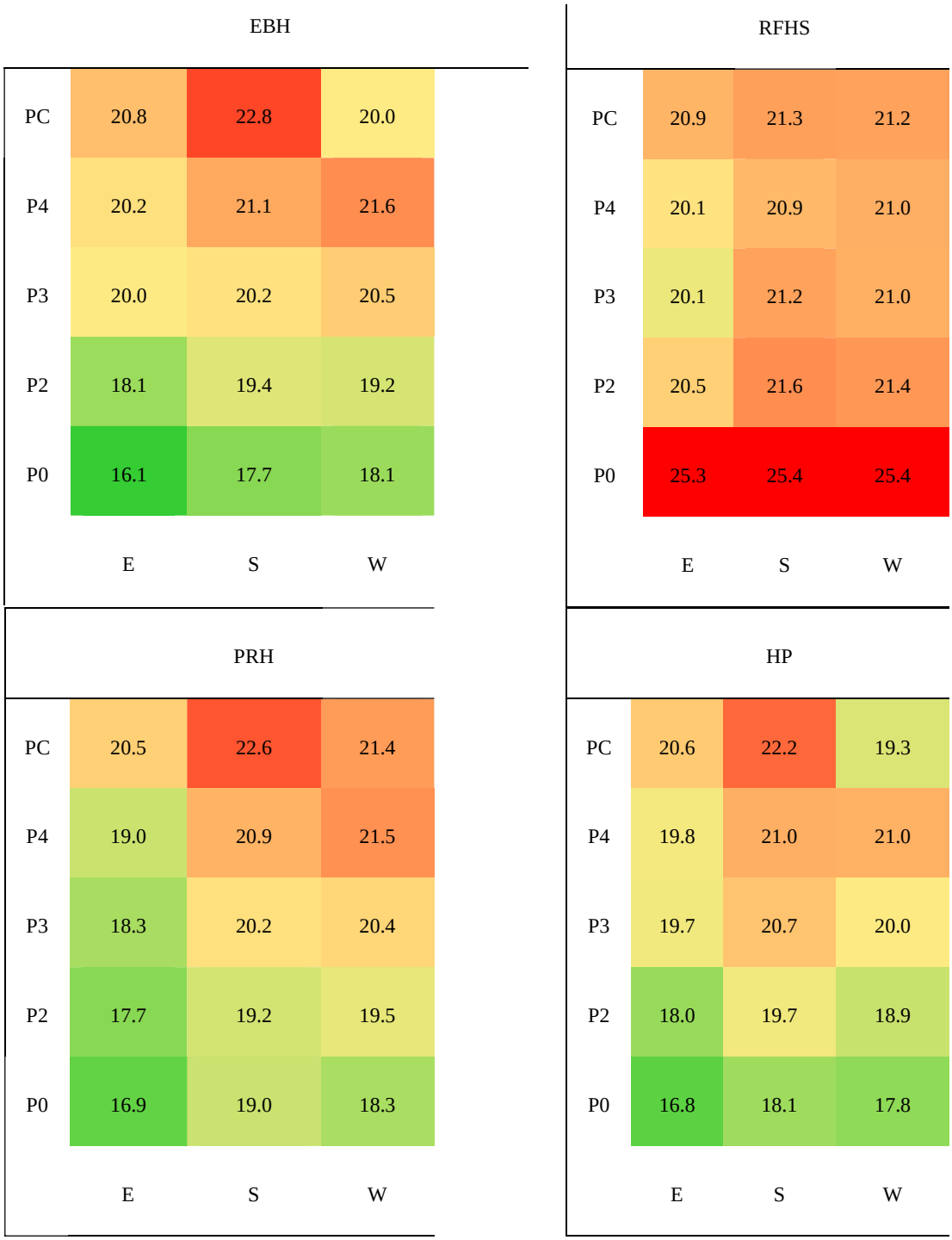

Figure 48 - Surface temperature distribution using four heating systems within the period where thermal energy is compared.

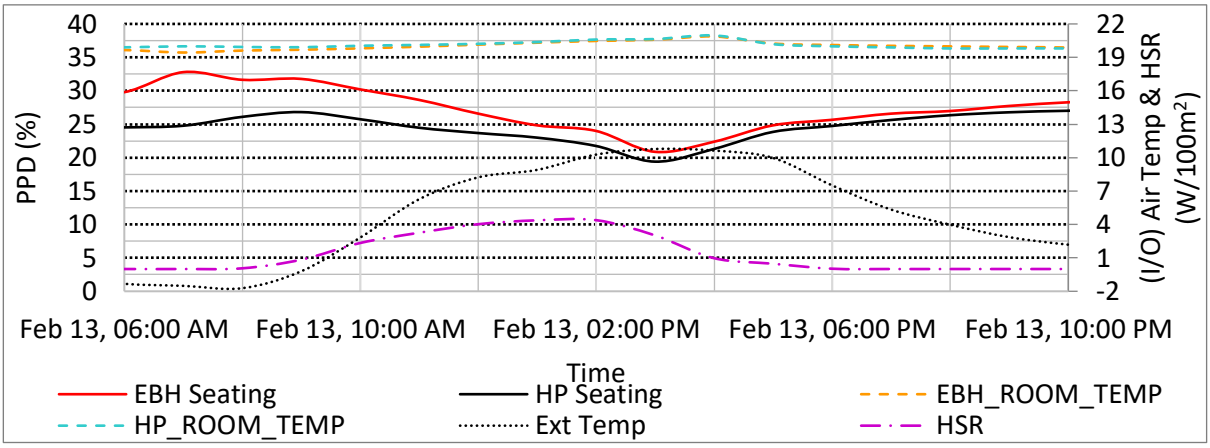

Figure 49 - Thermal comfort (PPD) for a seating person: EBH vs HP.

Figure 50 shows the thermal comfort in the test buildings with RFHS and HP. During this test case, the outdoor air average temperature is 5.4°C, which is warmer than the test case presented above (-1.3°C). In this test case, both buildings satisfy the ASHRAE general thermal comfort requirement (PPD < 20%). In relative terms, the building with RFHS shows a better thermal comfort than the building with the HP with about 4% PPD reduction. While the thermal comfort in the building with HP varies with the changing outdoor air temperature and solar radiation throughout the day, the thermal comfort in the building with RFHS seems to be stable. As can be learned from comparing this and the previous case, maintaining the same indoor air temperature by a mechanical system does not guarantee the same thermal comfort, but rather determined by outdoor air temperature and solar radiation conditions, which influence surface temperature and mean radiant temperature. That is why the test building with HP is thermally acceptable in the current test case but was not in the previous case. To remain comfortable, occupants might need to adjust their clothing levels, depending on outdoor weather conditions, to avoid thermal discomfort.

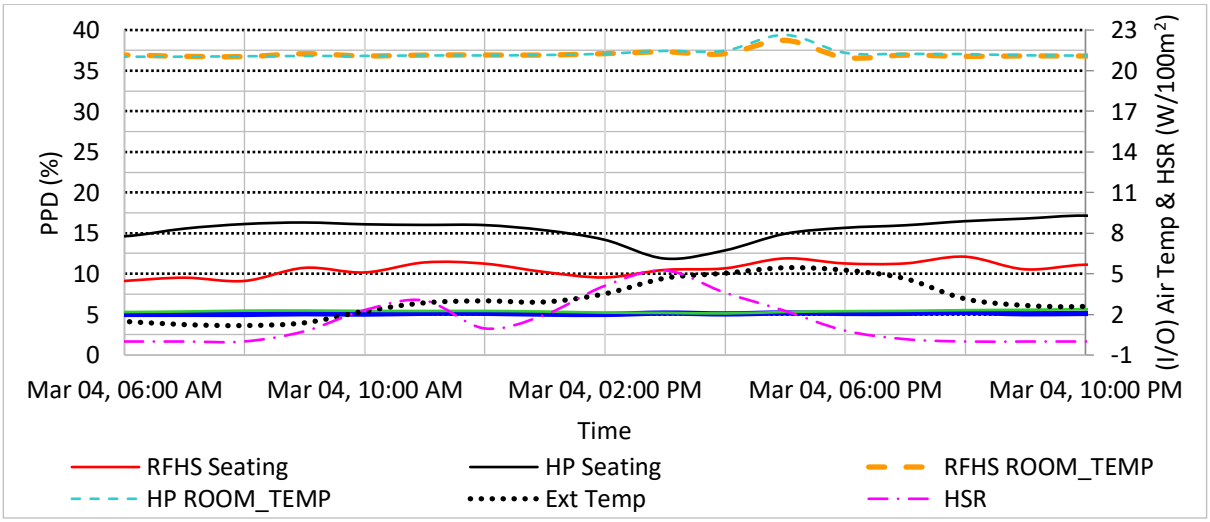

Figure 50 - Thermal comfort (PPD) for a seating person: RFHS vs HP.

6.1.3.7 Local thermal comfort

This section presents the local thermal comfort variations in buildings with different heating systems. The local thermal comfort indicators that are considered here are vertical temperature difference, floor surface temperature, and radiant asymmetry.

Local thermal discomfort as the result of vertical temperature difference

The local thermal discomfort due to the vertical temperature difference is calculated along the test room centre position (L3). In the test buildings with HP and PRH, the maximum percentage of dissatisfied (PD) is 2.25%, and 2.75% and 0% while using EBH and RFHS, respectively. In general, the local thermal comforts associated with vertical temperature differences are acceptable in all the four heating systems because their respective PDs are less than the maximum 5% PD threshold set in ASHRAE 55 (2013).

Local thermal comfort as the result of floor surface temperature

The average floor temperature reading from five thermocouples is used to calculate PD due to floor temperature. The percentage of dissatisfied while using RFHS is within 6 ± 1%. While running HP, PRH, and EBH, the PD increases between 12% and 15%. Out of the four heating systems, only the RFHS provides thermally acceptable floor surface temperature. The remaining three heating systems yielded PD beyond the acceptable limit set in ASHRAE 55 (10%). Accordingly, the occupant can experience thermal discomfort as the result of cold floor temperature while using HP, PRH, and EBH heating systems. One of the reasons for the cold floor and higher PD values obtained here is due to the significant perimeter heat loss that the small buildings are subjected to.

Local Thermal Discomfort Due to the Floor to Ceiling Radiant Asymmetry

The radiant asymmetry can be due to a cool ceiling or warm floor. The RFHS creates a warm floor compared to the ceiling; the corresponding asymmetry then is cool ceiling radiant asymmetry. The other three systems (EBH, PH, and HP) create a warm ceiling in comparison to the floor; thus, the asymmetry becomes warm ceiling radiant asymmetry. According to ASHRAE 55 (2013), the maximum allowable thermal discomfort due to radiant asymmetry is 5%. The test building with RFHS exhibits close to 0% PD due to the floor to radiant ceiling asymmetry, and the other heating systems (EBH, HP, and PRH) create a nearly acceptable floor to ceiling radiant asymmetry (4% to 6% PD). Overall, RFHS provides the best thermal comfort environment (both general and local) to occupants.

6.1.4 Conclusion

To sum up, this study conducts six pairs of field experiments comparing four heating systems. The comparison involves analyzing the relative thermal energy performance and general/local thermal comfort of the heating systems as well as investigate various aspects of the indoor environmental condition by the systems such as temperature distribution and RH distribution to understand how the system performs.

All heating systems supply similar thermal energy into the test building. The temperature distribution shows that EBH, HP, and PRH provide cold floor temperature. Whereas, RFHS produce warm floor temperature (over 24°C). Above the floor, the RFHS also creates a more uniform temperature distribution in contrast to the rest of the heating systems, while the temperature distribution with EBH, HP, and PRH heating systems depicts a less uniform temperature profile. In addition, the coldest wall is the east wall and the coldest spot is the north window since they are far from the heat source/heating systems. The indoor environment produced by the heating systems is assessed for thermal comfort for a seated person. The thermal comfort of buildings with EB, PRH, and HP is dependent on outdoor air temperature and solar gain, whereas in buildings with RFHS, the thermal comfort is found to be stable and within an acceptable range (PPD < 20%).

The local thermal comfort in buildings with the four heating systems is assessed using local thermal discomfort indicators associated with radiant asymmetry, vertical temperature difference, and floor temperature. All heating system creates acceptable local thermal discomfort (PD < 5%) due to vertical temperature difference. Out of the four heating systems, only RFHS deliver thermally acceptable floor surface temperature (PD < 10%). The building with RFHS exhibits close to 0% PD due to the floor to radiant ceiling asymmetry, and the other heating systems (EBH, HP, and PRH) yielded close to the PD limit set by ASHRAE (5%).

Acknowledgments

The authors are thankful for the financial support from Natural Science and Engineering Council Canada (NSERC), Canada Research Chair (CRC) and the School of Construction and the Environment at the British Columbia Institute of Technology (BCIT), and technical support of Mr. Doug Horn.

6.2 Moisture Buffering and Ventilation Strategies to Control Indoor Humidity

6.2.1 Context

In the Lower Mainland of BC, many buildings have undergone rehabilitation to prevent water ingress and deterioration following widespread poorly constructed leaky condos from the 1980's and 1990's. To prevent future rainwater penetration from the exterior, the building enclosures are designed for better water shedding and watertightness. Rehabilitation of the building enclosure for preventing water ingress also presents opportunities to improve the airtightness. Building retrofits such as those extensively done in the Lower Mainland of British Columbia for water ingress prevention or elimination have resulted in significantly more airtight buildings. However, in many instances, the enclosures were made more airtight without consideration for the need to increase ventilation. Adequate ventilation is crucial especially when moisture production of occupants may exceed design moisture loading. Without adequate ventilation, tighter building enclosures will generally result in elevated humidity levels and higher humidity peaks, and increase the risk of condensation in the building enclosure and on cold surfaces such as window glazing.

Staying within this range is challenging for buildings located in marine climates such as the Pacific Northwest of the United States, and Southern West Coast of British Columbia. In these climates, outdoor air temperature is mild and the air is humid. Therefore, ventilation alone may not suffice in managing indoor moisture, especially if moisture generation of occupants exceeds the design moisture generation rate. In these climates, further passive measures such as the aid of moisture buffering materials, or active measures such as dehumidification may be required to manage indoor moisture. Condensation can adversely affect the durability of a building. Chronic condensation and moisture accumulation leads to deterioration of the building enclosure and structural materials, such as softening of gypsum drywall, wood decay, corrosion of steel, peeling of paint finishes, damage to moisture sensitive insulation, and growth of mould, mildew, and fungi which can be detrimental to health (HPO, 2006). With rehabilitation resulting in tighter building enclosures, sufficient ventilation measures are required to avoid building durability issues. Sufficient ventilation can be achieved by means of retrofitting mechanical systems such as installing exhaust fans where there are none existing, upgrading existing exhaust fans to a higher flow rate model, implementing make-up air supply systems or heat recovery ventilators. Physical constraints of the building or cost limitations may render mechanical ventilation retrofits infeasible, in which case opening windows or running exhaust fans more frequently or continuously are required to reduce indoor humidity. Opening windows and running ventilation fans more frequently may address condensation and durability issues, but since more heating energy is required for additional outdoor air intake, they are also measures that compromise energy efficiency.

The intent of ventilation is to promote good indoor air quality by diluting or displacing indoor air ridden with pollutants and odours and allowing outdoor air to replace displaced air. In cold climates, it also allows indoor moisture-laden air to be exhausted to the exterior and be replaced with dryer outdoor air. Ventilation of indoor air also allows for removal of excess indoor moisture and management of indoor humidity.

The upper and lower relative humidity threshold of indoor spaces is debated. In general, consensus is that interior relative humidity should not exceed 60% (70% at a building surface) to avoid mould growth and germination. The lower threshold is less concrete, however ASHRAE recommends that indoor relative humidity stay above 25% to avoid irritation of the respiratory mucus membrane and the eyes

(Lstiburek, 2002).

The motivation for this research comes from a low-income housing reference building in Vancouver, BC with high indoor humidity and building durability issues brought on by air-tightening the building enclosure following rehabilitation. Implementation of new ventilation exhaust fans and operating schemes were not sufficient in addressing the building humidity and durability issues. Field experiments were designed to mimic the scenario of a suite in the low-income housing reference building and used to develop solutions to address the high indoor humidity problem, while also considering heat loss through ventilation and indoor air quality. The effect of moisture buffering of interior gypsum board as a passive means to reduce indoor humidity was investigated.

6.2.2 Methods

Two test building facilities with identical roof and floor assemblies, dimensions, orientation, and location were monitored to compare the effects of moisture buffering properties of gypsum wallboard and varying ventilation schemes on indoor humidity and air quality conditions (Figure 51). The buildings are located in Burnaby, British Columbia, an area characterized by mild climate, warm summers and cool rainy winters. All exterior boundary conditions during the monitoring period were recorded by a weather station on site. Tariku et al. (2013) outline the design, construction, systems, and equipment of the buildings in more detail.

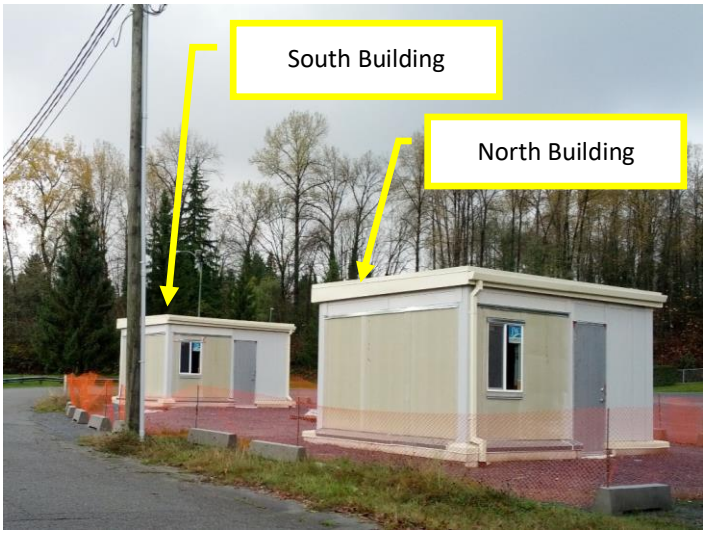

Figure 51 - Two test building facilities used for the experimental study.

A field experiment is designed to simulate the conditions of a residential suite and measure the response in indoor conditions under varying outdoor conditions, and ventilation strategies in the presence of moisture buffering and no moisture buffering. Daily indoor moisture and CO_2 generation profiles are determined based on analysis of real occupants in a 'Reference Building' described later in this paper. Indoor moisture and CO_2 is released in the field experiments based on the predetermined daily profiles using programmable occupant simulator units. The ventilation system operates as per pre-defined ventilation schemes for four different test cases. For each test case, the performances of hygroscopic versus non-hygroscopic interior finished buildings are directly compared for the same outdoor conditions. Performance of the buildings across test cases is also compared.

6.2.3 Experimental setup

Table 12 lists the parameters and variables for each of the buildings for test cases defined. Each test case is run for approximately one week. One or more days are dedicated to conditioning the materials for each test case, in order to reach quasi-equilibrium. With these field experiment test cases, it will be possible to assess the effects of the variable test parameters: the effect of ventilation strategy, and moisture buffering of gypsum wallboard on indoor relative humidity, indoor air quality, and ventilation heat loss.

Table 12 - Test cases and respective parameters and variables in each test and control buildings.

Test Period			Control Building (North Hut)	Test Building (South Hut)
Test run #1	Apr. 2-4/14	**Finish Material**	Polyethylene	Unpainted gypsum board
		Ventilation Rate	15 CFM (Cubic Feet per Minute)	15 CFM
		Ventilation Scheme	Constant	Constant
Test run #2	Apr. 12-14/14	**Finish Material**	Polyethylene	Unpainted gypsum board
		Ventilation Rate	30 CFM at 8am - 12pm and 7pm - 11pm, 7.5 CFM all other times	30 CFM at 8am - 12pm and 7pm - 11pm, 7.5 CFM all other times
		Ventilation Scheme	Time-controlled	Time-controlled
Test run #3	Jun. 22-24/14	**Finish Material**	Polyethylene	Unpainted gypsum board
		Ventilation Rate	7.5 CFM at 50% RH or less, 30 CFM at 60% RH or more, between 50-60% RH linearly increasing CFM between 7.5 and 30 CFM	7.5 CFM at 50% RH or less, 30 CFM at 60% RH or more, between 50-60% RH linearly increasing CFM between 7.5 and 30 CFM
		Ventilation Scheme	RH-controlled	RH-controlled
Test run #4	Jul.5-7/14	**Finish Material**	Polyethylene	Unpainted gypsum board
		Ventilation Rate	7.5 CFM at 800ppm or less, 30 CFM at 1000ppm or more, between 800-1000ppm linearly increasing CFM between 7.5 and 30 CFM	7.5 CFM at 800ppm or less, 30 CFM at 1000ppm or more, between 800-1000ppm linearly increasing CFM between 7.5 and 30 CFM
		Ventilation Scheme	CO_2-controlled	CO_2-controlled

One building is clad with unpainted gypsum board on the interior of the building enclosure, which has hygroscopic properties and is designated as the test building (South Building). The non-hygroscopic building is covered with 6 mil polyethylene sheet on all interior surfaces and is the designated control building (North Building). Both the test and control building are exposed to the same variables for a given test case, however, the test building has moisture buffering potential, while the control building has the moisture buffering effect eliminated. Other than vertical wall surfaces, all surfaces of the interior of the buildings exposed to test conditions were isolated during testing; the concrete floor, footings, and ceiling were sealed with 6 mil polyethylene sheet to prevent possible interactions between those materials and moisture inside the test space.

Indoor Moisture and CO_2 Load

Moisture generation is simulated by releasing moisture and CO_2 hourly based on occupants' behaviour in the real occupied 'Reference Building,' using the automated occupant simulator units. To isolate the moisture production of occupants and their activities, indoor conditions of a two-bedroom apartment

suite in a 'Reference Building' were analyzed. The suite is occupied by a family of four, two adults and two children and covers 643 ft^2 (59.7m^2) of area, and with a clear height of 8 ft encompasses 5144 ft^3 (149 m^3) of volume. The north-facing wall is the only exterior wall of the suite. This wall has one window in each bedroom, and a balcony adjacent to the living room. All other walls are adjacent to other suites or the building corridor. The kitchen is enclosed by interior walls on three sides and open to the living room on one side. The bathroom is located near the entrance door of the suite. The suite has a bathroom exhaust fan, which is intermittently on at 7-11 am and 6-10 pm. The kitchen is equipped with a range hood fan that is turned on manually. Fresh air is supplied to the suite through open windows, the balcony door, and the entrance door undercut.

Figure 52 show daily relative humidity profiles of the interior of the suite for 90 days of monitoring completed between December 1st, 2010 and February 28th, 2011. A typical daily moisture generation profile was determined from this data using statistical analysis, which is further outlined in Pedram & Tariku (2015). Typical moisture loading identified by Kunzel, et al. (2004) in studies of German homes is about 48g/m^3 per day. This corresponds to 1.9 kg of moisture per day for a building with a volume of 40.5m^3, the size of the ones at the test building facilities used. The total moisture production per day of the typical moisture generation profile obtained based on the monitoring data from the 'Reference Building' scaled down to the size of the test building facilities equates to 1.9 kg/day, which is in line with the findings from this study.

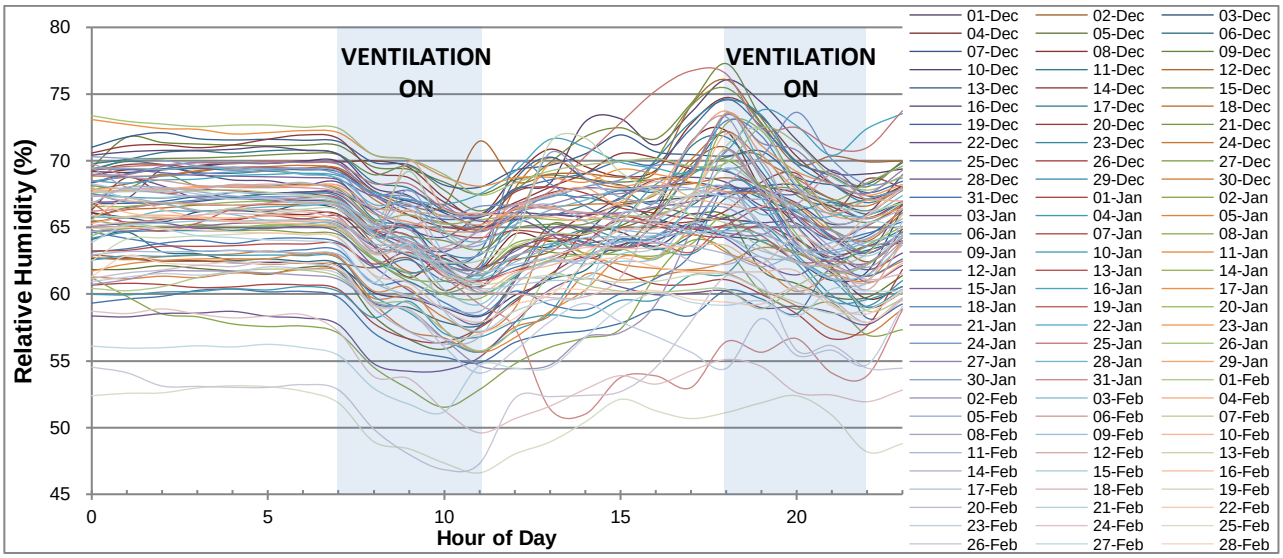

Figure 52 - Daily relative humidity profiles of suite in the 'Reference Building' for 90 days of monitoring.

An image of the occupant simulators' moisture dispensing unit is shown in Figure 53, which was used to release predetermined rates of moisture throughout the day in the field experiment, based on the typical daily moisture generation profile obtained from the 'Reference Building' data.

Because it is difficult to measure odour intensity in a space, CO_2 concentration is typically used as a surrogate indicator to evaluate the indoor air quality and ventilation adequacy of a space. CO_2 concentration in a building is dictated by the occupants, as well as the CO_2 levels in the ambient outdoor air. CO_2 production rate depends on the occupants' level of activity and diet. CO_2 generation per person can be estimated using the oxygen consumption rate, from Equation given in ASTM Standard D6245 (2012).

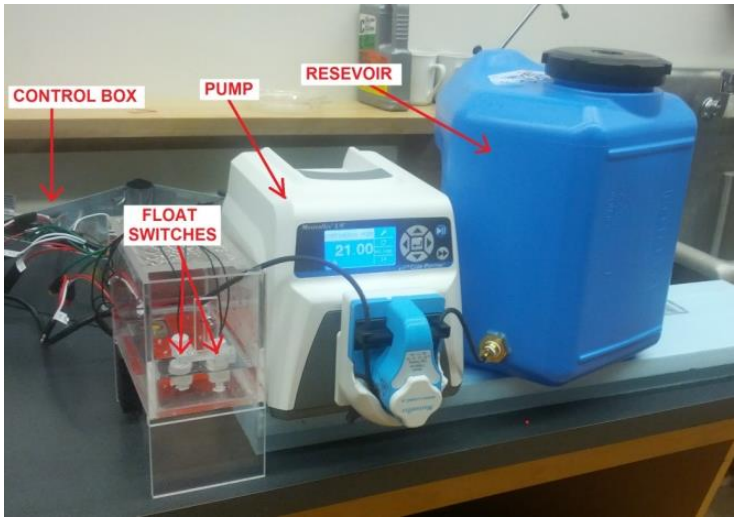

Figure 53 - Occupant simulator equipped with control box, humidifiers, water reservoirs, pumps, CO_2 release valve (not shown), and heat generating bulb (not shown)

Equation 9 - Oxygen Consumption of Occupants (ASTM D6245, 2012)

$$V_{O_2} = \frac{0.00276\ A_D\ M}{0.23\ RQ + 0.77}$$

V_{O_2}= Oxygen consumption rate (L s^{-1}),
A_D = DuBois body surface area (m^2),
M = Metabolic rate per unit of surface area (1 met = 58.2 W m^{-2})
RQ = Respiratory quotient, volumetric ratio of CO_2 produced to oxygen consumed (unitless)

To determine the rate of CO_2 emission of the occupant simulators for the testing, the level of occupants' activity was assumed for a typical day based on results of a questionnaire outlining their presence and typical activities in the suite. Figure 54 shows the assumed level of activity for the family of four throughout the day, assuming there are two adults, one who works from home with two children. The metabolic activity rates were estimated from each occupant's level of activity as outlined in Figure 54, from Equation 9, and corresponding CO_2 generation rates were determined based on oxygen consumption rate and RQ. Body surface area was assumed to be 1.8 and 1.0 m^2 for adults and children respectively. RQ was assumed to be 0.83. When scaled down by the volumetric ratio of the 'Reference Building' to the test buildings, the occupants' normal and peak activity CO_2 generation rates are 0.20 and 0.33 L min^{-1} respectively.

A solenoid valve on the occupant simulator units' CO_2 dispensing system requires voltage input for release of predetermined rate of CO_2 into the room. The rate of CO_2 release varies linearly with the voltage. CO_2 generation profile from Figure 54 was achieved in this way, by providing the resulting voltage for each hour of the day in occupant simulator control system program.

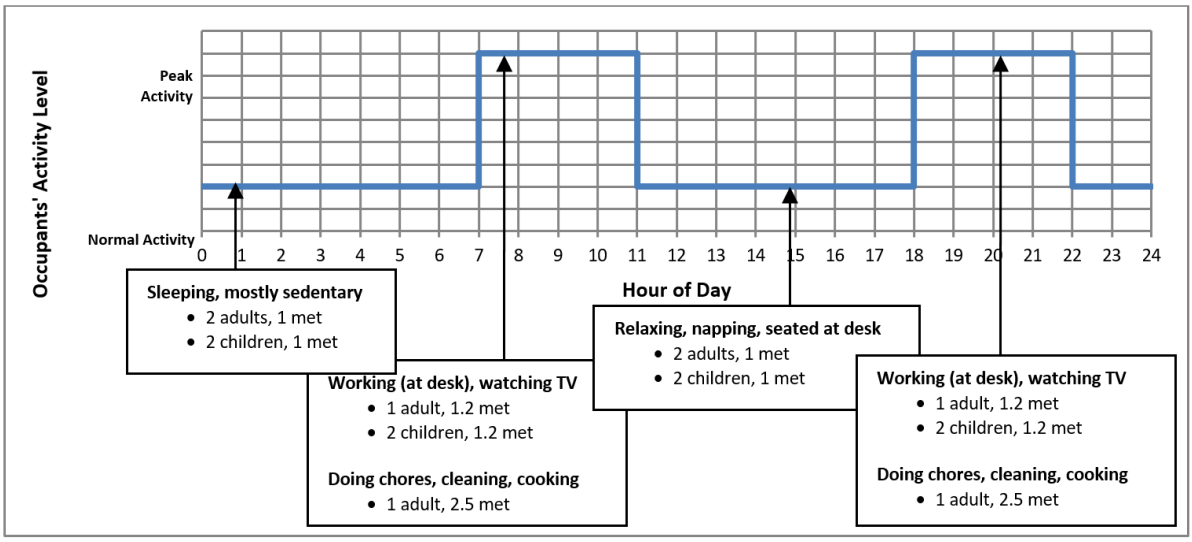

Figure 54 - Typical activities of a family of four throughout the day and their corresponding metabolic activity.

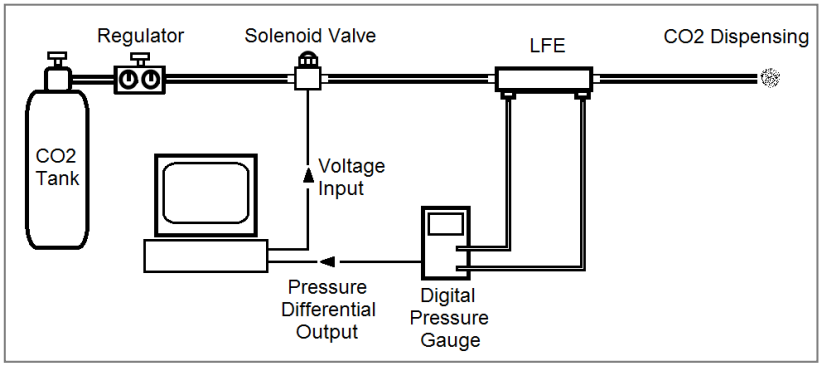

Figure 55 - Schematic of carbon dioxide dispersion system.

Ventilation Strategies

Both the test and control buildings are equipped with a supply ventilation system to provide outdoor air under continuous, time-controlled, relative humidity-controlled (RH-controlled), and CO_2-controlled ventilation schemes. For the purposes of the field experiments, 100% non-conditioned fresh air is supplied to the test space. This is so that the typically wet and moist marine climate air of coastal British Columbia is used to ventilate the building, as is typical of residential housing in the region. The four different ventilation schemes are tested as follows:

1) Constant: The supply ventilation system is run continuously at a constant rate of 15 $ft^3\ min^{-1}$ (CFM). The ventilation rate is determined based on ASHRAE recommended rates according to Standard 62.1, and scaled down for to the size of the test building facilities
2) Time-controlled: The ventilation system supplies fresh air at a ventilation rate of 30 CFM during predetermined on-times for 4 hour durations twice per day at 8am-12pm and 7pm-11pm, which correspond with periods of high moisture generation (typically showering in the morning time, and cooking in the evening). The maximum ventilation rate times are offset from the moisture peak times by one hour due to the gradual rise in humidity levels within the first hour of peak moisture loading. At all other times, ventilation rate is run continuously at 7.5 CFM.
3) RH-controlled: The ventilation system supplies fresh air at 7.5 CFM at relative humidity levels of 50% or less, and at 30 CFM at relative humidity levels of 60% or more. Between 50 to 60% relative humidity, the rate increases linearly between 7.5 and 30 CFM.

4) CO_2-controlled: The ventilation system supplies fresh air at 7.5 CFM at CO_2 levels of 800ppm or less, and at 30 CFM at CO_2 levels of 1000ppm or more. Between 800 to 1000 ppm, the rate increases linearly between 7.5 and 30 CFM.

The ventilation schemes are summarized graphically in Figure 56.

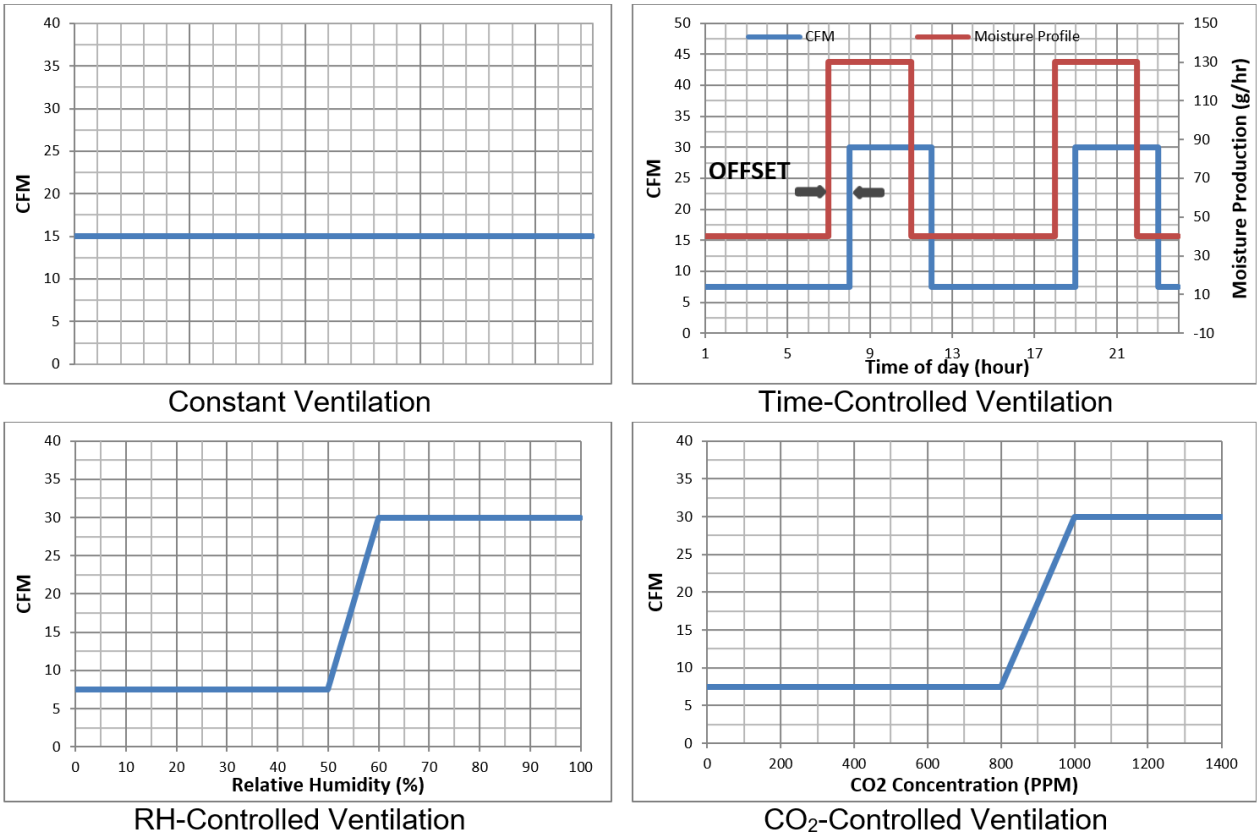

Figure 56 - Ventilation rates (in $ft^3\ min^{-1}$) and schemes for constant, time-controlled, RH-controlled, and CO_2-controlled ventilation.

6.2.4 Results

Previous field testing (Pedram & Tariku, 2014) reveals that moisture buffering properties of gypsum wallboard in the test building is generally effective in regulating the interior relative humidity levels, especially RH peaks, to varying degrees depending on ventilation rate and moisture loading.

The test cases presented here seek to couple the benefits of passive moisture management from moisture buffering, with active moisture management of various ventilation schemes. The effect of constant, time-controlled, RH-controlled, and CO_2-controlled ventilation on indoor humidity, indoor air quality, and ventilation heat loss are further analysed.

6.2.4.1 Indoor Humidity

Figure 57 shows the relative humidity levels for the test and control buildings, and their respective ventilation flow rates over time for each of the test cases. The effect of the moisture buffering of gypsum board in regulating relative humidity amplitudes is apparent between the test building and the control building, as demonstrated in Figure 57 for constant ventilation; the relative humidity peaks and lows are dampened. A similar effect is seen under the time-controlled ventilation scheme. However, the effect of moisture buffering under the demand-controlled ventilation schemes (RH- and CO_2-controlled) is not as pronounced.

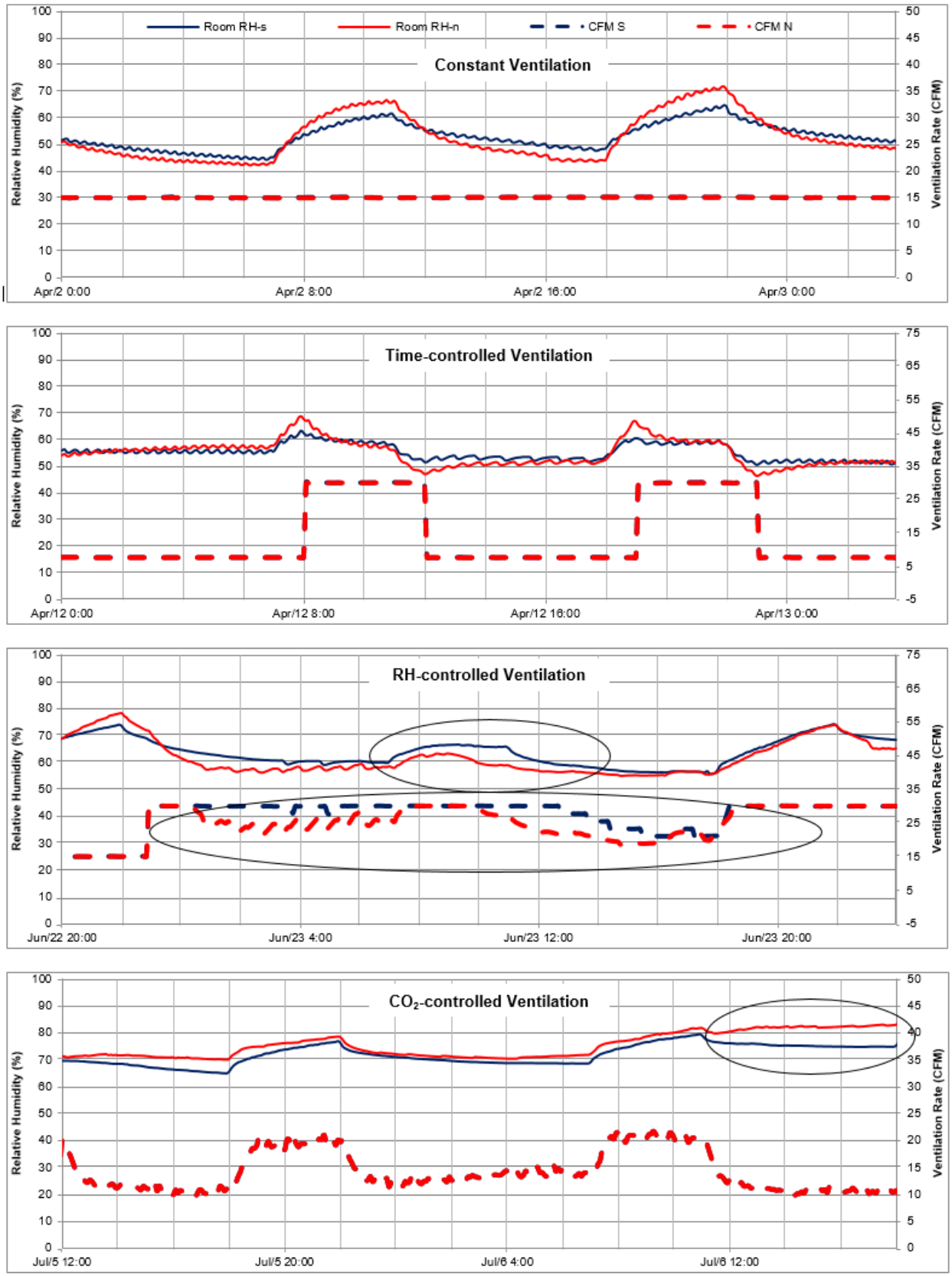

Figure 57 - The indoor relative humidity and ventilation rate of the control building (red) and test building (blue) under constant, time-controlled, RH-controlled, and CO_2-controlled ventilation.

Upon a closer look at the results, it appears that moisture buffering results in elevated relative humidity levels in comparison to the control building under RH-controlled ventilation. When the relative humidity threshold is exceeded, maximum ventilation rate causes relative humidity levels to drop more quickly

in the control building while the test building responds to changes in ventilation rate slowly due to the effect of moisture buffering. This phenomenon can also be seen in other test cases during decreasing relative humidity in the variation cycles. This is due to residual moisture in unfinished gypsum board gradually undergoing desorption back into the air as the relative humidity levels in the test space decrease.

In general, the moisture levels in the test building are not synergistic with RH-controlled ventilation due to slow change in relative humidity response to changing ventilation rates. Maximum ventilation rate is run for a longer duration in the test building, which can in fact increase ventilation heat loss, and have negative impacts on the building energy demand. In the case of continuous, time-controlled, and CO_2-controlled ventilation, moisture buffering effectively reduces humidity peaks and dampens the moisture level fluctuation cycles.

The best way to quantify the effectiveness of moisture buffering, is to look at the difference in amplitude of the relative humidity levels for each moisture loading cycle. Amplitude can be determined from the difference between the maximum relative humidity and minimum relative humidity for each cycle. Figure 58 demonstrates how to determine relative humidity amplitude. While moisture buffering reduces amplitude, it does not reduce the effective mean relative humidity. However, increase in ventilation will reduce mean relative humidity levels.

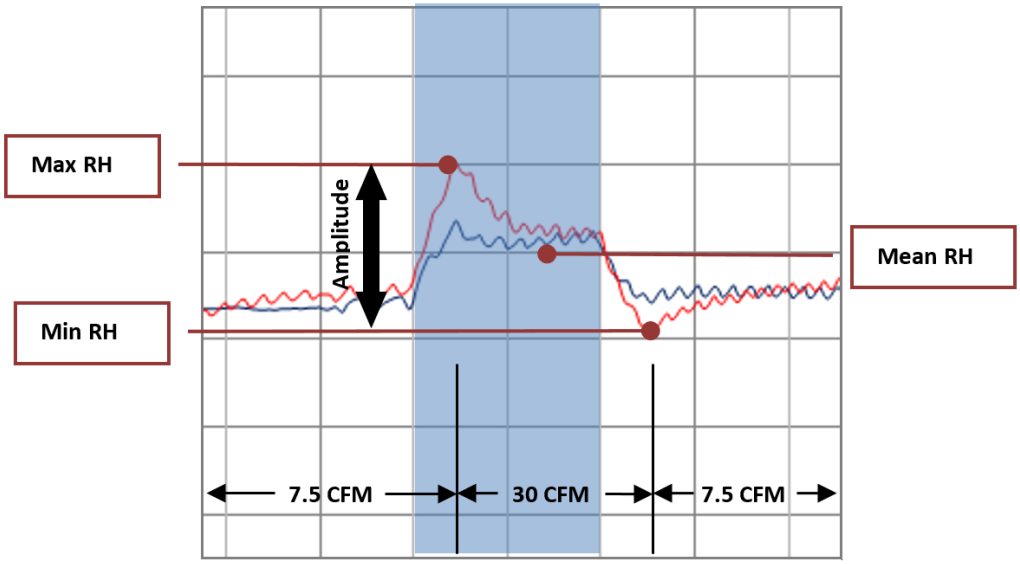

Figure 58 - Maximum RH, minimum RH, RH amplitude and mean RH levels in one moisture loading cycle as shown for the control building in red.

Figure 59 shows the relative humidity amplitude of Cycles 1 and 2 for each test case. Under time-controlled ventilation, the percent difference in relative humidity amplitudes between the control and test building are more than double, 157% and 111% for Cycles 1 and 2 respectively (Figure 60). This indicates that time-controlled ventilation is the ventilation scheme that successfully works best with the relative humidity regulating benefit of moisture buffering. Under RH-controlled and CO_2-controlled ventilation, the percent difference in relative humidity amplitude is much lower between the two buildings, equal to or less than 20%. This indicates that the regulating effect of moisture buffering is not effective under these ventilation schemes. Under the constant ventilation scheme, the percent difference in relative humidity amplitude between the two buildings is greater than 50% for each cycle. Thus, relative humidity is regulated under this scheme, but comparatively to a lesser degree than under time-controlled ventilation.

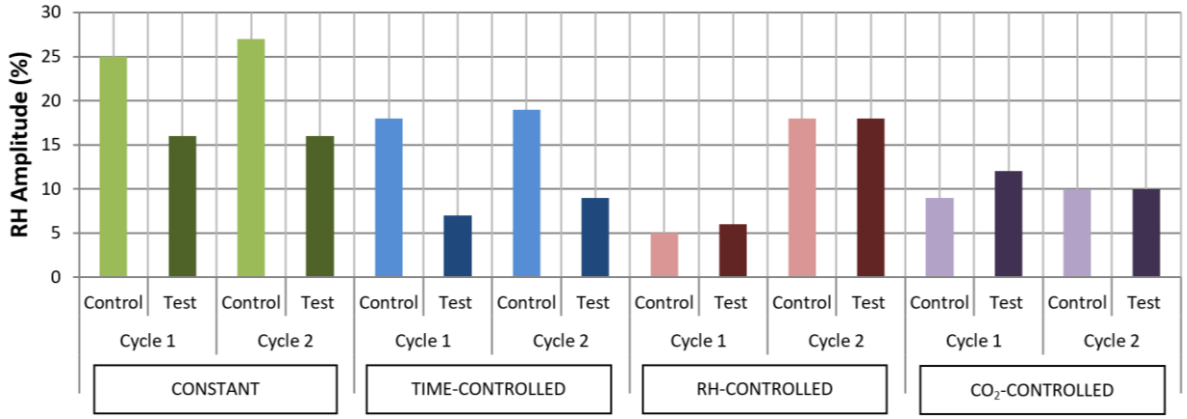

Figure 59 - RH amplitude (Max RH – Min RH) for Cycle 1 & 2 from test cases constant, time-controlled, RH-controlled, and CO_2-controlled ventilation schemes.

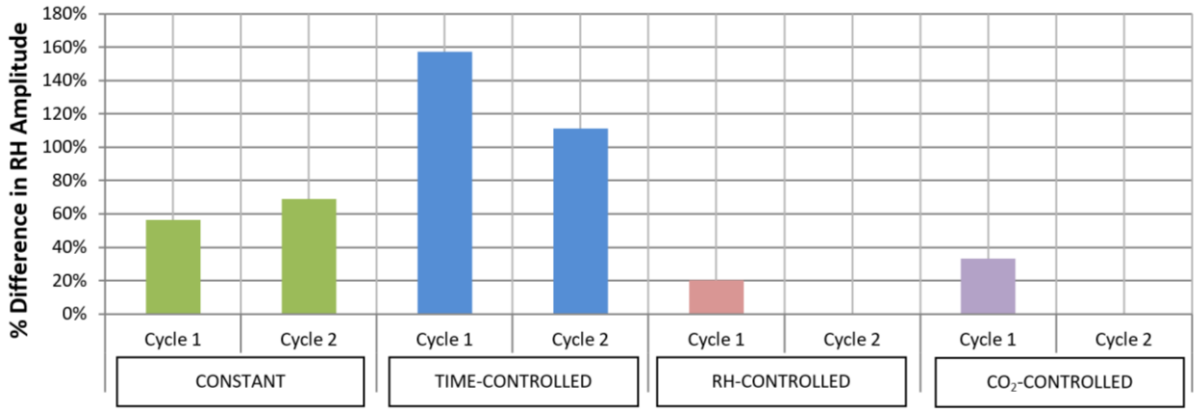

Figure 60 - % Difference in RH amplitudes between the control and test building from the test cases.

Based on these results, if RH-controlled ventilation is implemented as a means of controlling indoor humidity, the implementation of moisture buffering materials as means to control humidity peaks in tandem is not recommended. More exploratory investigations are required in this regards, such as modeling, sensitivity analysis, and further field testing.

6.2.4.2 Indoor Air Quality: CO_2 levels

In part, CO_2 levels are dependent on outdoor CO_2 levels which generally range between 350 to 450 PPM (Dlugokencky & Pieter, 2016). Locally, the outdoor CO_2 levels at the test facilities were measured to be within this range during testing.

Figure 61 shows the maximum, minimum and mean CO_2 levels for each cycle in all test cases. Under constant and time-controlled ventilation, the mean CO_2 levels are above or within 1000 PPM – ASHRAE recommended levels for good indoor air quality – and maximum CO_2 levels consistently exceed this level. Under RH-controlled and CO_2-controlled ventilation, the CO_2 levels are consistently below 1000 PPM.

Table 13 shows the total percentage of time CO_2 levels exceed 1000 PPM in each building for the total duration of the data presented for each test case. According to analysis of CO_2 levels, indoor air quality exceeds acceptable levels under constant and time-controlled ventilation for nearly half of the testing period.

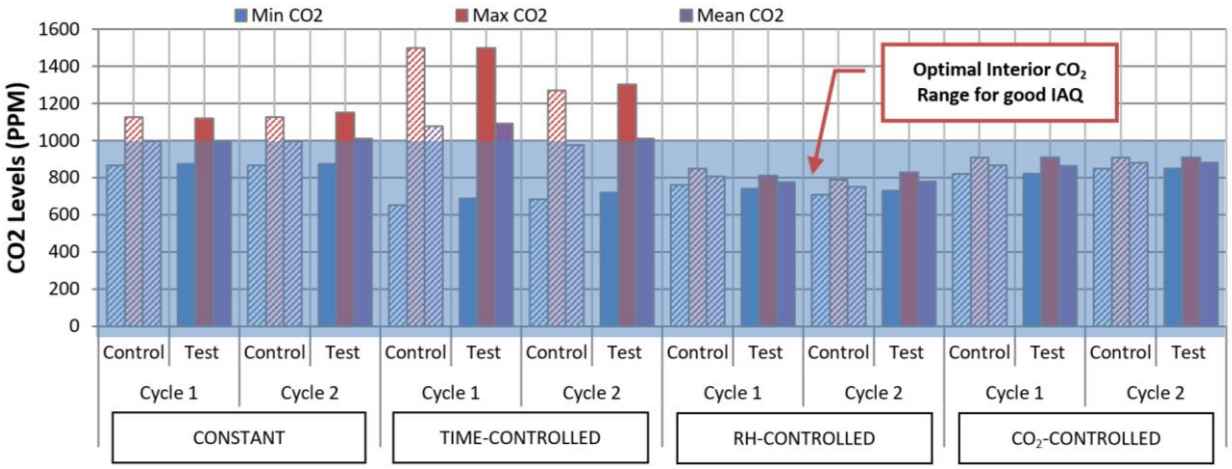

Figure 61 - Minimum, maximum, and mean CO_2 for Cycle 1 & 2 for all test cases. The test building is shown in solid and the control building is shown in hatched. Optimal interior RH range is highlighted in blue.

Table 13 - Percent of time CO_2 levels exceed 1000 PPM threshold.

Ventilation Scheme	Control Building	Test Building
Constant	40%	48%
Time-controlled	51%	55%
RH-controlled	0%	0%
CO_2-controlled	0%	0%

While RH-controlled and CO_2-controlled ventilation result in CO_2 levels being maintained at desirable levels, there are implications for heating energy of the buildings. When the space is over-ventilated, good indoor air quality is maintained, but energy consumption may be compromised. Therefore, there may be a tolerance for CO_2 levels exceeding the threshold for a short period of time, if RH levels and heating energy is optimized.

6.2.4.3 Energy: Ventilation Heat Loss

Heat loss of the buildings can occur by three ways: transmission losses to the exterior through the building envelope, radiation heat losses, and ventilation heat losses. Given that the building enclosure characteristics, indoor, and outdoor temperatures are similar for each building during each test case, the radiation and transmission heat losses can be considered equal. For a given ventilation scheme, if the ventilation rates are the same in both buildings, the ventilation heat losses are also considered equal.

However, ventilation heat loss varies between the buildings where demand-controlled ventilation results in different ventilation rates over time. The ventilation heat loss for the test cases is calculated per Equation 10:

Equation 10 - Ventilation heat loss (J s^{-1})

$$Q = \dot{m} \cdot c_p \cdot \Delta T$$

Q = ventilation heat loss [J s^{-1}]
$\dot{m}$ = airflow (ventilation) rate [m^3 s^{-1}]
c_p = specific heat of dry air, [1007 J kg^{-1} $°C^{-1}$]
ΔT = indoor-outdoor temperature differential [°C]

In order to compare the ventilation heat loss as a result of each ventilation scheme directly, the energy

required to maintain the interior temperature set points at around 20°C is obtained. The total ventilation heat loss energy is determined by calculating the estimated area under each *Q* curve.

For consistency, the ventilation heat loss energy for each building is calculated over a 28 hour period as shown in Figure 62. Note that cooling energy (area between negative *Q* values and 0 J s^{-1}) was included as an absolute value in the summation to include both heating and cooling energy. The RH- and CO_2-controlled experiments are carried out in the month of June and July, respectively. During day time, the difference between the outdoor and the indoor temperatures is small that the ventilation heat loss/gain is close to zero, however, as the outdoor temperature gradually decreases during night time the buildings enter into a heating mode and the ventilation heat loss increases.

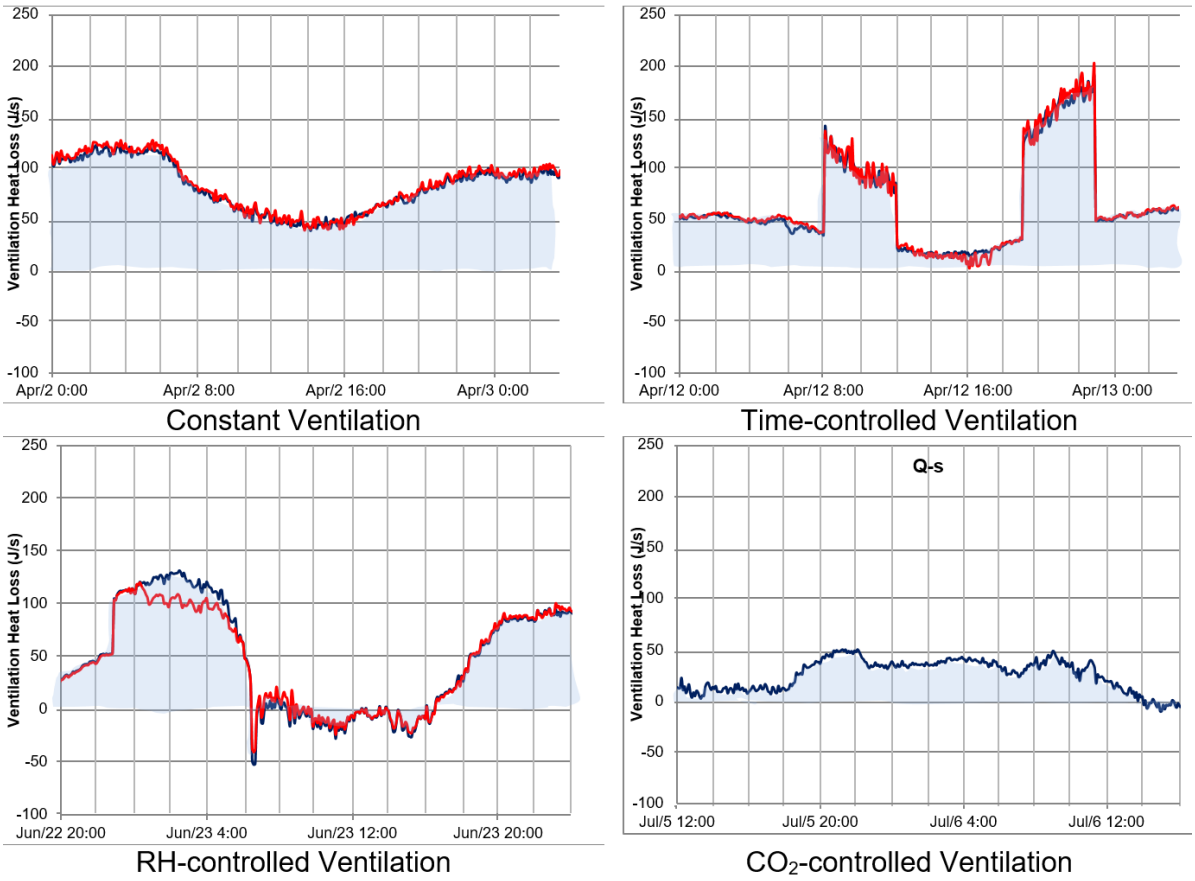

Figure 62 - Area under each ventilation heat loss (Q) curve used for calculation of heat loss energy each test case constant, time-controlled, RH-controlled, and CO_2-controlled ventilation scheme.

Figure 63 shows a summary of the total energy due to ventilation heat loss for each building under each test case. Energy is calculated in kilojoules, however, values are also converted to and indicated in kilowatt-hours above each bar for easy comparison. RH- and CO_2-controlled ventilation show improved ventilation energy savings in comparison to the latter two test cases. However, their comparison to constant and time-controlled ventilation can be misleading, as these tests are carried out during a warmer season. Accordingly, the comparisons shall be restricted to the ventilation energy of the test and the control buildings of the same ventilation scheme.

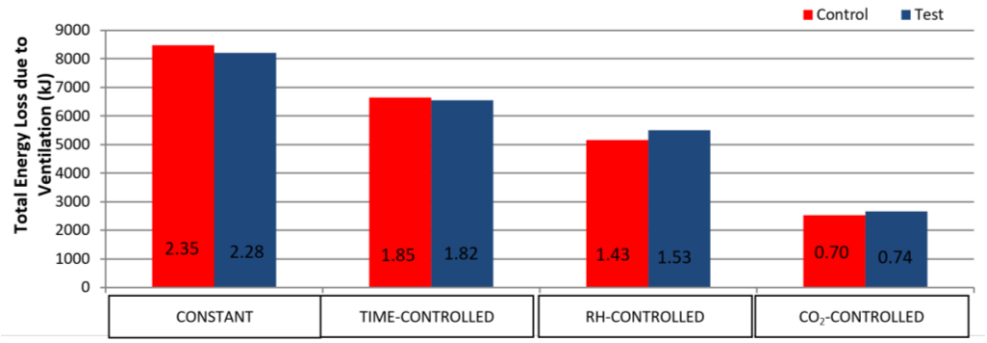

Figure 63 - Total energy loss (heating and cooling) due to ventilation for a duration of 28 hours under test cases. Values indicated on each bar are energy loss in kilowatt-hours.

6.2.5 Conclusion

Moisture buffering effect of unpainted gypsum board in the test building generally helped the building performance in regulating interior humidity levels under low ventilation rates. Amongst the active moisture management measures, time-controlled ventilation is most effective in maintaining both the test building and the control building's relative humidity levels below the 65%, close to the acceptable range. However, in practice, time-controlled ventilation may not be as successful as in field testing due to uncertainty in the duration and frequency of peak moisture loading of occupants. It may be a viable solution in spaces where peak moisture loading can be accurately predicted, such as a commercial kitchen, gymnasium, theatre, or spa.

CO_2-controlled ventilation is effective at maintaining CO_2 levels at acceptable levels for indoor air quality but fails to keep relative humidity levels below acceptable levels. In general, moisture buffering is not found to be synergistic with an RH-controlled ventilation scheme, which results in maximum ventilation rate run for a longer duration and as such increased ventilation heat loss and the building energy demand. Moisture buffering does not have an effect on ventilation heat loss in continuous, time-controlled and CO_2-controlled ventilation schemes. Beyond the assessment of moisture buffering impact on ventilation heat loss, establishing the relative energy performance of the ventilation schemes under the same outdoor climatic conditions is essential.

Acknowledgment

The authors are thankful for the financial support from Natural Science and Engineering Council Canada (NSERC), Canada Research Chair (CRC) and the School of Construction and the Environment at the British Columbia Institute of Technology (BCIT), and technical support of Mr. Doug Horn.

Chapter 7: Case study reports

7.1 Summary

As part of Annex 68 Subtask 5 activities, the energy use and indoor air quality data monitored in recently built high-performance buildings were presented at each annex meeting and, as a common exercise, collected using a common template. Data from 7 (groups of) buildings in 5 countries, namely Austria, Canada, France, New Zealand and United Kingdom, comprise the outcome of the second common exercise of Subtask 5. The buildings type include: house (New Zealand and France), low-rise multi-unit residential building (Canada), mid-rise multi-unit residential building (Austria), and high-rise buildings (UK). The characteristics of the French houses are not uniform across the sample. The houses (NZ) and the low-rise building are wood-frame construction with 30-35% wall-window ratio, and built-in 2017. The mid-rise and high-rise buildings are mass construction built in 2009 and 2014, respectively. The above-grade walls of the houses and the low-rise building have thermal resistance value of about 6 K $m^2 W^{-1}$. The mid and the high-rise buildings have slightly higher values, 7.7 to 8.3 K $m^2 W^{-1}$. The windows in the houses have higher U-value (1.25 W K^{-1} m^{-2}) compared to the other buildings, which have windows with U-values between 0.72 W K^{-1} m^{-2} and 0.92 W K^{-1} m^{-2}. The houses are heated with underfloor hydronic heating system and fresh air is supplied through the continuously running mechanical ventilation system (heat recovery units). The low-rise building is equipped with air-to-air heat pump for air-conditioning and energy recovery ventilator (ERV) for ventilation. Electric baseboard heaters are installed in the units as auxiliary heating system for times when the heating demand of the building is beyond the heat pump capacity. The mid-rise building uses solar thermal, gas boiler and wood pellets as heat sources and heat recovery ventilator (HRV) for ventilation. The high-rise buildings utilize community heating system based on natural gas-fired boilers with provision for integration of a CHP system in future. To control indoor humidity and optimize ventilation, humidity-controlled ventilation strategy has been implemented in the building. All the buildings have operable windows, allowing natural ventilation in all seasons through the opening of windows when weather permits. The low-rise building is equipped with mechanical cooling system and all the rest rely on natural ventilation to maintain the indoor temperature to acceptable level during summer and hot days. The snapshots of the indoor air quality and energy uses of the buildings are presented in the following sessions for each specific experiment. The measurement locations, sensors types and monitoring periods for each building are also included in the data collection sheet. In addition to the common indoor air measurements, temperature, relative humidity and CO_2, Formaldehyde, TVOC and particular matter (PM) are measured and reported in the houses, and other gaseous indoor pollutants in the high-rise buildings. Occupants in the seven building sites perceive their units' indoor-air-quality as good and thermally comfortable. The total energy use of the low-rise, mid-rise and the two high rise buildings are 73, 98, 138 and 179.6 KWh m^{-2} yr^{-1}, respectively.

One of the problems identified in the case study buildings is overheating in some top floor units of the low-rise and mid-rise buildings during hot summer days. To mitigate the problem internal and external shading devices are installed in the low-rise and high-rise buildings, respectively. The other problems reported, more specifically in the houses and the high-rise buildings case studies, are issues related to the use and the operation of mechanical ventilation (both HRV and DCV). For example, none of the 21 French dwellings fully complied with the ventilation requirements. It was suggested that the controllers need to be more dynamic and accessible to occupants to fine-tune the setting based on their needs and building users/managers need to be educated on type and function of ventilation components and recommended filter replacement frequency and methods to maintain good indoor air quality.

Details regarding each of these experiments can be found in the annexed document, as listed below.

7.2 Annexes:

1. Monitoring in Austria: *CaseStudy_AT_UIBK1.xlsx*
2. Monitoring in Canada: *CaseStudy_CA_Residential.xlsx*
3. Monitoring in France: *CaseStudy_FR_Houses.xlsx*
4. Monitoring in New Zealand: *CaseStudy_NZ_House_A.xlsx*
5. *CaseStudy_NZ_House_W.xlsx*
6. Monitoring in the United Kingdom: *CaseStudy_UK_UCL_BWR__CH003.xlsx*
7. *CaseStudy_UK_UCL_BWR_BC805.xlsx*

Chapter 8: References

Amaral, S. S.; Carvalho Jr., J. A.; Costa, M. A. M.; Pinheiro, C. (2015) An Overview of Particulate Matter Measurement Instruments. *Atmosphere*, v. 6, p. 1327-1345. doi:10.3390/atmos6091327

Arrhenius, K.; Brown, A. S.; van der Veen, A. M. H. (2016) Suitability of different containers for the sampling and storage of biogas and biomethane for the determination of the trace-level impurities – A review. *Analytica Chimica Acta*, v. 902, p. 22-32.

Asbach, C.; Alexander, C.; Clavaguera, S.; Dahmannd, D.; Dozol, H.; Faure, B.; Fierz, M.; Fontana, L.; Iavicoli, I.; Kaminski, H.; MacCalman, L.; Meyer-Plath, A.; Simonow, B.; van Tongeren, M.; Todea, A. M. (2017) Review of measurement techniques and methods for assessing personal exposure to airborne nanomaterials in workplaces. *Sci. Total Environ.*, v. 603–604, p. 793–806.

Ashokkumar, P.; Sahoo, B. K.; Raman, A.; Mayya, Y. S. (2014) Development and characterization of a silicon PIN diode array based highly sensitive portable continuous radon monitor. *J. Radiol. Prot.*, v. 34, p. 149–160.

ASTM (2012). ATSM Standard D6245, Standard Guide for Using Indoor Carbon Dioxide Concentrations to Evaluate Indoor Air Quality and Ventilation. Philadelphia: American Society for Testing and Materials, D6245-12.

ASTM D7675-15. (2015) Standard Test Method for Determination of Total Hydrocarbons in Hydrogen by FID-Based Total Hydrocarbon (THC) Analyzer, ASTM International, West Conshohocken, PA. DOI: 10.1520/D7675-15

Baskaran, M. (2016) Radon: A Tracer for Geological, Geophysical and Geochemical Studies. *Springer Geochemistry*, Springer International Publishing Switzerland. DOI: 10.1007/978-3-319-21329-3_2

Blake, R.; Monks, P.; Ellis, A. (2009) Proton-Transfer Reaction Mass Spectrometry. *Chem. Rev.*, v. 109, p. 861–896.

Booker, D.; Giannelli, R.; Hu, J. (2007) Road test of an on-board particulate matter mass measurement system. SAE 2007-01-1116. DOI: 10.4271/2007-01-1116.

Brostrøm, A.; Kling, K. A.; Koponen, I. K.; Hougaard, K. S.; Kandler, K.; Mølhave, K. (2019) Improving the foundation for particulate matter risk assessment by individual nanoparticle statistics from electron microscopy analysis. Scientific Reports, v. 9, n. 8093. DOI: 10.1038/s41598-019-44495-7

Caillou, S. (2018) Measurement issues of air flow at air terminal devices and perspectives. Proceedings: 39th AIVC - 7th TightVent & 5th venticool Conference, Antibes Juan-Les-Pins, France.

Carey, P. S.; Etheridge, D. W. (2001) Leakage measurements using unsteady techniques with particular reference to large buildings. *Building Serv. Eng. Res. Technol.*, v. 22, p. 69-82.

Ciobanu, M. C.; Catalina, T.; Dogaru, G. (2016) Analysis of radon concentrations in a radioactive working space. *Energy Procedia*, v. 85, p. 118–124.

Cooper, E.; Zheng, X. F.; Gillot, M.; Riffat, S.; Zu, Y. Q. (2014) A nozzle pulse pressurization technique for measurement of building leakage at low pressure. Proceedings: *35th AIVC conference, Poznan, September 2014*.

Coudray, N.; Dieterlen, A.; Roth, E.; Trouvé, G. (2009) Density measurement of fine aerosol fractions from wood combustion sources using ELPI distributions and image processing techniques. *Fuel*, v. 88, p. 947–954.

Crilley, L. R.; Shaw, M.; Pound, R.; Kramer, L. J.; Price, R.; Young, S.; Lewis, A. C.; Pope, F. D. (2018) Evaluation of a low-cost optical particle counter (Alphasense OPC-N2) for ambient air monitoring. *Atmos. Meas. Tech.*, v. 11, p. 709–720.

Dawson, M. E. (2005) Technical report: Interference with the LAL test and how to address it. *LAL Update*, v. 22, n. 3.

Dinh, T. -V.; Choi, I. -Y.; Son, Y. -S.; Kim, J. -C. (2016) A review on non-dispersive infrared gas sensors: Improvement of sensor detection limit and interference correction. Sensors and Actuators B: Chemical. DOI: 10.1016/j.snb.2016.03.040

Dlugokencky, E.; Pieter, T. (2016). Trends in Atmospheric Carbon Dioxide. Retrieved from http://www.esrl.noaa.gov/gmd/ccgg/trends/global.html

Du, Z.; Tsow, F.; Wang, D.; Tao, N. (2018) A miniaturized particulate matter sensing platform based on CMOS imager and real-time image processing. IEEE Sensors Journal, v. 18, n. 18.

Duenas, C.; Perez, M.; Fernandez, M. C.; Carretero, J. (1994) Disequilibrium of radon and its short-lived daughters near the ground with atmospheric stability. *J. Geophys. Res.*, v. 99, n. D6, p. 12865–12872.

Dungan, R. S.; Leytem, A. B. (2009) Qualitative and quantitative methodologies for determination of airborne microorganisms at concentrated animal-feeding operations. *World J. Microbiol. Biotechnol.*, v. 25, n. 9, p. 1505-1518. https://doi.org/10.1007/s11274-009-0043-1

Eappen, K. P.; Mayya, Y. S. (2004) Calibration factors for LR-115 (Type-II) based radon-thoron discriminating dosimeter. *Radiat. Meas.*, v. 38, p. 5–17.

Ellis, A. M.; Mayhew, C. A. (2014) *Proton Transfer Reaction Mass Spectrometry: Principles and Applications.* Ltd, Chichester: John Wiley & Sons.

EPA. (1990) *Indoor air – Assessment. Methods of analysis for environmental carcinogens*. EPA/600/8-90/041.

EPA. (1994) *Indoor air pollution: An Introduction for Health Professionals.* In association with: American Lung Association, the American Medical Association, The U.S. Consumer Product Safety Commission, and the U.S. Environmental Protection Agency. Available at: http://www.epa.gov/iaq/pubs/hpguide.html.

EPA. (1999) *Compendium Method TO-14*. The determination of Volatile Organic Compounds (VOCs) in ambient air using specially prepared canister with subsequent anamysis by gas chromatography; Second edition. EPA/625/R-96/010b

EPA. (2009) *A Citizen's Guide To Radon* - The Guide To Protecting Yourself And Your Family From Radon. EPA/402/K-09/001.

EPA. (2018) Criteria Air Pollutants. Available at: https://www.epa.gov/criteria-air-pollutants. Accessed on: January 14th 2020.

EUROPEAN STANDARD, (2015). Ventilation for buildings - Measurement of air flows on site – Methods. NS-EN 16211, European Committee for Standardization, Brussels, Belgium.

Foster, J.; Sharpe, T.; Poston, A.: Morgan, C.; Musau, F. (2016) Scottish passive house: insights into environmental conditions in monitored passive houses. *Sustainability*, v. 8, n. 5, p. 412, DOI:10.3390/su8050412.

Furbringer, J. M.; Roecker, C.; Roulet, C. A. (1988) *The use of a guarded zone pressurization technique to measure air flow permeabilities of a multizone building*. Proc AIVC 9th Conference.

Georgakopoulos, D. G.; Després, V.; Fröhlich-Nowoisky, J.; Psenner, R.,; Ariya, P. A.; Pósfai, M.; Ahern, H. E.; Moffett, B. F.; Hill, T. C. J. (2009) Microbiology and atmospheric processes: biological, physical and chemical characterization of aerosol particles. *Biogeosciences*, v. 6, p. 721-737. https://doi.org/10.5194/bg-6-721-2009

Giechaskiel, B.; Maricq, M.; Ntziachristos, L.; Dardiotis, C.; Wang, X.; Axmann, H.; Bergmann, A.; Schindler, W. (2014) Review of motor vehicle particulate emissions sampling and measurement: From smoke and filter mass to particle number. *J. Aerosol Sci.*, v. 67, p. 48–86.

Gilliam, J. H.; Hall, E. S. (2016) *Reference and Equivalent Methods Used to Measure National Ambient Air Quality Standards (NAAQS) Criteria Air Pollutants - Volume I*. Environmental Protection Agency - EPA/600/R-16/139.

Gutmann, A.; Rüdiger, J.; Bobrowski, N.; Hoffmann, T. (2017) Development and application of gas diffusion denuder sampling techniques with in situ derivatization for the determination of hydrogen halides in volcanic plumes. *Geophysical Research Abstracts*, v. 19, EGU2017-1264.

Hebisch, R.; Breuer, D., Krämer, W.; Maschmeier, C.-P.; Tschickardt, M. (2009) *Sampling and analysis of gases and vapours*. In: The MAK Collection, Part III – air monitoring methods, v. 11 (Deutsch Forschungsgemeinschaft, DFG). Weinheim, Germany: Wiley-VCH, pp. 13-47.

Hinds, W.C. (1999) *Aerosol Technology: Properties, Behavior, and Measurement of Airborne Particles*, 2nd ed.; John Wiley & Sons: Hoboken, NJ, USA.

Hodgkinson, J.; Smith, R.; Ho, W. O.; Saffell, J. R.; Tatam, R. P. (2012) A low cost, optically efficient carbon dioxide sensor based on nondispersive infra-red (NDIR) measurement at 4.2μm. Proceedings: SPIE Photonics Europe 2012, Brussels, Belgium. DOI: 10.1117/12.922258

Hossain, A. M. M.; Park, S.; Kim, J. S.; Park, K. (2012) Volatility and mixing states of ultrafine particles from biomass burning. *J. Hazard. Mater.*, p. 189–197.

Hosseini, S.; Li, Q.; Cocker, D.; Weise, D.; Miller, A.; Shrivastava, M.; Miller, J. W.; Mahalingam, S.; Princevac, M.; Jung, H. (2010) Particle size distributions from laboratory-scale biomass fires using fast response instruments. *Atmos. Chem. Phys.*, v. 10, p. 8065–8076.

HPO (2006). Building Envelope Maintenance Matters Bulletin No. 3: Avoiding Condensation Problems. Home Owner Protection Office Branch of BC Housing. Retrieved from http://www.hpo.bc.ca/files/download/MMR/MM3.pdf

Johnson, T. J.; Symonds, J. P. R.; Olfert, J. S. (2013) Mass–Mobility Measurements Using a Centrifugal Particle Mass Analyzer and Differential Mobility Spectrometer. *Aerosol Sci. Technol.*, v. 47, p. 1215–1225.

Larios, A. D.; Godbout, S.; Brar, S. K.; Palacios, J. H.; Zegan, D.; Avalos-Ramírez, A.; Sandoval-Salas, F. (2018) Development of passive flux samplers based on adsorption to estimate greenhouse gas emissions from agricultural sources. *Biosystems Engineering*, v. 169, p. 165-174.

Lehtinen, J.; Tolvanen, O.; Nivukoski, U.; Veijanen, A.; Hänninen, K. (2013) Occupational hygiene in terms of volatile organic compounds (VOCs) and bioaerosols at two solid waste management plants in Finland. *Waste Manag.*, v. 33, n. 4, p. 964-73. doi: 10.1016/j.wasman.2012.11.010.

Li, X. (2017) Application of Solid-Phase Microextraction in Gas Sampling. In: Ouyang G., Jiang R. (eds) *Solid Phase Microextraction*. Springer, Berlin, Heidelberg. Online ISBN: 978-3-662-53598-1.

Liddament, M. W. (1996) *A guide to energy efficient ventilation. IEA Energy Conservation in Building & Community Systems Programme*, publication prepared by Annex V Air Infiltration and Ventilation Centre. Code GV.

Lin, C.; Liou, N.; Sun, E. (2008) Applications of Open-Path Fourier Transform Infrared for Identification of Volatile Organic Compound Pollution Sources and Characterization of Source Emission Behaviors. *J. Air & Waste Manage. Assoc.*, v. 58, n.6, p. 821-828, DOI: 10.3155/1047-3289.58.6.821

Kamilli, K. A.; Poulain, L.; Held, A.; Nowak, A.; Birmili, W.; Wiedensohler, A. (2014) Hygroscopic properties of the Paris urban aerosol in relation to its chemical composition. *Atmos. Chem. Phys.*, v. 14, p. 737–749.

Kelly, T. J.; Holdren, M. W. (1995) Applicability of Canisters for sample storage in the determination of hazardous air pollutants. *Atmos. Environ*., v. 29, p. 2595–2608.

Kim, M. -H.; Jo, J. -H.; Jeong, J. -W. (2013) Feasibility of building envelope air leakage measurement using combination of air-handler and blower door. *Energy and Buildings*, v. 62, p. 436–441. DOI: 10.1016/j.enbuild.2013.03.034

Kim, K. –H.; Kabir, E.; Jahan, S. A. (2018) Airborne bioaerosols and their impact on human health. *J. Environ. Sci.*, v. 67, p. 23–35. https://doi.org/10.1016/j.jes.2017.08.027

Kito, A. -M. N.; Colbeck, I.; Kvetoslav, R. S. (ed.) (1999). Chapter 4: Filtration and Denuder Sampling Techniques. *Analytical Chemistry of Aerosols*. CRC Press. pp. 103–132. ISBN 156670040X.

Kuenzel, H.; Holm, A.; Sedlbauer, K.; Antretter, F.; Ellinger, M. (2004). Moisture buffering effect of interior linings made from wood or wood based products (No. HTB-04/2004/e). Fraunhofer Institut Bauphysik.

Kulkarni, P.; Baron, P. A.; Willeke, K. (2011) *Aerosol Measurement: Principles, Techniques, and Applications*, 3rd ed.; JohnWiley & Sons: Hoboken, NJ, USA.

Kuula, J.; Kuuluvainen, H.; Rönkkö, T.; Niemi, J. V.; Saukko, E.; Portin, H.; Aurela, M.; Saarikoski, S.; Rostedt, A.; Hillamo, R.; Timonen, H. (2019) Applicability of Optical and Diffusion Charging-Based Particulate Matter Sensors to Urban Air Quality Measurements. *Aerosol and Air Quality Research*, v. 19, p. 1024–1039. DOI: 10.4209/aaqr.2018.04.0143

Lstiburek, J. (2002). Relative Humidity (No. Research Report - 0203). Retrieved from http://www.buildingscience.com/documents/reports/rr-0203-relative-humidity.

Macher, J.; Chen, B.; Rao, C. (2008) Field evaluation of a personal, bioaerosol cyclone sampler. *Journal of Occupational and Environmental Hygiene*, v. 5, n. 11, p. 724-734, DOI: 10.1080/15459620802400159

Mainelis, G.; Willeke, K.; Adhikari, A.; Reponen, T.; Grinshpun, S. A. (2002) Design and collection efficiency of a new electrostatic precipitator for bioaerosol collection. *Aerosol Science and Technology*, v. 36, n. 11, p. 1073-1085, DOI: 10.1080/02786820290092212

Mandal, J.; Brandl, H. (2011) Bioaerosols in indoor environment - A review with special reference to residential and occupational locations. *The Open Environmental & Biological Monitoring Journal*, v. 4, p. 83-96.

McWilliams, J. (2003) Annotated bibliography 12: Review of airflow measurement techniques. *IEA Energy Conservation in Buildings & Community Systems Programme – Annex V, Air Infiltration and Ventilation Centre*. ISBN 2-9600355-3-4.

Meffert, K.; Blome, H. (2005) Messung von Gefahrstoffen – BGIA-Arbeitsmappe – Expositionser mittlung bei chemischen und biologischen Einwirkungen, Erich Schmidt Verlag Berlin.

Namieśnik, J.; Górecki, T.; ła, B. K. –Z.; Łukasiak, J. (1992) Indoor air quality (IAQ), pollutants, their sources and concentration levels. *Building and Environment*, v. 27, n. 3, p. 339-356.

Nussbaumer, T.; Czasch, C.; Klippel, N.; Johansson, L.; Tullin, C. (2008) *Particulate emissions from biomass combustion in IEA countries*. In Proceeding of the 16th European Biomass Conference and Exhibition, Zurich, Switzerland, 2–6 June, p. 40.

Olfert, J. S.; Reavell, K.; Rushton, M.; Collings, N. (2006) The experimental transfer function of the Couette centrifugal particle mass analyzer. *J. Aerosol Sci.*, v. 37, p. 1840-1852.

Olfert, J. S.; Kulkarni, P.; Wang, J. (2008) Measuring aerosol size distributions with the fast integrated mobility spectrometer. *J. Aerosol Sci.*, v. 39, p. 940–956.

Orecchio, S.; Fiore, M.; Barreca, S.; Vara, G. (2017) Volatile profiles of emissions from different activities analyzed using canister samplers and gas chromatography-mass spectrometry (GC/MS) analysis: A case study. *Int. J. Environ. Res. Public Health*, v. 14, n. 195. DOI:10.3390/ijerph14020195

Paralovo, S. L.; Barbosa, C. G. G.; Carneiro, I. P. S.; Kurzlop, P.; Borillo, G. C.; Schiochet, M. F. C.; Godoi, A. F. L.; Yamamoto, C. I.; de Souza, R. A. F.; Andreoli, R. V.; Ribeiro, I. O.; Manzi, A. O.; Kourtchev, I.; Bustillos, J. O. V.; Martin, S. T.; Godoi, R. H. M. (2019) Observations of particulate matter, NO_2, SO_2, O_3, H_2S and selected VOCs at a semi-urban environment in the Amazon region. *Sci. Total Environ.*, v. 650, p. 996–1006.

Patel, S.; Li, J.; Pandey, A.; Pervez, S.; Chakrabarty, R. K.; Biswas, P. (2017) Spatio-temporal measurement of indoor particulate matter concentrations using a wireless network of low-cost sensors in households using solid fuels. *Environmental Research*, v. 152, p. 59-65.

Pedram, S.; Tariku, F. (2014). Moisture Buffering Effect of Gypsum Board in a Marine Climate: A Field Experimental Study. *Advanced Materials Research*, v. 1051, p. 763-773. (ISSN: 1662-8985)

Pedram, S.; Tariku, F. (2015). Determination of Representative Daily Moisture Production Profile of Occupants in a Residential Setting. *International Conference on Energy and Environmental Systems Engineering* (EESE 2015), May 17-18, 2015, Beijing, China.

Persily, A. K. (2016) Field measurement of ventilation rates. *Indoor Air 2016*, v. 26, p. 97-111.

Pettersson, A.; Lovejoy, E. R.; Brock, C. A.; Brown, S. S.; Ravishankara, A. R. (2004) Measurement of aerosol optical extinction at with pulsed cavity ring down spectroscopy. *J. Aerosol Sci.*, v. 35, p. 995–1011.

Roulet, C.-A.; Vandaele, L. (1991) *Airflow patterns within buildings measurement techniques*. Handbook, Code TN 34, 284pp.

Sagheby, H.; Kriegel, M.; Mueller, B. (2012) Density effects in modeling contaminant dispersion in displacement ventilation. Proceedings: Healthy Buildings 2012, Brisbane, Australia.

Sandberg, M.; Sundberg J. (1987) The use of detector tubes with carbon dioxide as a tracer gas. *Air Infiltration Review*, v. 8, n. 3.

Sateri, J.; Jyske, P.; Majanen, A.; Seppanen, O. (1989) *The performance of the passive perfluorocarbon method*, Proc. 10th AIVC Conference Vol 1.

Sherman, M. H. (1989) Analysis of errors associated with passive ventilation measurement techniques. *Building and Environment*, v. 24, n. 4, p. 365-374.

Sherman, M. H. (1990) Tracer-gas techniques for measuring ventilation in a single zone. *Building and Environment*, v. 25, n. 2, p. 131-139.

Shinohara, N.; Kataoka, T.; Takamine, K.; Butsugan, M.; Nishijima, H.; Gamo, M. (2010) Modified perfluorocarbon tracer method for measuring effective multizone air exchange rates. *International Journal of Environmental Research and Public Health,* v. 7, p. 3348-3358. DOI: 10.3390/ijerph7093348

Skoog, D. A.; Holler, F. J.; Crouch, S. R. (2018) Principles of instrumental analysis. Cengage Learning, 7th ed., Boston, MA, USA. ISBN 978-1-305-57721-3.

Sousan, S.; Koehler, K.; Thomas, G.; Park, J. H.; Hillman, M.; Halterman, A.; Peters, T. M. (2016) Inter-comparison of low-cost sensors for measuring the mass concentration of occupational aerosols. *Aerosol Sci. Technol.*, v. 50, n. 5, p. 462-473.

Sparkman, O. D. (2000). *Mass spectrometry desk reference*. Pittsburgh: Global View Pub. ISBN 0-9660813-2-3.

Spietelun, A.; Pilarczyk, M.; Kloskowski, A.; Namieśnik, J. (2010) Current trends in solid-phase microextraction (SPME) fibre coatings. *Chem. Soc. Rev.*, v. 39, p. 4524-4537.

Spinelle, L.; Gerboles, M.; Kok, G.; Sauerwald, T. (2015) Sensitivity of VOC Sensors for Air Quality Monitoring within the EURAMET Key-VOC project. Proceedings: Fourth Scientific Meeting EuNetAir, p. 6-9. DOI: 10.5162/4EuNetAir2015/02

Spinelle, L.; Gerboles, M.; Kok, G.; Persijn, S.; Sauerwald, T. (2017) Review of portable and low-cost sensors for the ambient air monitoring of benzene and other volatile organic compounds. *Sensors*, v. 17, p. 1520. DOI:10.3390/s17071520

Sun, J.; Guan, F.; Cui, D.; Chen, X.; Zhang, L.; Chen, J. (2013) An improved photoionization detector with a micro gas chromatography column for portable rapid gas chromatography system. *Sensors and Actuators B*, v. 188, p. 513–518.

Szulczynski, B.; Gebicki, G. (2017) Currently Commercially Available Chemical Sensors Employed for Detection of Volatile Organic Compounds in Outdoor and Indoor Air. *Environments*, v. 4, n. 21, 15p. DOI: 10.3390/environments4010021

Tariku, F.; Simpson, Y.; Pedram, S.; Horn, D. (2013). Development of a Whole-Building Performance Research Laboratory for Energy: Indoor Environment and Building Envelope Durability Study. *Proceedings from ZEMCH 2013 International Conference*. Miami, FL.

Therkorn, J.; Thomas, N.; Scheinbeim, J.; Mainelis, G. (2017) Field performance of a novel passive bioaerosol sampler using polarized ferroelectric polymer films. *Aerosol Science and Technology*, v. 51, n. 7, p. 787-800. DOI: 10.1080/02786826.2017.1316830

Tsekenis, G.; Garifallou, G. –Z.; Davis, F.; Millner, P. A.; Gibson, T. D.; Higson, S. P. J. (2008) Label-less immunosensor assay for myelin basic protein based upon an ac impedance protocol. *Anal. Chem.*, v. 80, p. 2058-2062.

Van Schaik, W.; Grooten, M.; Wernaart, T.; Van der Geld, C. (2010) High accuracy acoustic relative humidity measurement in duct flow with air. *Sensors*, v. 10, p. 7421-7433. doi:10.3390/s100807421.

Venkataraman, C.; Rao, G. U. M. (2001) Emission Factors of Carbon Monoxide and Size-Resolved Aerosols from Biofuel Combustion. *Environ. Sci. Technol.*, v. 35, P. 2100–2107.

Vincent, J. H. (2007) *Aerosol Sampling: Science, Standards, Instrumentation and Applications*; JohnWiley & Sons: Hoboken, NJ, USA.

Wentzel, M.; Gorzawski, H.; Naumann, K. -H.; Saathoff, H.; Weinbruch, S. (2003) Transmission electron microscopical and aerosol dynamical characterization of soot aerosols. *J. Aerosol Sci.*, v. 34, p. 1347–1370.

Wight, G. D. (1994) Fundamentals of air sampling. Taylor & Francis Group, LLC. Boca Raton, FL.

World Health Organization – WHO (2006) Air Quality Guidelines: Global Update 2005. WHO Regional Office for Europe, Copenhagen.

Wouters, P.; Vandaele, L. (Eds.) (1990) The PASSYS Test Cells (5th edition), EUR 12882 EN, Commission of the European Communities, DGXII, Brussels.

Zhao, Y.; Aarnink, A. J. A.; Hofschreuder, P.; Koerkamp, P. W. G. G. (2009) Evaluation of an impaction and a cyclone pre-separator for sampling high PM_{10} and $PM_{2.5}$ concentrations in livestock houses. Aerosol Science, v. 40, p. 868 – 878.

Appendix: Detailed measurement methods for IAQ pollutants

A.1 PM measurement: Concentration methods

A.1.1 Gravimetry

The gravimetric method is the simplest one, measuring the PM air concentration on a mass basis. In this method, the air is pumped through a sampling tube, passing then through a filter, which retains the particles. By weighing the filter before and after the sampling period and knowing the volume of air pumped in the same period, the average PM mass concentration in that period can be calculated. The filters collect PM in all granulometric fractions (total PM); unless a mechanism to pre-filter the incoming air (e.g. cyclones or impactors) is used in order to remove particles larger than the fraction of interest, usually > 10 μm or 2.5 μm (Giechaskiel et al., 2014; Nussbaumer et al., 2008). The biggest disadvantage of the gravimetric method is its low time resolution (in general varying from 15 min to several hours or days for collecting one sample, depending on the expected level of PM pollution), hindering the identification of fast processes. On the other hand, the particles collected in the filters can later be analyzed by different techniques to determine other characteristics of the collected PM, e.g. X-ray fluorescence spectrometry to determine the PM elemental composition and chromatography to determine the concentration of adsorbed chemical compounds (Paralovo et al., 2018; Nussbaumer et al., 2008).

A.1.2 Optical methods

In the optical detection methods, a light beam is lit onto the pumped airflow and the present particles reflect the beam in all directions (scattering). Part of this light is simultaneously transformed in other energy forms, e.g. heat (absorption) (Giechaskiel et al., 2014). The PM concentration can then be inferred by the difference between the intensity of the incident light and the intensity of the light detected after interaction with the particles. Optical instruments used for measuring PM concentration can be based on the principles of scattering, absorption or light extinction.

Light scattering instruments are possibly the real-time sensors most commonly used by researchers. These instruments are primarily classified in two types: light dispersion by single particles or by an ensemble of particles. The instruments of light scattering by an ensemble of particles include dispersion photometers that measure the intensity of scattered light (which may vary in wavelength) in one or more angles (varying between 90°, 45° or less than 30°). Examples of this type of instrument are the DataRAM 4, the UCB-PATS, the Sidepak and the DusTrak (Amaral et al., 2015; Giechaskiel et al., 2014). Several low-cost options of light scattering instruments are commercially available (Patel et al., 2017; Sousan et al., 2016; Kuula et al., 2019). Instruments of light scattering by single particles are very similar to the ones by particles ensemble, the main difference is that the optical detection volume of the single particles instrument is smaller compared to the ensemble instrument, so that only one particle is lit at once. The single particles instrument most commonly used is the Optical Particle Counter (OPC) (Giechaskiel et al., 2014). The more widely used and available low-cost PM sensors are “miniature versions” of OPCs (Crilley et al., 2018). The Condensation Particle Counters (CPCs), also classified as light scattering counters, are employed to measure the concentration of small particles that do not scatter light sufficiently for detection by conventional OPCs. In CPCs, small particles have their size

increased by condensation of vapor, produced from a working fluid. After the particles are enlarged by condensation, the operation of the CPC is similar to OPCs.

Optical instruments based on the principle of light absorption are used to measure the concentration of black carbon (BC), i.e. particles composed exclusively of carbon. BC strongly absorbs light and is therefore a positive radiative agent, contributing to climate change. The techniques based on aerosol absorption measurement can be subdivided in (Amaral et al., 2015; Giechaskiel et al., 2014):

- **Difference method**: absorption is obtained from the difference between extinction and scattering (e.g. Spotmeters). These have the advantage of assessing the whole PM size range, but the disadvantage of not providing real-time data;
- **Filter-based methods**: measure light attenuation by the PM collected in a filter (e.g. Aethalometer and Particle Soot Absorption Photometer);
- **Photoacoustic spectroscopy-based methods**: light absorbing particles contained in the samples are heated by absorption of amplitude-modulated light. The heat conducted from the particles to the surrounding gas generates acoustic pressure waves that are registered by a microphone (e.g. Photoacoustic Soot Sensor - PASS);
- **Laser Induced Incandescence (LII)**: particles are heated right below the carbon sublimation temperature by a short laser pulse, reaching incandescence and further decomposition, which is measured by a photomultiplier. The number and average size of particles and the soot volume are calculated from the incandescence intensity and decomposition rate.

The last type of optical instrument is the one based on light extinction or opacity, which occurs due to the combination of light absorption and scattering, i.e. opacity is the difference between incident and transmitted light. Measurements based on light extinction depend on path length and light wavelength, as well as on particles shape and composition. Opacity meters are the most used light extinction instruments (Amaral et al., 2015), but cavity-ring-down spectroscopy systems can also be used (Pettersson et al., 2004).

Beta-attenuation monitors utilize an analogous principle as the optical instruments based on light extinction, but replacing the light beam by beta rays. In these instruments, a constant source of air is drawn into the monitor through a ribbon filter, in which particles are deposited. The ribbon then passes through a detector, in which beta radiation from a source of radiation pass through the particles. The attenuation of the flow of beta radiation is proportional to the mass of the particles present in the airflow (Gilliam and Hall, 2016).

A.1.3 Microbalance

In the microbalance method, the particles are collected over the surface of an oscillatory microbalance element, which alters the frequency of oscillation. Based on the correlation between mass and frequency, total particle mass can be calculated (Gilliam and Hall, 2016). Two main instruments use the microbalance method: The Tapered Element Oscillation Microbalance (TEOM) and the Quartz Crystal Microbalance (QCM). The TEOM measures PM mass based on the alteration of resonance frequency of a tapered quartz wand, due to the accumulation of particles in a sampling filter connected to the wand tip. TEOM is a well-established instrument for measurements of PM_{10} and $PM_{2.5}$ in real time during biomass combustion (Nussbaumer et al., 2008). In QCMs, particles are deposited by electrostatic precipitation in a fine quartz crystal resonator, i.e. the quartz crystal has a piezoelectric property of changing its resonance frequency according to the mass added in its surface. The accumulation of mass can be calculated from the decrease of the resonance frequency (Booker et al., 2007).

A.1.4 Electrical charge

Electrical charge based methods, in which the ability of particles to acquire electrical charge is used to determine the PM concentration, can also be employed. The charging of aerosol particles can be achieved by a number of different approaches, e.g. static electrification, thermionic emission, photoemission, and charging by small ions (Kulkarni et al., 2011; Hinds, 1999). Photoelectric sensors and diffusion chargers are examples of instruments that employ this principle.

A.2 PM measurement: Size distribution methods

A.2.1 Microscopy

One method that can be used for size distribution measurement is microscopy. The PM sampling for analysis in a microscope generally involves collection of particles on filters followed by filter preparation to improve visibility (Vincent, 2007). Besides the dimensions of solid particles, electronic microscopy also examines their morphology and may provide information on useful information such as rotation radius, size distribution of aggregates, fractal dimension, number of primary particles per aggregate, and size distribution of primary particles (Wentzel et al., 2003). Furthermore, when combined with energy dispersive x-ray spectroscopy (EDS or EDX), electronic microscopy can measure the elemental composition of individual particles, enabling a more detailed description of aerosol populations than real time instruments. However, the long time spent to analyze a statistically relevant number of particles may be a disadvantage. Automated image processing methods and recognition by artificial intelligence algorithms may help to further develop this technique (Du et al., 2018; Brostrøm et al., 2019).

A.2.2 Impaction

Impactors can be used in conjunction with pumps normally used for total PM sampling in order to separate the particles in several parcels of known size. The technique is based on simple gravimetry, but using multiple impact stages/filters or multiple orifices. A simple type of impactor is the dichotomous sampler, also called the virtual impactor (Wight, 1994). In this technique, particles impact onto a surface allowing separation of particles into two size ranges, usually PM_{10} and $PM_{2.5}$. However, the most commonly used impactor is the cascade type, which operates based on the inertial classification of particles (Hinds, 1999). In a Cascade Impactor, the pumped air passes through a sequence of stages. In each stage, the incoming air reaches an impacting plate, where particles larger than the cutoff diameter for the stage are collected. Smaller particles pass through or around the collection plate, where the process is repeated in a plate of smaller cutoff diameter. This process continues until smaller particles are removed in the last collection plate (Vincent, 2007). Some of the most used low pressure cascade impactors are the Andersen Impactor, Dekati Low Pressure Impactor (DLPI) and Berner Low Pressure Impactor (BLPI) (Nussbaumer et al., 2008). Conventional cascade impactors operate at atmospheric pressure and generally do not select particles smaller than 0.4 µm. For smaller particles, there is a family of precision cascade impactors based on Micro-Orifice Uniform Deposit Impactor (MOUDI). Their operating flow rate ranges from 10 to 100 L min^{-1} and several combinations of impacting stages are available (Vincent, 2007). There are models with 10 stages that collect particles smaller than 0.056 µm on a quartz fiber (Venkataraman and Rao, 2001). Models with rotation of impacting plates are also available, providing a more uniform deposition of particles over the plates, reducing bounce related problems as well as evaporation of semi-volatile material (Vincent, 2007).

A.2.3 Cyclones

An alternative to impactors is the use of cyclones to select the particles' aerodynamic diameter. When the airflow passes through a cyclone, the larger particles will deposit on the cyclone walls, while the smaller particles will be collected by an after-filter. The size fraction of the collected particles is determined by the air flow rate. Cyclones can collect large quantities of PM and are less vulnerable to the problem of particle bouncing than cascade impactors, but have the disadvantage of sampling only one particle size fraction (Zhao et al., 2009). Although the addition of an impactor or cyclone represents an increase in size/weight to the basic gravimetry equipment, most devices with impactors/cyclones are still portable. The Very Sharp Cut Cyclone (VSCC) is an example of a method using a cyclone for size selectivity (Gilliam and Hall, 2016).

A.2.4 Diffusion

Particles with diameters smaller than 0.1 μm (ultrafine PM, i.e. PM of nanoscale size) are not strongly influenced by gravitational and inertia forces, meaning that their behavior is not well represented by aerodynamic diameter, the property commonly measured in traditional equipment. In this range, particle movement is generally dominated by diffusion (Vincent, 2007). Thus, the equivalent diameter in volume, obtained in a Diffusion Battery, becomes more appropriate for nanometric PM measurement.

Diffusion Batteries were developed to determine the diffusion coefficients of the particles (Hinds, 1999). These instruments separate particles by their mobility, being typically used as a switching valve to vary the effective length of the diffusion path and with a CPC to measure the concentration in number (Giechaskiel et al., 2014). A new approach for Diffusion Batteries is the Electrical Diffusion Battery (EDB), in which particles are carried by a corona charger before getting into the Diffusion Battery, which can be of two types: tube or screen. The EDB collection efficiency is a function of geometric properties of the tube or screen, the flow rate, and particle size, expressed in terms of equivalent diameter in volume (Vincent, 2007). In recent years, personal samplers for nanoscale PM have been developed, most of them based on diffusion charging (Asbach et al., 2017; Kuula et al, 2019).

A.2.5 Mobility analyzers

Another type of instrument that uses the principle of mobility is the so-called Mobility Analyzer. The Electrical Aerosol Analyzer (EAA) is the oldest mobility analyzer, and the Differential Mobility Analyzer (DMA) is a more recent model. DMAs use bipolar diffusion charging to bestow a well-defined charge distribution in the aerosol. After loading, particles are inserted into an electrostatic classifier, allowing particles to pass in a narrow range of electrical mobility. Classified particles are then measured by an electrometer or CPC (Giechaskiel et al., 2014). Another model is the Volatility Tandem Differential Mobility Analyzer (VTDMA), a system composed by two nano-DMAs, two long-DMAs (covering a large size range), a heating tube and one Ultrafine Condensation Particle Counter (UCPC) (Hossain et al., 2012).

A.2.6 Centrifugal

Particle mass can also be measured by the centrifugal method using a Centrifugal Particle Mass Analyzer (CPMA) or an Aerosol Particle Mass (APM). The CPMA is composed of two coaxial cylindrical electrodes, an internal one and an external one. The internal electrode turns slightly faster than the external electrode (Olfert et al., 2006). When the loaded particles pass through the electrodes, they experience electrostatic and centrifugal forces acting in opposed directions. The particles then penetrate the CPMA in a rate depending on the rotation speed and tension between the electrodes. The CPMA classifies the aerosol by the mass-to-charge ratio and is used in conjunction with a DMS (Differential Mobility Spectrometer) to measure the mobility size distribution of the mass-classified

particles in real-time (Johnson et al., 2013). The main difference between the CPMA and APM is that in the APM both electrodes turn in the same angular speed. These instruments present the advantage of registering particle mass without the need to collect particles for weighing (Giechaskiel et al., 2014).

A.2.7 Spectrometry

Spectrometers based on particle mobility may also be used to measure particle dimensions. These spectrometers are composed of a particle loader, a classification column and a series of detectors (Giechaskiel et al., 2014). The mobility spectrometers most known are the Differential Mobility Spectrometers (DMS) and the Fast Mobility Particle Sizer (FMPS) (Hosseini et al., 2010; Hossain et al., 2012). Other similar instruments include the Scanning Mobility Particle Sizer (SMPS) and the Twin Differential Mobility Particle Sizer (TDMPS). The FMPS is made of two concentric cylinders (classification columns), a diffusion loader and 32 electrometers that cover the particle size range from 5 to 560 nm. The current containing positively charged particles flow along the sheath. High voltage between the two cylinders transports the particles from the point they are introduced to the other side that houses the electrometers. Next to the column top, the particles with greater electrical mobility are collected, and the particles with inferior electrical mobility are collected downstream. Instead of a CPC, the FMPS spectrometer uses multiple, low-noise electrometers for particle detection, providing particle-size-distribution measurements with high time resolution, enabling the visualization of particle events and changes in particle size distribution in real time. The SMPS uses a technique analogous to that used in the FMPS, but with higher precision and lower time resolution (Giechaskiel et al., 2014; Hosseini et al., 2010; Nussbaumer et al., 2008). The TDMPS in turn is composed of two DMAs, an Ultrafine CPC and a CPC. Particles are charged and brought into charge equilibrium. With the help of two regenerative diffusion driers, relative humidity conditions can be continuously monitored (Kamilli et al., 2014).

A.2.8 Combined systems

Some instruments combine two or more of the techniques previously mentioned to measure the size distribution and concentration of PM. One example is the Fast Integrated Mobility Spectrometer (FIMS), composed by a charger, a size classifier, a condenser and a detector. In the FIMS, the aerosol passes through a neutralizer, where the particles receive a charge distribution of bipolar equilibrium. Then, the aerosol passes through a mobility analyzer, through which a butanol-saturated gas flows. In the electrical field of the mobility analyzer, charged particles are separated based on their electrical mobility. Classified particles are then transported by the flow to the condenser, where supersaturation of butanol condensates over the classified particles, increasing their size. At the condenser exit, one laser beam lights the drops, and the images are captured at 10 Hz with a camera. The images not only provide particle concentration but also the particle mobility diameter (Kulkarni et al., 2011; Olfert et al., 2008).

The Electrical Low Pressure Impactor (ELPI) classifies particles according to their aerodynamic diameter and measures the concentration and particle distribution in number (7 nm to 10 µm) close to real time (Giechaskiel et al., 2014; Vincent, 2007). In an ELPI, the particles are electrically charged as they are aspirated by a unipolar corona charger. Charged particles pass through a low pressure Cascade Impactor composed by collection steps electrically isolated. Since the particles impact in one specific stage, they produce an electrical current that is registered in real time by an electrometer. This technique is dependent on the aerosol density, which can compromise the precision of size distribution measurement in particle number if the density is not well known (Coudray et al., 2009).

There are also instruments used to measure aerodynamic size, such as the Aerodynamic Particle Sizer (APS), the Particle Size Distribution (PSD) and the Aerosol Mass Spectrometer (AMS). The working principle of the APS is based on the acceleration of the aerosol sample flow through an orifice. The

particle aerodynamic size determines its acceleration rate (larger particles have larger inertia and thus accelerate slower). At the nozzle exit, the particles cross each other through two laser beams partially overlapped in the detection area. The light is scattered when each particle passes through the overlapped beams. An elliptical mirror, placed 90 degrees in relation to the laser beam axis, collects and concentrates the light over an avalanche photodetector (APD). Next, the APS converts light pulses in electrical pulses. The APS is capable of measuring size distribution of particles in the size range of 0.5 to 20 μm. Sample particles are accelerated when the transporter gas flows through a converging nozzle. Due to inertia, particles cannot accelerate as fast as the gas, and there is a lack of speed comparing to the gas. Particle size is correlated to this lack of speed, measured in the exit of the nozzle, where the particles go through two closely spaced laser beams. Flight time between the two laser beams is then used to calculate the aerodynamic diameter (Hosseini et al., 2010).

A.3 Gases/vapors measurement: Enrichment methods

A.3.1 Enrichment by adsorption

Several types of samplers may be used for substance enrichment. Adsorbent samplers are widely used to capture organic gases, either passively or actively. Such samplers vary with regards to their desorption method (thermal or using solvents), to their capacity and to their range of adsorbed compounds (some are not suitable for very light, highly volatile compounds; others do not capture compounds of higher molecular weight). Commonly used adsorbent materials are: activated carbon, silica gel, XAD-2 and XAD-4 for solvent desorption and Tenax (TA, GR), Chromosorb and Porapak for thermal desorption (EPA, 1990; Hebisch et al., 2009). Recent developments include the use of zeolite 5A as adsorbent medium in passive flux sampling for greenhouse gases emissions estimates (Larios et al., 2018).

A.3.2 Enrichment by absorption

Impingers or bubblers are specially designed tubes used for collecting air pollutants (both gaseous and solid) into a liquid medium. In this method, a known volume of air is bubbled through a tube containing a specific liquid. The liquid collects the substance of interest by physically dissolving it (i.e. by absorption). Impingers are particularly useful for sampling unstable compounds, as they can be used to stabilize very reactive substances (EPA, 1990). Considering the need to employ pumps for bubbling air into the tube, this method is essentially an active one. The impingement method is commonly applied in the sampling of biogas and biomethane (Arrhenius et al., 2016).

Solid-phase microextraction (SPME) technology has been widely used in the analysis of complex environmental matrices over the last two decades. Among its several possible applications, SPME is often used for gas sampling in a range of different types of assessments (Li, 2017), e.g. urban air assessment, vehicle exhaust gas analysis, breath analysis and IAQ assessments, which is the focus of the present review. An SPME device consists of a silica fiber coated with a thin layer of a polymeric sorbent or immobilized liquid, adequate to collect the analyte of interest. The coated fiber is placed inside a needle, which is then placed within a syringe-like arrangement. SPME can directly extract analytes from gaseous and liquid media, by immersion of the syringe, or it can be used indirectly to analyze the composition of liquid and solid samples by extracting the analytes from the headspace above them (HS-SPME). After extraction, the fiber is placed within the feeder of the measuring instrument, where the extracted analytes are desorbed. SPME is based on a partition mechanism and the establishment of equilibrium between the analyte and the sample matrix. (Spietelun et al., 2010).

The SPME method is considered an environmentally friendly process because it is solvent-free and reusable (Li, 2016).

A.3.3 Reaction samplers

Reaction samplers are also an option for gaseous pollutants sampling. This method, in which a chemical reaction between substance of interest and the sampling medium allows the indirect measurement of the substance by measuring the reaction product(s), is applied when (a) the investigated substance is reactive and the reaction products are more stable (as mentioned above for impinger sampling), or (b) when the enrichment or desorption of the substance is enhanced due to the chemical reaction, or (c) when the reaction product can be detected with higher sensitivity than the targeted substance or (d) when the direct analysis of the substance of interest is hindered due to other present components (Hebisch et al., 2009). The sampling occurs using either an impinger or a solid sampler that has been pretreated with a specific reagent. The reaction between the substance of interest and the reagent takes place in situ during sampling, and then the resulting samples are transported to a lab for analysis (e.g. chromatography, spectrophotometry). Examples of this type of sampling are: the collection of aldehydes using enrichment systems impregnated with dinitrophenylhydrazine; of diisocyanates collected on filters coated with 2-methoxyphenyl-piperazine; of hydrogen peroxide in solutions containing titanium; of nitrogen and sulfur dioxides on filters coated with triethanolamine; of ozone on silica gel coated with 4,4'-dipyridylethylene; of hydrogen sulfide on filters impregnated with zinc acetate and of ammonia on filters impregnated with phosphoric or oxalic acid (Hebisch et al., 2009; Larios et al., 2018; Paralovo et al., 2019).

A denuder is an active sampling system similar to the reaction samplers. It is based on the diffusion principle, comprising a cylindrical or annular conduit or tube internally coated with a reagent that selectively reacts with the gases in the airflow drawn through the conduit. In a laminar flow, the separation of gaseous substances relies on the diffusion of gas molecules in a direction transverse to the flow. If the airflow in the tube is adjusted to obtain laminar flow conditions, gaseous air components can diffuse to the walls, while the analyte contained in the gas is transmitted outwards, collected, and analyzed. The gaseous and vaporous substances can be separated and enriched in different stages through adequate coating of the wall. Thus, enrichment occurs due to absorption or reaction mechanisms. Denuders usually are only applicable for stationary sampling (Hebisch et al., 2009; Kito et al., 1999). Recently, a denuder method was developed for the determination of hydrogen halides in volcanic plume. The method uses selective derivatization reaction of gaseous hydrogen halides, employing an organic compound (5,6-Epoxy-5,6-dihydro-1,10-phenanthrolin) for the enrichment and immobilization. The reaction with HBr results in the formation of 5-Bromo-5,6-dihydro-6-hydroxy-1,10-phenanthrolin. Other hydrogen halides give corresponding products. The denuder based sampling system with in situ derivatization enabled to differentiate also between gaseous and particulate hydrogen bromine. The derivatized analytes were analyzed with high pressure liquid chromatography-mass spectrometry (Gutmann et al., 2017).

A.4 Gases/vapors measurement: Non-enrichment methods

A.3.1 Collection of air samples in original state

When the gases enrichment is neither possible nor necessary, or when the indoor air composition is unknown and a complete screening is intended, gas storage vessels/flasks or gas sample bags (e. g. Tedlar™-bags) can be used. Gas storage bags and vessels are available in different sizes. Sampling

using bags usually requires a connection to a pump and that the air sample is drawn with a flow rate of 1 to 3 l min^{-1}. Metal canisters are also often used as vessels for air sampling. In this case, the canister is completely emptied beforehand in lab, generating a vacuum inside and thus rendering the use of a pump for sampling unnecessary (Orecchio et al., 2017). Several VOCs and their halogenated derivatives are known to be very stable in canisters (Kelly and Holdren, 1995). The sampling of air in electropolished canisters, followed by pre-concentration with a cryofocusing step, is described by the USEPA (EPA, 1999). After sampling using canisters or sample bags, either an aliquot is taken in laboratory and analyzed afterwards, or a volume portion is separated from the gas storage and enriched on adequate adsorption materials prior to analysis.

A.4.2 Color test tubes

A possibility for measuring gaseous compounds without enrichment is the use of color test tubes. The concentration of the substance (or substance class) of interest is determined by means of a reaction between the substance and the tube filling. This reaction, which leads to a change in color, is used both for verifying the occurrence of the substance of interest and for determining its concentration. The sampling procedure is performed drawing a defined air volume through the test tube using a pump. The resulting length of a colored layer is proportional to the concentration of the substance (or substance class) under investigation. The advantage of using color test tubes is that the gas concentration is obtained quickly and directly after sampling, without the need of further lab analysis. In practice, color test tubes have been proven valuable specially to determine carbon monoxide, carbon dioxide, hydrogen sulfide, ozone, nitrogen dioxide, ammonia, chlorine, phosphine, hydrogen cyanide and sulfur dioxide in air (Meffert and Blome, 2005). However, this method also presents some disadvantages, including a restricted selectivity, restrictions in determining shift average values, possible cross-reactions with other substances and problems in reading the colored edge, hindering the determination of the concentration of the assessed analyte (Hebisch et al., 2009).

A.4.3 Direct-reading instruments

Another way of assessing gaseous pollutants concentration in air without enrichment is to use direct-reading instruments, combining real-time sampling and analysis. Similarly to the color test tubes, these instruments do without the post phase of lab analysis, saving time and materials. Some commercial sensors are very small and affordable (cheapest options costing from €10 to €30), being especially suitable for applications where portability is more important than accuracy, for e.g. control purposes which do not require accurate absolute values of a specific compound. On the other hand, the more advanced instrument options, which provide high levels of accuracy and low detection limits, can be quite costly.

Direct-reading instruments can be either selective for a specific substance (e.g. carbon monoxide) or non-selective for a mixture of substances (e.g. organic gases). The simplest devices work by solely warning and signaling optically and/or acoustically once a threshold limit value is reached, without displaying the actual concentration value (Hebisch et al., 2009). These simple direct-reading instruments are relatively inexpensive and easy to handle but are not suitable for more elaborate assessments. A second group of direct-reading instruments can, in addition to the warning function, store the concentration values measured over time. This enables to examine the concentration average shifts and short-term values and peaks. Some of the most commonly used direct-reading devices are mentioned in the following sections.

A.4.3.1 Flame ionization detector (FID)

A flame ionization detector (FID) can be used for determining the sum of flammable gases and vapors occurring in indoor air. An FID can be used either as a direct-reading in situ device or coupled to a gas chromatograph in lab. In an FID, the air is drawn with an internal pump and fed to the FID. The operation of the FID is based on the detection of ions formed during combustion of the organic compounds (present in the inflow air) in a hydrogen flame. The ions and electrons formed during combustion generate a current, and the intensity of this current is proportional to the concentration of all flammable gases and vapors. Due to its dimensions and the need of hydrogen gas, the portability of the FID is hindered (Sun et al., 2013). The FID is advantageous due to its high time resolution, allowing to record the concentration of total flammable gases over time and to observe peaks. However, due to the restricted selectivity, the monitoring of specific substances in mixtures is not possible, not allowing a direct comparison with threshold limit values. The range of measurement with FID goes from 0.1 ppm up to 1000 ppm (ASTM, 2015). FID measurements are often labelled total hydrocarbons or total hydrocarbon content (THC), although a more accurate name would be total volatile hydrocarbon content (TVHC), as hydrocarbons, which have condensed out are not detected. Carbon monoxide, carbon dioxide and inorganic compounds are not detectable by FID (Hebisch et al., 2009).

A.4.3.2 Photoionization detector (PID)

Another option for direct-reading device is the photoionization detector (PID). The principle of operation of photoionization sensors consists in the ionization (decay into charged particles) of neutral molecules of chemical compounds. The air is drawn by an internal pump into the PID and passes a discharging tube, usually a UV-lamp, where diffusing molecules are ionized by photons. The substance to be determined is ionized when its ionization potential is lower than the energy of the irradiating beam. Then, the formed ions are directed between two polarized electrodes. The ions move towards the electrodes in an electric field, generating a current flow which is then converted into a voltage signal proportional to the concentration of the ionized compounds (Szulczynski and Gebicki, 2017). Depending on the given conditions, the PID delivers a sum signal of all ionizable substances. The selectivity of the detector can be varied within limits according to the chosen lamp. PIDs are usually affordable, compact and portable devices with battery operation and do not require any extra gas to operate, thus they can be used for personal air sampling (Hebisch et al., 2009; Sun et al., 2013). Similarly to the FID, the PID also presents high time resolution, being able to record sets of spatial and time-dependent concentrations and to determine concentration peaks. Classes of substances that can be detected by the PID include aromatic hydrocarbons, chlorinated hydrocarbons, amines, oxygen containing substances, and inorganic compounds such as ammonia or hydrogen sulfide. However, as the selectivity for mixtures is restricted to VOCs with proper ionization potential, a substance-specific measurement for direct comparison with threshold limit values is not possible. Recent developments in PIDs allow a response time less than 30 ms and a detection limit less than 5 ppb (Sun et al., 2013; Szulczynski and Gebicki, 2017).

A.4.3.3 Infrared spectrophotometer detector (IRSD)

Infrared spectrophotometer detectors can be used for the qualitative and quantitative determination of gases and vapors that are infrared active. The air is drawn with an internal pump through a measurement chamber, which is irradiated by infrared light with wavelength between 2.5 and 15 µm. The IR-active molecules in the sample are excited to induce oscillations at characteristic IR frequencies, leading to the absorption of light. Additionally, variations of the gas pressure can be measured (photo acoustic IR spectroscopy). Both phenomena can be utilized for measurements of airborne gases and vapors (Hebisch et al., 2009). The concentration of the analyzed species can then be calculated from the IR absorbance or transmittance in each wavelength, and the selectivity of the process can be controlled within limits by the correct choice of the monitoring wavelength (Skoog et al., 2018). The sensitivity reaches the low ppm levels. In measurement instruments that utilize the photo acoustic

effect, the monochromatic light irradiates through the gas chamber whereupon a changing in the gas pressure can be measured. The selectivity is equal to the infrared spectral photometer, but the measurement range reaches the lower ppb levels. Due to their large size, IRSDs are generally not feasible for personal air sampling. Both methods, however, have the capability of recording concentration values with more or less reasonable selectivity, and can be used to detect short-term concentration peaks. The response time of IRSDs is higher when compared to FID and PID due to the construction of the system (volume of the chamber) (Hebisch et al., 2009).

A type of IRSD widely used is the nondispersive infrared (NDIR) sensor. A typical NDIR consists of a light source, gas chamber and detector. The NDIR sensor is nondispersive in the sense of optical dispersion, as the infrared energy is allowed to pass through the atmospheric sampling chamber without deformation. The NDIR technique targets the absorption of specific wavelength in the infrared spectrum as a way to identify specific gases, such as CO, CO_2, SO_2, NOx, N_2O, NH_3, HCl, HF and CH_4 (Dinh et al., 2016). Initially, NDIR sensors were as large and costly as conventional IRSDs, but over the last decade, the commercial market has become populated with small low-cost gas sensors based on the NDIR principle, especially for CO_2 detection (Hodgkinson et al., 2012).

Another type of IRSD is the Fourier transform type (FTIR), which employs a Fourier transform to convert the raw data into the actual spectrum. FTIRs collect higher-spectral-resolution data over a wider spectral range when compared to conventional dispersive IR spectrometers. A variety of analysis techniques are available to retrieve trace gas concentrations from measured single-beam spectra acquired by FTIR instrumentation, generally involving comparison of the measured spectra with reference spectra of the gas of interest under standard conditions. One option is the open-path FTIR (OP-FTIR), widely used for methane, CO, CO_2, SO_2, NO and ammonia monitoring, mainly because these species have unique absorptions in the IR range, and thus have good detection sensitivity and less interference from water vapor. However, OP-FTIR can also be applied for VOC monitoring (Lin et al., 2008).

A.4.3.4 Electrochemical sensors (ECS)

Electrochemical or amperometric sensors can be applied for both the qualitative and quantitative determination of indoor gases and vapors, and are usually affordable, small, portable and suitable for personal sampling. Such sensors measure the concentration of a target gas by oxidizing or reducing it at an electrode and measuring the resulting current. In these sensors, air is drawn with a pump and passes by a gas-permeable membrane, or reaches it due to diffusion, where they diffuse through the internal electrolyte (most frequently aqueous solution of strong acids or bases, although mixtures with aprotic solvent are also utilized) towards the surface of a working electrode suitably polarized with respect to a reference electrode, inducing a controlled potential difference. On the measurement electrode, depending on the substance to be determined, either reduction or oxidation occurs, leading to a current that can be measured (Szulczynski and Gebicki, 2017). ECSs are often applied as warning devices, but it is also possible to record time dependent changes in concentrations of hazardous substances in air. Substances commonly monitored by electrochemical sensors include chlorine, carbon monoxide, hydrogen sulfide, sulfur dioxide, nitric oxide, glutaraldehyde, formaldehyde, ammonia, hydrogen cyanide, ethylene oxide and vinyl chloride (Hebisch et al., 2009; Szulczynski and Gebicki, 2017). The measurement range normally extends between the middle and upper ppb level. The lifetime of ECSs is limited due to expiration of the sensors, on which reactions may take place permanently and irreversibly. The response time of these sensors is slower if compared to FIDs and PIDs (Hebisch et al., 2009).

A.4.3.5 Metal oxide semiconductor (MOS) sensors

In this type of sensor, the gas of interest diffuses towards the receptor surface, which is a metal oxide surface, where it undergoes either oxidation or reduction. This interaction between the gas and the metal oxide changes either the conductivity or resistivity of the receptor from a known baseline value, a change which can be measured and is proportional to the gas concentration. Two types of metal oxide semiconductors are commonly used in measurement practice: (1) type n (e.g. ZnO, SnO_2), which changes resistance of the receptor element in the case of reducing gases presence, and (2) type p (e.g. NiO, CoO), which changes resistance of the receptor element in case of oxidizing gases presence. The sensor sensitivity depends mainly on the thickness of the receptor layer, the catalytic metal particles placed in it and the temperature of the receptor layer. MOS sensors applications include measurement of hydrocarbons and their derivatives, alcohols, ethers, ketones, esters, carboxylic acids, nitroalkanes, amines or aromatic compounds (Szulczynski and Gebicki, 2017). Similarly to the PIDs, MOS sensors are small size, low weight and inexpensive, being appropriate for personal monitoring. On the other hand, like PID sensors, MOSs are not specific to individual organic compounds. These sensors do additionally respond to inorganic reducing and oxidizing gases (e.g. CO or NOx). To improve their selectivity, manufacturers typically incorporate different dopants or filters (Spinelle et al., 2017).

A.4.3.6 Mass spectrometry (MS)-based monitors

Mass spectrometry (MS) is an analytical technique very useful in air quality assessments. This technique ionizes chemical species and sorts the ions based on their mass-to-charge ratio. A mass spectrum is a plot of the ion signal as a function of the mass-to-charge ratio. These spectra are used to determine the elemental or isotopic signature of a sample, the masses of particles and of molecules and to elucidate the chemical structures of molecules. In a typical MS procedure, a sample (solid, liquid or gas) is initially ionized, causing some of the sample's molecules to break into charged fragments. These ions are then separated according to their mass-to-charge ratio, typically by accelerating them and subjecting them to an electric or magnetic field: ions of the same mass-to-charge ratio will undergo the same amount of deflection. The ions are detected by a mechanism capable of detecting charged particles, such as an electron multiplier. Results are displayed as spectra of the relative abundance of detected ions as a function of the mass-to-charge ratio. The atoms or molecules in the sample can be identified by correlating known masses (e.g. an entire molecule) to the identified masses or by a characteristic fragmentation pattern. An MS consists of an ion source, a mass analyzer and a detector. There are several options for each component, especially for ion source (e.g. chemical ionization, electron bombardment), allowing for many different design combinations (Sparkman, 2000).

Mass spectrometers are commonly used in the lab as detectors coupled to gas chromatographs, but some devices use this principle for real-time, in situ monitoring. Selected ion flow tube mass spectrometry (SIFT-MS) is a form of direct mass spectrometry that monitors VOCs in air with typical detection limits at low ppbv (Ellis and Mayhew, 2014). SIFT-MS uses ultra-soft, precisely controlled chemical ionization coupled with mass spectrometric detection to quantify VOCs in real-time. Eight chemical ionization agents (reagent ions) are applied in SIFT-MS instruments: H_3O^+, NO^+, O_2^+, O^-, O_2^-, OH^-, NO_2^-, and NO_3^-. These eight reagent ions react with analyte VOCs and inorganic gases in very well controlled ion-molecule reactions, but they do not react with the major components of air (N_2, O_2, and Ar), enabling SIFT-MS to analyze air at trace levels without enrichment.

Another type of direct mass spectrometry monitor is the proton transfer reaction mass spectrometry (PTR-MS). The PTR-MS technique is analogous to the SIFT-MS, both employing the kinetics taking place in a flow tube to determine the concentration of the constituents of an air sample in real-time. The PTR-MS replaces the flow tube of the SIFT-MS by a relatively short drift tube, using an electric field instead of a carrier gas to transport ions, resulting in a gain of several orders of magnitude in the detection sensitivity for VOCs compared to SIFT-MS. On the other hand, in the PTR-MS the reagent ions are produced with very high purity by a hollow-cathode discharge, rather than select reagent ions

with a quadrupole, granting the SIFT-MS a higher selectivity (Blake et al., 2009; Ellis and Mayhew, 2014).

Most SIFT-MS and PTR-MS instruments use quadrupole mass analyzers, which are filtering devices that allow ions of a single mass-to-charge ratio to strike the detector at any moment. Quadrupole mass analyzers typically have unit mass resolution, meaning they cannot resolve ions that have the same nominal mass-to-charge ratio. To solve that, the time-of-flight (TOF) technique has arisen. TOF mass analyzers separate ions based on differences in their velocities after acceleration by a fixed potential. TOF mass analyzers inherently measure all mass-to-charge ratios simultaneously and can have much higher mass resolving power than quadrupole mass analyzers. TOF-based PTR-MS systems also provide better time resolution and mass range than quadrupole-based systems.

A.4.3.7 Gas chromatography (GC)-based monitors

These monitors combine low power consumption, sample processing, column programming, detection systems and data handling in reduced size and weight for portable use. The simplest may consist of an ambient temperature injector, column and detector, while the most complex may have every feature of an advanced lab instrument. Portable GCs may be based on semiconductor chip processing or assembled from discrete components (Spinelle et al., 2017). The ion mobility spectrometer (IMS) can be considered as a sub-class of chromatographic separators. The principle of every IMS is a time-of-flight measurement. After a gaseous sample enters the spectrometer, it is ionized by a radioactive source, the resulting positive and negative charged species are accelerated over a short distance and the time-of-flight is determined. The IMS is different from the mass spectrometer in that it operates under atmospheric conditions and does not need large and expensive vacuum pumps, meaning that the IMS can be easily miniaturized. The instruments of this category present high sensitivity and selectivity, but the price of such instruments (between €20.000 and €100.000) limit their applicability (Spinelle et al., 2015).

A.5 Radon concentration measurement methods

A.5.1 Scintillation flask

One of the most important devices to measure radon is the scintillation flask, originally developed by Henry F. Lucas and commonly known as the Lucas cell. Scintillation devices include cells for gaseous and liquid samples and plates for samples of radon collected on filters. Commercially, different volumes of cells are available (e.g. 270, 160, 100 cm^3). The plates and gas cells are coated with silver-activated zinc sulfide (ZnS(Ag)) phosphor and one side of the cell is a transparent flat surface, constituting a viewing window, to which a photomultiplier tube is coupled. When an alpha particle produced within the cell strikes the phosphor, a flash of light is produced and is sensed by the photomultiplier tube and associated electronics and is counted using a multichannel analyzer (recorded as a count) (Baskaran, 2016).

A.5.2 Online detectors

Online radon monitors are most commonly used for continuous radon measurements. The most common ones available in the market are the RAD7 (Durridge, Boston, USA), the Radon Scout Plus (SARAD, GmbH, Dresden, Germany), the RTM 2200 (SARAD, Dresden, Germany) and the CRM (BARC, Mumbai, India; Ashokkumar et al., 2014). Conventional detectors used in the development of radon monitors include pulse ionization chambers, scintillation detectors coupled with photomultiplier

tubes and silicon PIN diodes. Scintillation cell-based continuous radon monitors (Smart Radon Duo and Scintillation Radon Monitors) have been developed by the Bhabha Atomic Research Center in Mumbai (Bombay, India). These detectors take into account the ingrowth of progeny in a given counting interval without making equilibrium assumptions. An advantage of this technique is that its performance is not affected by relative humidity (Baskaran, 2016).

A.5.3 Electrets

Usually, measurements of radon concentration in the air of occupied indoor environments are carried out by means of integrated sampling over a period time (usually weeks to months) (EPA, 1990). Electrets are an example of integrating detectors, which are passive, lightweight and relatively inexpensive. They consist of electrically charged Teflon discs, which serve both as a source of electric field and sensor. When an alpha particle decays in the detector chamber, ionization of the air takes place and leads to a decrease in the total charge on the electret. This results in a voltage drop over the measurement period, which is used to quantify the ^{222}Rn concentration (Baskaran, 2016).

A.5.4 Thermoluminescent dosimeter (TLD)

A TLD is a type of radiation dosimeter that may be used to provide an integrated measurement of radon or its decay products. The TLD measures ionizing radiation by measuring the intensity of visible light emitted from a crystal (made of a material exhibiting thermoluminescence in response to ionizing radiation) when it is heated. During the sampling period, the radiation interacts with the crystal, causing electrons in the crystal's atoms to jump to higher energy states, where they stay trapped due to intentionally introduced impurities, until heated. Heating the crystal causes the electrons to drop back to their ground state, releasing a photon of energy equal to the energy difference between the trap state and the ground state. The intensity of light emitted is proportional to the radiation exposure. A TLD crystal (chip) is typically lithium fluoride or calcium fluoride (EPA, 1990).

A.5.5 Track detectors

Alpha track detectors are dosimeters based on solid-state nuclear track detectors (SSNTD), and are also commonly used as integration monitors for radon measurements by recording the alpha-particles emission. This method of detection consists of placing a thin piece of an appropriate plastic in a holder and exposing it to air containing radon and its decay products for an extended period of time (reaching up to a year). During this exposure period, the alpha particles that are emitted by decaying nuclei strike the surface of the plastic piece, making microscopic gouge marks (alpha tracks). The exposed plastic is then removed from its holder and chemically etched to enlarge the tracks, facilitating their visualization. The alpha tracks are visually counted using a wide-screen microscope or other counting system (e.g. spark counter, CCD camera, etc.) (EPA, 1990). Original discovery of the alpha-particle tracks was seen in cellulosic materials such as cellulose nitrate and cellulose acetate butyrate. Subsequently, alpha-particle tracks were also seen in polycarbonates such as bisphenol-A polycarbonate, i.e. Lexan and allyl diglycol carbonate (CR-39). Due to good ionization sensitivity and stability against various environmental factors, the CR-39 (polycarbonate material) has been used as the state-of-the-art track detector for environmental radon (Baskaran, 2016). The LR-115 track detector-based twin-cup dosimeter has also been developed for indoor ^{222}Rn and ^{220}Rn measurements (Eappen and Mayya, 2004).

In the two-filter method, a small tube (30-100 cm long) is equipped with an entrance filter, which removes the decay products from the sample as it is drawn into the tube, and an exit filter, which traps the ^{218}Po formed by the decay of some of the radon atoms as they move through the tube. After

sampling, the filter is removed and counted by measurement of the alpha decays. This method has been adapted to continuous and integrated monitoring by the use of a TLD chip at the exit filter (EPA, 1990).

Radon concentrations can also be determined by measuring the beta-particle activity of ^{214}Pb and ^{214}Bi collected on filter papers, assuming secular equilibrium between ^{222}Rn and its progeny in the air. Beta-particles can be assessed using plastic scintillators mounted on photomultiplier tubes or the filter paper can be directly counted in a beta counter (a Geiger-Muller counter), with appropriate use of absorber film (Baskaran, 2016). Alternatively, radon concentration can be inferred by gamma-ray spectrometry (Duenas et al. 1994).

A.5.6 Solid media collection

As previously mentioned, activated charcoal can be used to capture radon from air by means of adsorption, both to obtain grab samples or for integrated sampling. The resulting sample can be then analyzed by different means, such as: de-emanation of the adsorbed radon from the charcoal into a scintillation cell and alpha-counting; heating the charcoal and counting the gamma emissions from the desorbed radon using a sodium iodide system; dissolving the charcoal in liquid scintillation fluid and counting in a liquid scintillation detector (EPA, 1990).

The measurement principles used for radon decay products determination are similar to those used for radon, with some alterations in the sampling and analysis approach. Radon decay products are largely attached to the surface of suspended particulate matter, and thus may be separated from radon during sampling by collecting the particulate matter (with the adsorbed decay products) from the air sample using a filter. The filter can then be analyzed by alpha-particle spectroscopy, which allows the determination of the activity of each decay product on the filter and the subsequent computation of the potential alpha energy or working level concentration (EPA, 1990).

A.6 Bioaerosols: Sampling methods

A.6.1 Impaction plates

Collection of bioaerosols can be done using the same principles applied to common PM sampling, but employing plates of solid nutrient media instead of common filters. Simply gravitational sampling on such open plates (settle plate method) is not considered an efficient sampling method, as the number of large particles collected on the surface will be overestimated while smaller particles, with slower settling velocity, will be underestimated. Thus, inertial samplers can include setups to distinguish the collection of particles by size (Haig et al., 2016). The Andersen cascade impactor, for example, is a convenient sampling method that uses pre-poured plates, in which the distribution of particle sizes can be determined, and a high sampling rate (28 l min^{-1}) (Mandal and Brandl, 2011). Cyclone samplers with multiple tubes are also efficient for collecting size-fractionated bioaerosol samples (Macher et al. 2008).

A.6.2 Rotorod

Changes in aerosol concentration with time can be observed with the rotating slit or slit-to-agar sampler, in which a large petri dish of medium is placed on a turntable beneath a stationary slit inlet. Air filters or rotorod samplers are used to know the particles quantitatively recovered per unit of air sampled. The rotorod sampler is a volumetric, rotation impaction device capable of quantitatively sampling airborne particles in the size range of 1 to 100 µm at sampling rates up to 120 liters per minute (Mandal and Brandl, 2011). There is also the possibility of real-time analysis of viable particles in the air, using for

example a Biotrak from TSI®. The Biotrak particle counter detects total and viable particle counts in real time and incorporates laser induced fluorescence to determine particle viability.

A.6.3 Electrostatic precipitator

Another sampling possibility for bioaerosol sampling is the electrostatic precipitator, which utilizes an electric field to deposit charges on bacterial samples and a solid agar as bacterial growth media. In this device, two ionizers in the inlet charge the incoming biological particles (in case they carry insufficient charge for efficient collection). The particles are then subjected to a precipitating electric field and are collected onto agar plates placed along the flow axis. In electrostatic precipitators, the particle velocity component perpendicular to the collection medium is much lower than that in impactors and impingers at comparable sampling flow rates, being thus less damaging to the microorganisms (Mainelis et al., 2002).

There are also options for passive bioaerosol sampling, such as the Rutgers Electrostatic Passive Sampler (REPS), developed based on the use of ferroelectric polymer film (PVDF), which remains permanently polarized for typical environmental applications. This sampler uses polarized PVDF to electrostatically attract charged particles in addition to capture particles settling by gravity. It uses a spiral film shape to increase total collection surface area (Therkorn et al., 2017).

A.6.4 Impingers

In contrast to impactors, particle collection by impingement is based on liquid media. Liquid impingers are mostly used when the organisms require rapid rehydration and to collect soluble materials (e.g. Tyco- or bacterial endo-toxins and some antigens). In this technique, sampled air is drawn with a known flow rate through a narrow inlet tube into a recipient containing the appropriate collection medium. When the air hits the surface of the liquid, any suspended particles are impinged into the collection liquid. After sampling, aliquots of the collection liquid can be cultivated in adequate growth medium to enumerate viable microorganisms. Results allow for quantitative determinations, as both the sampling volumes and times are known (Mandal and Brandl, 2011).

A.7 Bioaerosols: Analytical methods

A.7.1 Culture

The most frequently used method is to culture the collected organisms. In some methods, the sampling is done directly onto a solid nutrient medium and in others (e.g. impingement) the bioaerosol is placed on the nutrient medium after sampling. The organisms are then identified by their distinctive individual colonies. The samples must be inoculated onto as many types of media and incubated under whatever conditions of temperature, humidity and lighting as all present organisms need to grow (Mandal and Brandl, 2011). There are several medias used to cultivate sampled bioaerosols, such as sabourauddextrose agar (SDA), dichloran rose-bengalchloramphenicol (DRBC), and yeast extract glucose chloramphenicol (YGC), tryptic soy agar, MacConkey agar and malt extract agar (MEA) (Kim et al., 2018).

Culturing of sample is most suitable for identifying infectious agents that must be alive or active to produce diseases. However, this means of quantification underestimates actual levels of microorganisms, since some may have been damaged by the sampling procedure, not all will reproduce under the given culturing conditions, and the presence of some will inhibit the growth of others. Cells

that are not alive are also not revealed but they may still be important, as even dead cells of allergenic material are capable of causing reactions.

A.7.2 Microscopy and optical methods

A second useful method of identification of bioaerosols after sampling is examination by microscope. In this method, bioaerosol particles are identified by morphology and a certain level of expertise is required. Fluorescent probes can be applied to stain and determine specific bacterial groups or even species in a sample (Amann and Ludwig, 2000). The total number of bacteria are normally determined after staining with a fluorescent dye such as DAPI (4, 6 diamidino-2-phenylindol) or SYBR Green (asymmetrical cyanine dye) that bind to DNA. Acridine Orange is used to detect viable cells (Mandal and Brandl, 2011).

Flow cytometric analysis on air samples can also be performed after air collection by impingement. In this analysis, a suspension of cells is passed rapidly through a capillary in front of a measuring window. Light emitted from a source is scattered by particles in the liquid and several characteristics such as size, shape, biological and chemical properties can be measured simultaneously. Fluorescence in situ hybridisation (FISH) and flow cytometry might be combined resulting in a more powerful analysis of air samples (Mandal and Brandl, 2011).

The ATP-bioluminescence assay is also used to detect the presence of microorganisms in a sample, and even a real-time instrument for airborne microbe analysis has been developed (Lee et al., 2008). Spectroscopic techniques such as matrix assisted laser desorption/ionization time of flight - mass spectrometry (MALDI-TOF-MS) or Raman-spectroscopy have been recently introduced for the analysis of bioaerosols (Mandal and Brandl, 2011).

A.7.3 Polymerase chain reaction (PCR)

The polymerase chain reaction (PCR) technique can be used to detect and quantify microorganisms, by copying and amplifying many million-fold specific regions of the genome for analyses. This method is more rapid than culture techniques and is sensitive enough for the detection of specific microorganisms, which are slow growing and difficult to culture. However, it does not allow to distinguish between non-viable and viable microorganisms. Currently, there is also the option of real-time PCR analysis (RT-PCR) (Dungan and Leytem, 2009; Georgakopoulos et al., 2009).

A.7.4 Bioassays and immunological tests

Bioassays can be conducted on eluates of air samples or bulk samples of dust. Such assays determine concentration or potency of a substance by its effect on living cells or tissues. A common bioassay is the *Limulus* amoebocyte lysate (LAL) test, widely used for the detection and quantification of bacterial endotoxins (Dawson, 2005). The common scratch test used by allergists is another example in which concentrated extracts of dust or pollen are applied to the skin to test a person’s sensitivity to specific antigens.

Immunological tests may also be used in IAQ assessments to present biological pollution in terms of allergen levels. Such tests are used to measure the presence in human blood serum of antibodies that indicate exposure to specific microorganisms (Tsekenis et al., 2008). Among these tests are the enzyme-linked immunosorbent assay (ELISA), the immunoelectrophoresis (RIE), the radioimmunoassay (RIA), immunoradiometric assay (IRMA) and the radio-allergo-sorbent test (RAST).